

https://dspace.org/

Study of the expression of hepatitis B surface antigen (HBsAg) by different African genotypes of hepatitis B virus (HBV) using subcellular fractionation

Pillay, Thanusha

2019
https://hdl.handle.net/10539/29779

Downloaded from a DSpace repository. https://dspace.org/



STUDY OF THE EXPRESSION OF HEPATITIS B SURFACE ANTIGEN (HBsAg) BY DIFFERENT AFRICAN GENOTYPES OF HEPATITIS B VIRUS (HBV) USING SUBCELLULAR FRACTIONATION

Thanusha Pillay

A dissertation submitted to the Faculty of Health Sciences, University of the Witwatersrand, Johannesburg, in fulfilment of the requirements for the degree of Master of Science in Medicine.

July, 2019

DECLARATION

I, Thanusha Pillay declare that this dissertation: **Study of the Expression of Hepatitis B Surface Antigen (HBsAg) by Different African Genotypes of Hepatitis B Virus (HBV) Using Subcellular Fractionation** is my own, unaided work. It is being submitted for the degree of Master of Science in Medicine at the University of the Witwatersrand, Johannesburg, South Africa. It has not been submitted before for any degree or examination at any other University.

_____

(Signature of candidate)

_____day of _____20____at_____

PUBLICATIONS AND PRESENTATIONS ARISING FROM THIS DISSERTATION

This work was presented with the title “Optimization of Subcellular Fractionation Protocol to Ensure the Purity of Subcellular Fractions of Huh-7 Liver Cancer Cells” in poster format at the 2018 Faculty of Health Sciences Biennial Postgraduate Research Day, University of the Witwatersrand, Johannesburg (September 2018).

ABSTRACT

Hepatitis B Virus (HBV) is hyperendemic in sub-Saharan Africa, and of the 292 million people chronically infected with HBV worldwide, approximately 30% reside in Africa – an approximation that is likely underestimated because of poor surveillance. Chronic HBV infection is a significant risk factor for the development of hepatocellular carcinoma (HCC), and correspondingly, the predominant strain circulating in South Africa – subgenotype A1 – is associated with hepatocarcinogenic potential.

Studies have demonstrated that HBV genotypes vary in their clinical manifestation and disease progression, accompanied by differences in expression of HBV viral proteins. Hepatitis B surface antigen (HBsAg) is one of the first virological biomarkers to appear upon the onset of HBV infection, and plays an indispensable role both in the viral life cycle as the major HBV surface protein, and in the clinical setting as an indicator of HBV infection, disease progression and treatment response. HBsAg is the term used to collectively refer to small- (S-HBs), middle- (M-HBs) and large (L-HBs) surface antigens, and distinct differences in the proportion of these antigens have been observed extracellularly and intracellularly. Additionally, variations in the subcellular localisation of HBV viral proteins have been shown to influence the severity of HBV infection and its associated hepatocarcinogenesis. However, no studies have comparatively analysed the differences in S-HBs, M-HBs and L-HBs expression or their subcellular localisation, within the HBV strains predominantly circulating in South Africa. Thus, the aim of the study was to determine the subcellular localisation of HBsAg in HCC cells transfected with wild type subgenotypes A1, A2 and D3, and further characterise the relative proportions of S-HBs, M-HBs and L-HBs expressed intracellularly and extracellularly.

To achieve this, human HCC (Huh7) cells were transiently transfected with 1.28 mer replication competent plasmids containing HBV wild type subgenotypes A1, A2 or D3. Supernatants were collected on days 1, 3 and 5 post-transfection and transfected Huh7 cells were harvested on day 5 post-transfection. Using the Thermo Scientific Subcellular Protein Fractionation Kit for Cultured Cells, Huh7 cell pellets were then fractionated into cytoplasmic, membrane, soluble-nuclear, chromatin-bound nuclear and cytoskeletal fractions. The identity of each fraction was confirmed with fraction-

specific housekeeping proteins and the subcellular fractionation protocol was optimised to provide pure, enriched fractions suitable for downstream Western blotting analysis. HBsAg was detected using a mouse monoclonal antibody targeted towards the S-domain of HBsAg, thus all forms of HBsAg were successfully detected. HBsAg was found to localise exclusively within the membrane fraction with subgenotype A1 exhibiting the lowest expression and subgenotype D3 the highest. To determine the expression of HBsAg extracellularly, supernatants collected on days 1, 3 and 5 from the culture of transfected Huh7 cells were precipitated for HBsAg using a PEG precipitation protocol developed and optimised for this study. Extracellular HBsAg was secreted the highest from cells transfected with subgenotype A1. This result was confirmed with an HBsAg enzyme-linked immunosorbent assay (ELISA).

A novel finding in this study was differences in the proportions and glycosylation patterns of S-HBs, M-HBs and L-HBs extracellularly and intracellularly between the different subgenotypes. It was observed that S-HBs is consistently expressed in the highest proportion, with variable expression in M-HBs and L-HBs expression between the subgenotypes. Furthermore, there was generally a lower proportion of glycosylated S-HBs and biglycosylated M-HBs, with nonglycosylated and glycosylated L-HBs expressing at a ratio of approximately 1:1. The relative proportions of S-HBs to M-HBs and L-HBs as well as their rates of glycosylation have important implications for HBV viral infectivity and the associated host immune response.

An HBeAg ELISA was also performed to determine the rate of HBeAg expression over days 1, 3 and 5 post-transfection. HBeAg expression increased over each consecutive day, and subgenotype A1 was noted to have the highest expression. The comparatively high extracellular HBeAg and HBsAg expression in association with low intracellular HBsAg expression in subgenotype A1 would seem to indicate that this strain has high production and secretion efficiency of HBV viral proteins – characteristics which may allow subgenotype A1 to circumvent the immune system, establish chronic HBV infection and ultimately result in HCC.

ACKNOWLEDGEMENTS

This research project would not have been possible without the kindness and assistance from many people. I would like to express my sincere thanks to the following:

To my supervisor, Professor Anna Kramvis, I would like to express my immense gratitude for your guidance, understanding, and wisdom. Thank you for doing your best to encourage and help me grow. You are an inspiration both as a scientist and as a leader.

To my co-supervisor, Dr Nimisha Bhoola, thank you so much for all your help throughout the course of my degree. Thank you for sharing your expertise, encouraging me when experiments didn't work and getting excited with me when I finally achieved results.

To the members of the Hepatitis Virus Diversity Research Unit, thank you for the intellectual conversations and for assisting me with various aspects of my project; I learned a lot from every one of you.

To Boipelo Kgosinkwe, thank you for being a great friend, and for going over and beyond your role as a finance officer.

To Luicer Olubayo, thank you for being an amazing friend and colleague. It was a pleasure working with you and you made my days in the lab so much easier and more enjoyable.

To the individuals from the following departments for their generosity and assistance: To the Antiviral Gene Therapy Unit for their assistance with the procurement of cell lines for optimisation, and for allowing me to use various equipment. A special thanks to Dr Kuben Naidoo for all his guidance regarding viral protein precipitation.

To Dr Clement Penny, for kindly allowing use of his FLoid™ Cell Imaging Station.

To Raquel Duarte and the members of her team, for their support and for generously allowing me to use their Western blotting equipment. Thanks to Dr Caroline Dickens for her assistance with the statistical analyses in this study. A special thanks to Nicolas Tagliatti, for his support and for always being willing to help no matter the time or occasion.

To Kiashanee Moodley, for your boundless support and positivity. Thank you for always reminding me of my value as a scientist and as an individual, and for being there through my times of sadness and joy. Thank you for being the big sister I never knew I needed, but certainly the one I have always wanted.

To Leeshania Sarappa and Prajna Naidu, for sticking with me through thick and thin for the last six years. Thank you both for being the ultimate pillars of love and support, for keeping me grounded, and at other times helping me keep my head above water when I otherwise would have drowned. I am truly blessed to call you my best friends.

To my amazing family, where words cannot begin to express my gratitude:
To my Dad, thank you for (literally) everything. Thank you for chauffeuring me around and waiting those long, *long*, hours while I was in the lab. Thank you for your words of advice and reason, and for always trying to make my life easier where you could.
To my Mom, for always being willing to lend a listening ear and shoulder to cry on. Thank you for taking care of me when I couldn't take care of myself, and for the on-demand supply of hugs.
To my brother and closest friend, Divyan. Thank you for showing me the importance of never giving up, and for being the ultimate role model of someone who is strong and brave. Thank you for inspiring me to become a scientist that leaves a positive imprint on people's lives.

I would finally like to sincerely thank the National Research Foundation, Poliomyelitis Research Foundation, and The University of the Witwatersrand's Postgraduate Merit Award Programme, for making this study financially possible.

TABLE OF CONTENTS

DECLARATION i

PUBLICATIONS AND PRESENTATIONS ARISING FROM THIS DISSERTATION ii

ABSTRACT iii

ACKNOWLEDGEMENTS v

TABLE OF CONTENTS vii

LIST OF FIGURES x

LIST OF TABLES xiii

ABBREVIATIONS xiv

CHAPTER 1: INTRODUCTION 1

1.1. The Hepatitis B Virus: Classification and Epidemiology 1

1.2. Clinical Manifestation and the Natural History of HBV 3

1.3. HBV Structure and Biology 5

1.4. HBV Genome and Viral Proteins 5

1.4.1. HBV Polymerase/Reverse Transcriptase 6

1.4.2. HBcAg and HBeAg 6

1.4.3. HBV X Protein 7

1.4.4. HBsAg 8

1.5. HBV Replication Cycle 12

1.6. HBV Genotypes and Subgenotypes 13

1.6.1. Genotype A 14

1.6.2. Genotype D and Subgenotype D3 15

1.6.3. The Role of HBsAg and HBeAg in Different Genotypes and Subgenotypes 16

1.7. Rationale 17

1.8. Aims and Objectives 17

CHAPTER 2: MATERIALS AND METHODS 18
2.1. Ethics 18
2.2. Materials 18
2.3. Methodology 21
2.3.1. Plasmid Preparation 22
2.3.2. Transient Transfection of Huh7 Cells 30
2.3.3. Expression of HBV Proteins 32
2.3.4. Statistical Analysis 43
CHAPTER 3: RESULTS 44
3.1. Plasmid Preparation 44
3.1.1. Restriction Digestion 44
3.2. Transient Transfection of Huh7 Cells 46
3.2.1. Mycoplasma Detection 46
3.2.2. Measurement of Transfection Efficiency with eGFP 46
3.3. Expression of HBV Proteins 48
3.3.1. Subcellular Fractionation Optimisation 48
3.3.2. Detection of Intracellular HBsAg 53
3.3.3. Quantification of Intracellular HBsAg Expression 54
3.4. Quantification of Extracellular HBeAg and HBsAg Expression 60
3.4.1. ELISA 60
3.4.2. PEG Precipitation 63
3.5. Comparison of Intracellular and Extracellular HBsAg Expression 68
CHAPTER 4: DISCUSSION 72
4.1. Optimisation of Subcellular Fractionation and PEG Precipitation 72
4.2. Subcellular Localisation of Intracellular HBsAg 73
4.3. The Composition of Intracellular and Extracellular HBsAg Differs Between Genotypes 74

4.4. Glycosylation of HBsAg Differs Between Genotypes 76
4.5. Extracellular Expression of HBeAg Differs Between Genotypes 78
4.6. ER Stress and HBV-associated Hepatocarcinogenesis 79
4.7. Limitations and Future Studies 80
CHAPTER 5: CONCLUSION 83
REFERENCES 85
APPENDIX I: ETHICS CLEARANCE CERTIFICATE 91
APPENDIX II: REPLICATION COMPETENT CLONE PLASMID MAPS 92
APPENDIX III: PROTOCOLS 94
A. Agarose Gel Electrophoresis 94
B. Mycoplasma Detection 94
APPENDIX IV: COMPOSITION OF REAGENTS AND SOLUTIONS 96
A. Plasmid Preparation 96
B. Cell Culture and Transient Transfection 98
C. Subcellular Fractionation, Whole Cell Lysis, and Protein Quantification 99
D. Western Blotting 100
E. ELISA and PEG Precipitation 104
APPENDIX V: DNA AND PROTEIN LADDERS 106
Appendix VI: ENZYME-LINKED IMMUNOSORBENT ASSAY 110
96-well Plate Layout 110
APPENDIX VII: PLAGIARISM DECLARATION 112

LIST OF FIGURES

Figure 1. Estimated global prevalence of HBV 2
Figure 2. Major phases of HBV chronic infection 4
Figure 3. Schematic illustration of the organisation of the hepatitis B virus genome 6
Figure 4. Electromicrograph of HBV viral particles 8
Figure 5. Illustration of the transmembrane domains present in small, middle and large hepatitis B surface antigen 11
Figure 6. Schematic diagram of the HBV life cycle 13
Figure 7. Geographical distribution of hepatitis B virus genotypes and subgenotypes 14
Figure 8. Flow diagram illustrating an overview of the methodology in this study 21
Figure 9. Flow diagram illustrating the methods used for preparation of 1.28 mer replication competent HBV plasmids 22
Figure 10. Flow diagram illustrating the methodology established for cell culture and transient transfection of Huh7 cells. 30
Figure 11. Flow diagram illustrating the methods used to quantify the extracellular expression of HBsAg 32
Figure 12. Schematic illustration of subcellular fractionation protocol used in this study 33
Figure 13. Schematic diagram illustrating the assembly of the Western blot "transfer sandwich" 37
Figure 14. Flow diagram illustrating the methodology employed to quantify extracellular expression of HBsAg and HBeAg. 39
Figure 15. Agarose gel electrophoresis of A1-WT, A2-WT, D3-WT and pCDNA™4/TO DNA restriction digest 44
Figure 16. Agarose gel electrophoresis of PCR products for *Mycoplasma* detection 46
Figure 17. Representative photomicrographs of Huh7 cells transfected with eGFP 47
Figure 18. Ponceau S stains of whole lysate and subcellular fractions extracted from Huh7 cells 48

Figure 19. Composite Western blot image comparing subcellular fractions extracted from freshly harvested Huh7 cells versus Huh7 cells previously stored at -70 °C 50
Figure 20. Composite Western blot image of Huh7 subcellular fractions validated with fraction-specific housekeeping proteins 52
Figure 21. Western blot image of intracellular HBsAg expression in HBV subgenotypes A1, A2 and D3, over short and long exposure times 53
Figure 22. Composite Western blot images of HBsAg expression in subcellular fractions for HBV subgenotypes A1, A2 and D3 55
Figure 23. Semi-quantitative analysis of intracellular HBsAg expression in A1-WT, A2-WT and D3-WT 58
Figure 24. Composite Western blot images of HBsAg expression within whole cell lysates of Huh7 cells transfected with either HBV subgenotypes A1, A2, or D3 . 59
Figure 25. Normalised HBeAg expression in cell culture supernatant of transfected Huh7 cells 61
Figure 26. Normalised HBsAg expression in cell culture supernatant of transfected Huh7 cells 62
Figure 27. Western blot image of extracellular HBsAg expression in HBV subgenotypes A1, A2 and D3 66
Figure 28. Semi-quantitative analysis of extracellular HBsAg expression in A1-WT, A2-WT and D3-WT on day 5 post-transfection 67
Figure 29. Comparison of intracellular and extracellular S-HBs, M-HBs and L-HBs expression in wild type HBV subgenotypes A1, A2 and D3 69
Figure 30. Relative amounts of nonglycosylated to glycosylated S-HBs and monoglycosylated to biglycosylated M-HBs, in wild type HBV subgenotypes A1, A2 and D3 71
Figure 31. Ethics clearance certificate 91
Figure 32. Schematic illustration of the 1.28 mer replication competent plasmid containing HBV wild-type subgenotype A1, A2, or D3 92
Figure 33. Schematic illustration of the pCDNA 4/TO mammalian expression vector 93
Figure 34. O'GeneRuler™ 1 kb DNA Ladder, Ready-to-Use 106
Figure 35. O'GeneRuler™ 1 kb Plus DNA Ladder, Ready-to-Use 107

Figure 36. Precision Plus Protein™ WesternC™ Standards.....108
Figure 37. Pierce™ Prestained Protein MW Marker.....109
Figure 38. ETI-EBK PLUS HBeAg ELISA plate layout.....110
Figure 39. Murex HBsAg Version 3 HBsAg ELISA plate layout.....111

LIST OF TABLES

Table 1. Antibody information 20
Table 2. Restriction digestion reaction set-up used to confirm size and orientation of HBV DNA 26
Table 3. Expected fragment sizes following restriction digestion of 1.28 mer HBV plasmid DNA 27
Table 4. Sequencing primers (700 bp) used to confirm the presence and orientation of HBV DNA within each plasmid 28
Table 5. Summary of modifications tested to improve purity of the cytoskeletal fraction extracted from Huh7 cells previously stored at -70 °C 51
Table 6. Summary of polyethylene glycol (PEG) precipitation optimisation for Western blotting analysis of cell culture supernatants containing HBV viral proteins 64
Table 7. Reaction Set Up for the Detection of Mycoplasma in Cell Culture 95
Table 8. Cycling Conditions for the Detection of Mycoplasma in Cell Culture 95

ABBREVIATIONS

%	Percentage
°C	Degrees Celsius
µg	Micrograms
µl	Microlitre
A1-WT	Wild-type HBV Subgenotype A1
A2-WT	Wild-type HBV Subgenotype A2
A_{260}/A_{280}	Absorbance Ratio at 260 nm to 280 nm
APS	Ammonium Persulphate
bp	Base Pairs
CBEB	Chromatin-Bound Nuclear Extraction Buffer
CBNE	Chromatin-Bound Nuclear Extract
cccDNA	Covalently Closed Circular DNA
CEB	Cytoplasmic Extraction Buffer
CK-18	Cytokeratin 18
cm	Centimetre
CMV	Cytomegalovirus
CO_2	Carbon Dioxide
CPE	Cytoplasmic Extract
CSE	Cytoskeletal Extract
D3-WT	Wild-type HBV Subgenotype D3
D3-WT (CMV+)	Wild-type HBV Subgenotype D3 with an Exogenous CMV Promoter
DMEM	Dulbecco's Modified Eagle's Medium
DNA	Deoxyribonucleic Acid

dNTP	Deoxyribonucleotide Triphosphate
E. coli	*Escherichia coli*
eGFP	Enhanced Green Fluorescent Protein
ELISA	Enzyme-Linked Immunosorbent Assay
ER	Endoplasmic Reticulum
ERGIC	Endoplasmic Reticulum-Golgi Intermediate Compartment
ESCRT	Endosomal Sorting Complexes Required for Transport
EtOH	Ethanol
FBS	Foetal Bovine Serum
GFP	Green Fluorescent Protein
HBcAg	Hepatitis B core Antigen
HBeAg	Hepatitis B e Antigen
HBsAg	Hepatitis B Surface Antigen
HBV	Hepatitis B Virus
HBx	Hepatitis B X Protein
HIV	Human Immunodeficiency Virus
HRP	Horseradish Peroxidase
Hsp90	Heat Shock Protein 90
Huh7	Human Hepatocellular Carcinoma Cells
kb	Kilobase Pairs
kDa	Kilodaltons
LB	Luria-Bertani
L-HBs	Large Hepatitis B Surface Antigen
ME	Membrane Extract
MEB	Membrane Extraction Buffer
MEM NEAA	Minimum Essential Medium Non-Essential Amino Acids

mg	Milligrams
M-HBs	Middle Hepatitis B Surface Antigen
min	Minutes
ml	Millilitre
mRNA	Messenger RNA
MVBs	Multivesicular Bodies
NaCl	Sodium Chloride
NaN_3	Sodium Azide
NaOH	Sodium Hydroxide
NEB	Nuclear Extraction Buffer
ng	Nanograms
nm	Nanometre
NMP p84	Nuclear Matrix Protein p84
NTCP	Sodium Taurocholate Co-transporting Polypeptide
PBS	Phosphate Buffered Saline
PCV	Packed Cell Volume
PEB	Pellet Extraction Buffer
PEG	Polyethylene Glycol
pgRNA	Pregenomic RNA
RNA	Ribonucleic Acid
rpm	Revolutions Per Minute
SDS	Sodium Dodecyl Sulphate
SDS-PAGE	Sodium Dodecyl Sulphate Polyacrylamide Gel Electrophoresis
S-HBs	Small Hepatitis B Surface Antigen
SNE	Soluble-Nuclear Extract
TEMED	Tetramethylethylenediamine

Tris	Tris(hydroxymethyl)aminomethane
U	Units
V	Volts
x g	Relative Centrifugal Force
YT	Yeast Extract and Tryptone

CHAPTER 1: INTRODUCTION

1.1. The Hepatitis B Virus: Classification and Epidemiology

Hepatitis B virus (HBV) has successfully infected a third of the world's population, confirming its position as a global health challenge [1]. Indicated by HBV surface antigen (HBsAg) prevalence, of the 2 billion people showing evidence of past or present HBV infection (anti-HBsAg-positive), roughly 292 million people are chronically infected, of which 10% have actually been diagnosed and 1.6% receiving antiviral treatment [2]. Chronic HBV infection is a significant risk factor for the development of hepatocellular carcinoma (HCC), which is the 7th most common cancer. The burden of HBV varies geographically, with Africa and the Asia-Pacific region accounting for a disproportionate 68% of chronic HBV infections [3]; this is a result of high rates of perinatal mother to child transmission of HBV genotypes B and C in Asia [4-6] and genotype E in Africa [7]. HBV vaccination coverage in these regions is also not optimal, and Africa in particular was delayed in initiating an HBV vaccination programme [8].

The HBV burden in Africa is difficult to ascertain because of underreporting as well as the poor quality of serosurveys conducted, particularly within the sub-Saharan region [2, 7]. However, currently available modelled data for sub-Saharan Africa indicates HBV prevalence at approximately 10% in the central regions, 5% in the east, 9.8% in the west and 8.5% in southern sub-Saharan Africa; HBV is hyperendemic in those regions with a prevalence of ≥8%. Northern African regions are of relatively low endemicity (<2%) (**Figure 1**). Of the 292 million chronically infected, approximately 30% reside in Africa – which is likely underestimated owing to the lack of serosurveillance [2]. HBsAg prevalence is higher in rural areas versus urban areas [7], low income versus high income countries [2], and chronic infection is higher in men versus women [9-11]. HBV is multi-faceted, with several viral factors including genotype, viral mutations and viral loads influencing clinical manifestation and disease progression.

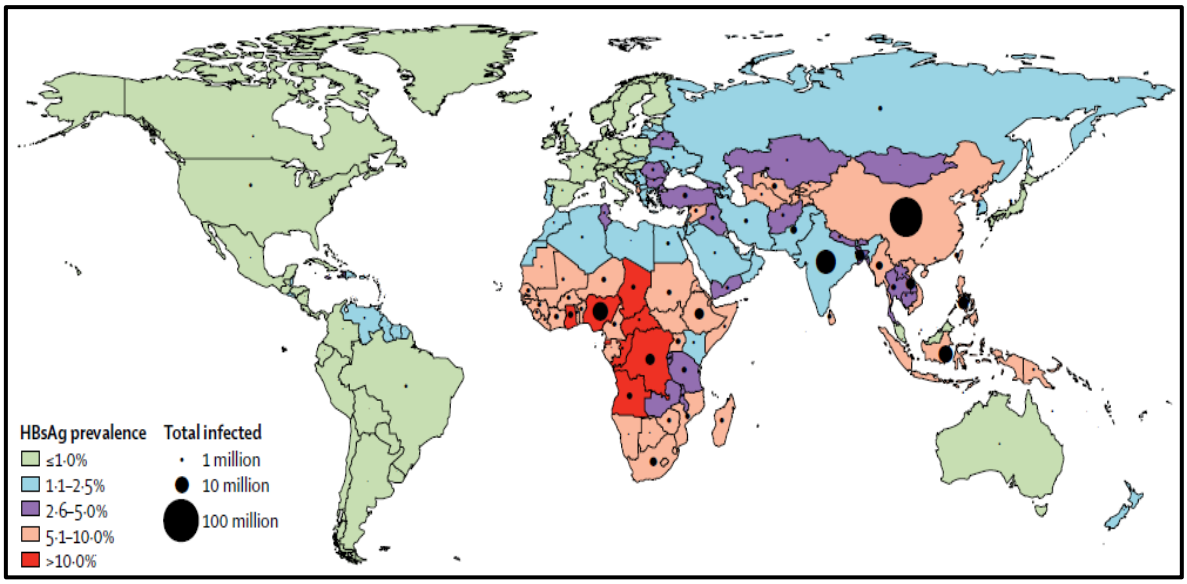


Figure 1. Estimated global prevalence of HBV

This figure shows the estimated prevalence of HBV infection worldwide, indicated by estimated HBsAg prevalence. The relative size of the black circles indicates the number of infected individuals and the red areas indicate areas of hyperendemicity. HBsAg prevalence of <2.5% indicates low endemicity, >2.5 moderate endemicity and >5% indicative of highly endemic regions. Africa and the West Pacific region are shown as having the highest endemicity. Reprinted from The Lancet Gastroenterology and Hepatology, Razavi-Shearer *et al.* Global prevalence, treatment, and prevention of hepatitis B virus infection in 2016: a modelling study. Copyright (2018), with permission from Elsevier.

As the prototype member of the family *Hepadnaviridae*, HBV is a small double stranded DNA pararetrovirus, whose only known natural hosts are humans and greater apes [12]. Hepadnaviruses include two species-specific genera infecting mammals such as ground squirrels, woolly monkey and orangutans (orthohepadnaviruses) as well birds such as ducks, herons and storks (avihepadnaviruses) [12, 13]. Hepadnaviruses can be reliably dated to their origins in fish over 400 million years ago [14], and a recent study in *Nature* described the sequencing of the oldest viral genomes ever recovered in human remains, revealing the existence of HBV since at least the Bronze age [15]. This long-lived nature of HBV has allowed it to evolve efficient methods that enable it to circumvent both the host immune system and various treatment modalities. HBV has employed extremely effective transmission and infection strategies enabling it to successfully replicate and persist in humans for thousands of years [16].

1.2. Clinical Manifestation and the Natural History of HBV

Consistent with all hepadnaviruses, HBV causes hepatotropic infections specifically isolated in liver tissue [16]. HBV infection may result in liver disease spanning a wide range of clinical manifestations such as acute and chronic hepatitis, as well as cirrhosis and HCC [13].

HBV is transmitted through percutaneous or mucosal exposure to infected blood and body fluids [1], and presents with high-titre viremia at a concentration of approximately 10^8 – 10^9 particles circulating per ml of blood in infected individuals [17, 18]. Furthermore, only a minimal amount HBV virions circulating in the bloodstream is required to infect hepatocytes [19]. The primary route of transmission varies according to the geographical endemicity of HBV infection.

In highly endemic regions where HBV affects more than 8% of the population, HBV is primarily acquired via perinatal transmission of neonates at birth from infected mothers. Regions with high to intermediate endemicity generally have horizontal transmission in children through close personal contact with HBV-infected people, whereas in low-endemicity regions the primary route of transmission is via risky behaviour during adolescence and adulthood [20]. Additionally, progression towards chronic infection is inversely proportional to the age at which acute infection occurs [21]; whereby adults have a less than 5% risk of chronic infection, infants and children under 5 years having up to a 35% risk of infection, and more than 90% of neonates eventually developing chronic hepatitis B infection [20].

HBV is a highly transmissible virus, capable of resisting extreme conditions [22] and can survive outside the body for an indeterminate period of time while still retaining the capability to infect a susceptible host [1, 23]. A number of viral antigens can be found in serum following infection with HBV, and an accurate diagnosis of the clinical forms of HBV infection and its associated disease is based on multiple biochemical, histological and clinical findings [13]. Generally, HBV infection is not considered directly cytopathic, with hepatitis and any subsequent histological alterations in the liver as a result of the host's immune-mediated response [16, 24]. The natural history and progression of HBV

infection is influenced by the complex interplay of the virus and the host immune response.

Different phases of chronic HBV each presenting with characteristic biochemical and virological profiles have been described by the European Association for the Study of the Liver (EASL), and are summarised in **Figure 2**:

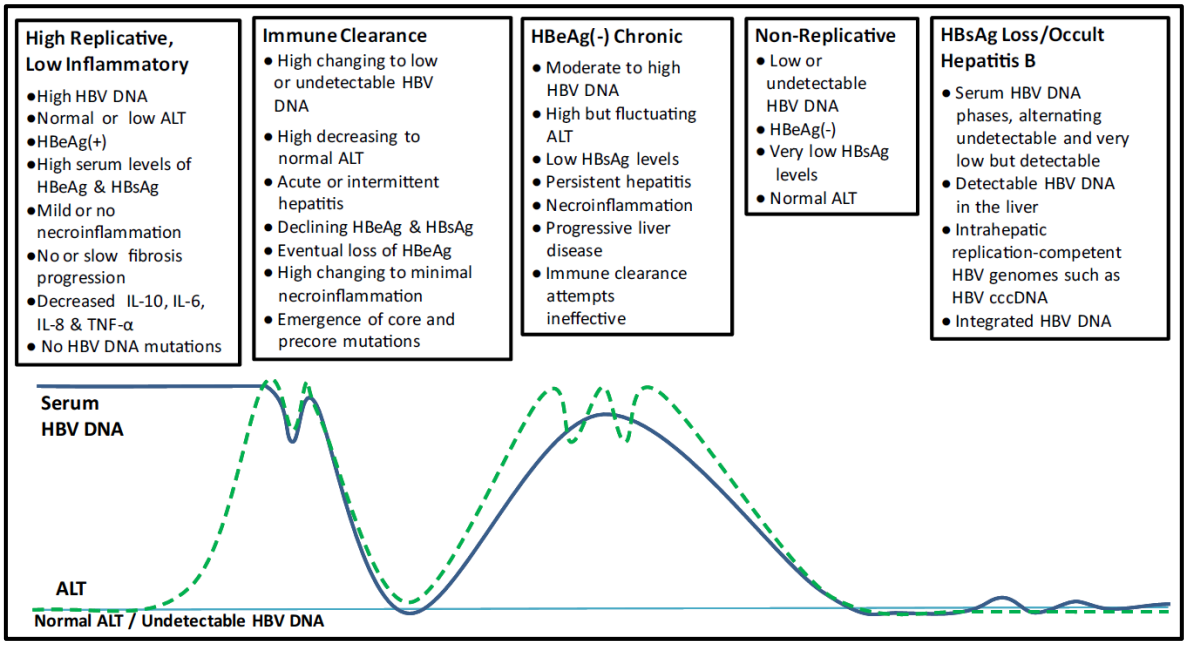


Figure 2. Major phases of HBV chronic infection

Schematic illustration of the various stages of chronic HBV infection. **ALT,** Alanine aminotransferase; **HBeAg,** hepatitis B e antigen; **HBsAg,** hepatitis B surface antigen; **IL,** interleukin; **TNF-α,** tumour necrosis factor-α. Reprinted from Antiviral Research, Gish *et al*. 2015, Chronic hepatitis B: Virology, natural history, current management and a glimpse at future opportunities. Copyright (2015), with permission from Elsevier.

The risk of cirrhosis and HCC development is variable, with a 2 – 5% annual risk of HCC in patients with cirrhosis [25]. Progression towards HCC is currently the main concern for patients diagnosed with chronic hepatitis B and may develop even in those patients who have been successfully treated. There is increased risk of developing HCC in patients with one or more host (including cirrhosis, chronic necroinflammation of the liver) or viral (such as high DNA and HBsAg levels, genotype of the virus, and the presence of HBV variants) risk factors [26].

1.3. HBV Structure and Biology

In 1965, Blumberg and colleagues noticed infectious particles in the sera of haemophiliac Australian Aboriginal patients. The particles were initially termed "Australia antigen" and was later recognised as the envelope proteins of HBV [27]. Five years later, the small HBV DNA virus was identified using electron microscopy by Dane *et al*. [18], owing to the name of the HBV virion, the Dane particle. The HBV virion, is a spherical structure roughly 42 nm in diameter, enveloped in a lipid bilayer containing transmembrane viral envelope proteins; or HBsAg [24, 28]. Beneath this lipid envelope is an icosahedral viral nucleocapsid core composed of hepatitis B core antigen (HBcAg), encasing the partially double-stranded HBV 3.2 kb DNA genome, which is covalently linked to a reverse transcriptase. HBV can be classified as a pararetrovirus, replicating via reverse transcription of an RNA intermediate, similar to traditional RNA retroviruses [12, 16].

1.4. HBV Genome and Viral Proteins

The HBV genome consists of a small 3.2 kb partially double-stranded DNA strand, found in a relaxed circular conformation [29]. The strands overlap at the 5' end with a complete minus strand and an incomplete plus strand with a variable position of the 3' end. During viral replication, the HBV endogenous polymerase completes the genome via the addition of nucleotides, creating a full covalently closed circular DNA (cccDNA) [30, 31] conformation. This cccDNA is a minichromosome providing the template for viral transcription, generating mRNA transcripts of 3.5 kb, 2.4 kb, 2.1 kb and 0.7kb each. The HBV genome consists of four overlapping, frame-shifted open reading frames (ORFs), namely viral transcriptase/polymerase, core, X and surface ORFs, which encode for the seven HBV proteins [32] (**Figure 3**) .

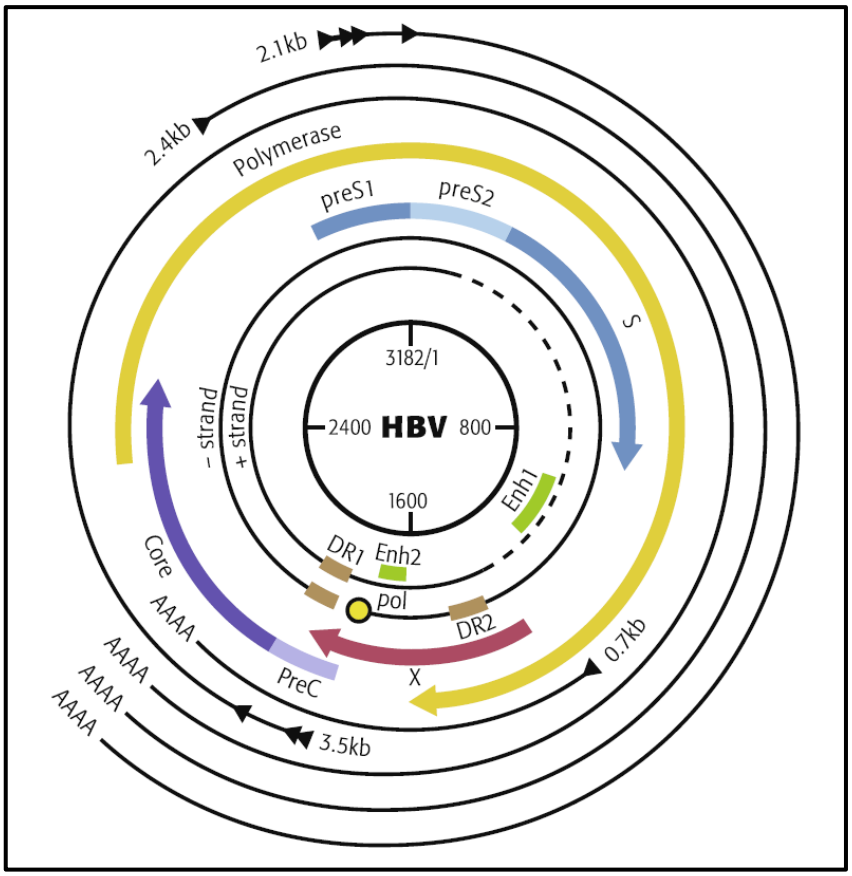


Figure 3. Schematic illustration of the organisation of the hepatitis B virus genome

Reprinted from Antiviral Research, Gish *et al*. 2015, Chronic hepatitis B: Virology, natural history, current management and a glimpse at future opportunities. Copyright (2015), with permission from Elsevier.

1.4.1. HBV Polymerase/Reverse Transcriptase

The HBV polymerase gene has the longest ORF encoding a large viral polymerase of approximately 800 amino acids, and is composed of four subdomains; the terminal domain involved in viral encapsidation and DNA synthesis, a spacer domain, the reverse transcriptase domain catalysing genome synthesis, and a carboxy terminal domain that has ribonuclease H activity critical for degrading pregenomic RNA (pgRNA) and facilitating replication [13, 33].

1.4.2. HBcAg and HBeAg

The *C* gene encodes either the viral nucleocapsid HBcAg or hepatitis B e antigen (HBeAg) depending on whether translation begins at the core or precore regions, respectively. HBcAg has the intrinsic ability to assemble into capsids around the

ribonucleoprotein complex constituted by pgRNA and the polymerase, and can also assemble into empty capsids [34-36].

Full translation of the *C* gene results in the formation of HBeAg which is secreted in large excess of the virions. HBeAg is the only protein modified post-translationally prior to secretion, and is an accessory protein not required for viral structure stability, secretion, infectivity or replication [37-39]. Despite much investigation the true function of HBeAg remains largely unknown, but it is highly conserved evolutionarily amongst *Hepadnaviridae*, increasing the likelihood that it plays a critical role in HBV propagation [40, 41]. HBeAg is suspected to play an immunomodulatory and tolerogenic role to enable immune escape, and is a serological marker indicating active HBV replication [42, 43].

HBeAg is clinically used as an indicator of HBV infectivity, disease severity and treatment response [42]. Normally, the presence of HBeAg antibodies (anti-HBe) and disappearance of HBeAg is correlated with the clearance of HBcAg from hepatocytes, HBV DNA from serum, and stabilisation of normal hepatic histology [44]. In some cases, HBV infection and liver damage persist, despite the presence of anti-HBe. These instances have been attributed to translational defects, which result in the failure of HBeAg secretion. Such patients often develop aggressive forms of chronic hepatitis, characterized by flare-ups and exacerbated liver disease. It has been thought that this is due to the lack of HBeAg mediated immune tolerance, leading to a potent inflammatory immune response [44].

1.4.3. HBV X Protein

The X ORF encodes for the hepatitis B X protein (HBx), which is not required as a structural protein, but is necessary for cccDNA transcription and is plays a key role in viral replication[16]. While not much is definitively known about the HBx protein, it has been implicated as playing a critical role in oncogenesis and the development of HCC. Studies describe HBx as having the capacity to modulate apoptosis and the cell cycle, as well as regulation of various signal and transduction pathways [45, 46].

1.4.4. HBsAg

A unique feature of HBV infection is that infected hepatocytes produce numerous types of virus-related particles, including infectious virions and non-infectious subviral particles, which are primarily composed of HBsAg and host-derived lipids [47]. HBsAg is unusually complex, consisting of three structurally related but functionally distinct surface proteins, termed small (S-HBs), middle (M-HBs) and large (L-HBs) surface antigens [13, 48]. These surface proteins do not solely constitute the viral envelope, but also spontaneously assemble into sphere and filament-shaped subviral particles lacking any viral capsid or genome [49] (**Figure 4**).

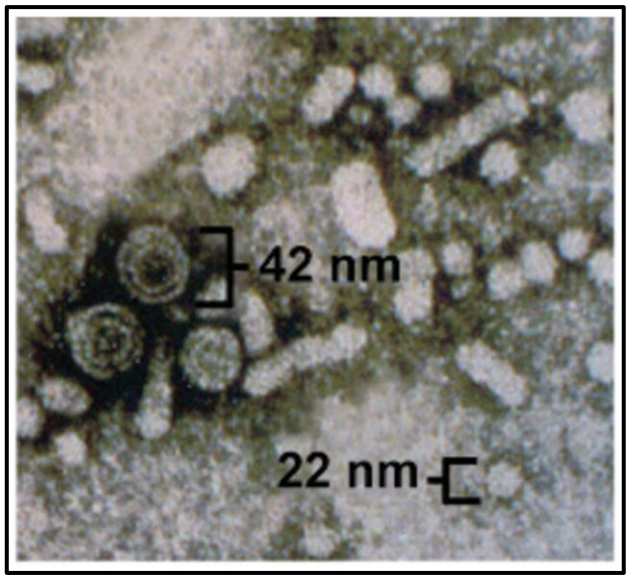


Figure 4. Electromicrograph of HBV viral particles

The 42 nm particle is the HBV virion, surrounded by 22 nm tubular filaments and spherical subviral particles. Reprinted from Hepatology, Liang 2009. Hepatitis B: The Virus and Disease. Copyright (2009), with permission from Wiley and Sons.

HBsAg is coded by the *S* gene, which is divided by three in-frame translation initiation sites, giving rise to the PreS1, PreS2, and S domains. S-HBs is coded by the S domain, M-HBs by the PreS2 and S domains, and L-HBs by the PreS1, PreS2 and S domain [50]. The PreS1 domain contains an N-terminal myristoylation site which is essential for viral infectivity and binding to the primary HBV receptor [51, 52]. Additionally, the PreS1 domain contains immunodominant epitopes recognised by T cells and B cells, and the PreS2 domain includes an epitope recognised by B cells [53, 54].

Similar to typical membrane proteins, HBsAg assembly occurs through a series of steps at the endoplasmic reticulum (ER); firstly, S-HBs is inserted into the ER followed by partial translocation into the ER lumen, crossing the ER membrane via four transmembrane domains [55]. This results in a transmembrane configuration consisting of an amino acid loop at the cytosolic side of the ER membrane, and an inner luminal loop [56] containing the conformational epitope of HBsAg known as the "a" determinant – the major antigenic HBV epitope that is especially clinically significant [45] [57]. S-HBs is the smallest envelope protein and contains low affinity binding sites for heparan sulphate proteoglycans (HSPG), which are believed to bring the virus in close enough proximity to hepatocytes to allow for binding of HBV to its primary hepatocyte receptor [58, 59]. N-glycosylation at asparagine residue 146 occurs in roughly half of S-HBs proteins, giving rise to 25 kDa nonglycosylated and 27 kDa glycosylated forms [60].

The transmembrane topology of M-HBs is identical to that of S-HBs, and the N-terminal of the PreS2 domain in translocated into the ER lumen [61]. M-HBs is N-glycosylated at asparagine residue 146 on the S domain and asparagine residue 4 on the PreS2 domain, resulting in either a 33 kDa monoglycosylated conformation or a 36 kDa biglycosylated form [60]. M-HBs has been reported to bind to human serum albumin [62], but the role of M-HBs in the viral life cycle remains uncertain and it does not appear to be necessary for HBV propagation. The absence of M-HBs *in vivo* in infected hepatocytes does not disrupt viral particle secretion, morphogenesis or infectivity [63].

L-HBs plays an indispensable role in the viral life cycle, where the envelopment of mature nucleocapsids and virion budding is strictly dependant on the presence of L-HBs[28]. Indeed, absence of L-HBs completely stops the production of new virions[64], and studies with duck HBV show that absence of L-HBs results in shuttling of the viral genome back to the nucleus, whereas capsids are generally secreted as enveloped virions when L-HBs is expressed [65, 66]. Furthermore L-HBs is an essential component for viral entry as its PreS1 domain binds to the sodium taurocholate co-transporting polypeptide (NTCP), a bile receptor located on the membrane of hepatocytes that grants hepatotropic specificity to HBV [67]. The PreS1 domain is myristoylated at glycine residue 2 to confer binding ability, and L-HBs has nonglycosylated and glycosylated forms of 39 kDa and 42 kDa respectively [68].

HBV surface proteins budding intracellularly from post-ER pre-Golgi membranes [69, 70], without enveloping of nucleocapsids, appear as octahedral spherical subviral particles 22 nm in diameter, or as filamentous particles of variable length. S-HBs and M-HBs are the major components of the spherical particles, which contain low amounts of L-HBs, while the relative amount of L-HBs is higher in filaments and greatest in the viral envelope [50]. Spherical subviral particles self-assemble initially in a filamentous form within the perinuclear space, which is part of the ER. The filaments are then packed and transported via ER-derived vesicles to the ER-Golgi intermediate compartment (ERGIC) [71]. The vesicles are released into the ERGIC lumen and the filaments unpacked and converted into spherical particles, followed by secretion through the Golgi apparatus and out the cell via the constitutive cellular secretory pathway of vesicular transport [47, 69].

Distinct from the secretory pathway of spherical subviral particles, filaments are instead assembled within the same intracellular compartment and secreted via the same secretory pathway as virions [72-74]. Like other retroviruses and enveloped RNA viruses, studies show that HBV maturation and secretion is dependent on intraluminal maturing endosomal multivesicular bodies (MVBs) [75, 76]. These MVBs form part of the host sorting complex machinery known as ESCRT (Endosomal Sorting Complexes Required for Transport), and are generally involved in the sorting of ubiquitinated and misfolded proteins targeted for degradation [77]. To further emphasise that the mechanism of spherical particle assembly is distinct and independent of the ESCRT pathway, endocytic host receptors strongly bind to L-HBs but does not recognise S-HBs [78, 79], and inhibition of ESCRT sorting complexes does not disrupt the release of spherical subviral particles [75]. How the ESCRT system mediates HBV viral budding is unclear but it is likely similar to the mechanism used by the human immunodeficiency virus (HIV) in macrophages, whereby ESCRT complexes are recruited and MVBs are assembled around HBV virions prior to secretion via exosome [80].

Persing *et al.* documented a study where a high proportion of L-HBs tends to result in retention of L-HBs within the infected cell [81]. The inability of infected hepatocytes to secrete L-HBs as filaments or otherwise appears to influence the direct cytopathic effect known as “ground glass” hepatocytes [71, 72] – the histopathological hallmark of

chronic HBV infection indicating the presence of ER congested with HBsAg [82]. Retention of HBsAg within the ER can cause ER stress which is a pro-apoptotic and pro-carcinogenic response [82-84].

Figure 5 provides a schematic illustration of S-HBs, M-HBs and L-HBs. Subviral particles are produced up to 100000-fold in excess relative to virions and it is suspected that this overproduction allows subviral particles to act as decoys, overwhelming the host immune response and eliciting an immunomodulatory effect advantageous for the virus [47]; subviral particles are strongly immunogenic and induce a potent protective immune response – a property which contributed towards the development of an effective HBV vaccine [85].

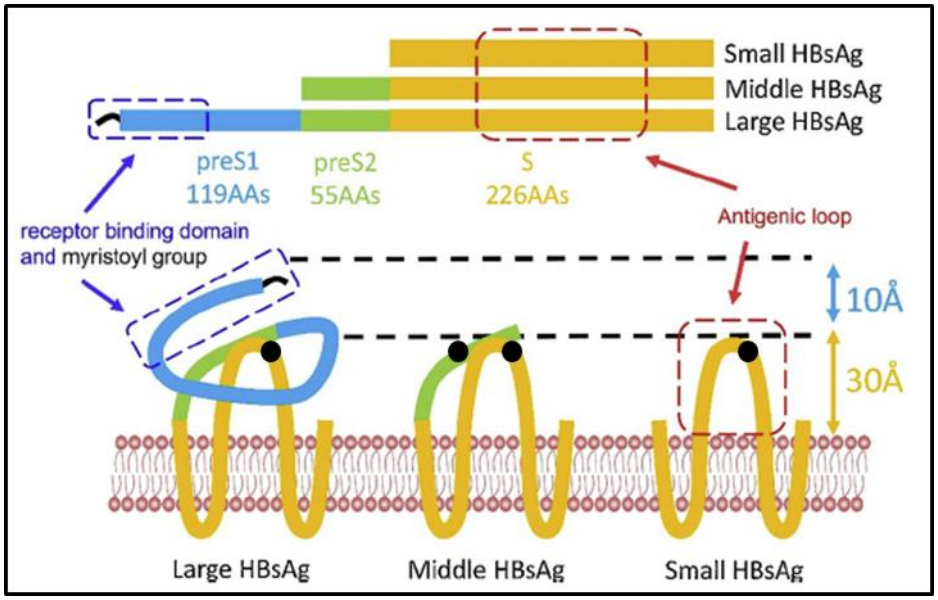


Figure 5. Illustration of the transmembrane domains present in small, middle and large hepatitis B surface antigen

The red dotted line indicates the "a" determinant. The black dotted line indicates the myristoyl group at the amino-terminus of the large hepatitis B surface antigen. The blue dotted line indicates the PreS1 domain involved in the binding of HBV to the NCTP located on hepatocytes. The small black dots indicate N-linked glycosylation sites; Note that there is a difference in the number of glycosylation sites depending on the genotype. Genotype A and genotype D express one and two glycosylation sites in the PreS2 domain, respectively. Reprinted from Virus Research, Cao *et al.* 2019. Cryo-EM structure of native spherical subviral particles isolated from HBV carriers. Copyright (2019), with permission from Elsevier.

HBsAg is extensively observed and measured as a principal marker of HBV infection [86, 87], as research shows that HBsAg concentrations can be correlated to viral loads [88].

When quantified, HBsAg has important clinical significance in that it allows for the distinction between acute and chronic infections, as well as the monitoring of disease progression and treatment response [62]. Unfortunately, the efficacy of this technique is diminished by the presence of HBsAg mutations, which produce false-negatives and allow mutant variants to develop unnoticed [89]. HBsAg quantitative assays contain antibodies specific to the S domain "a" determinant epitope [62], resulting in the collective targeting of all three forms of HBsAg [88]. Since S-HBs is the primary constituent of the viral envelope and is secreted in high amounts from infected hepatocytes [62, 90], it plays an essential diagnostic role in the detection of HBV [89]. However, it is important to differentiate between the different types of HBsAg, as S-HBs, M-HBs and L-HBs each contribute differently to viral propagation.

1.5. HBV Replication Cycle

Following the binding of the virus to the hepatocyte via the NTCP receptor [67] the virion enters the host cell via endocytosis. The viral envelope is removed and the nucleocapsid is actively transported to the nuclear pore, after which the viral DNA is released into the nucleoplasm and converted into cccDNA [24, 91]. The DNA is transcribed and the RNA is translated into proteins. Thereafter, the pgRNA together with the viral polymerase is assembled into the core particle. This is followed by the synthesis of the double-stranded HBV DNA genome through reverse transcription of the pgRNA. The nucleocapsid, consisting of HBcAg and the viral genome is enveloped by the HBsAg proteins and host-derived lipids in the ER, resulting in the formation of the mature virion that is secreted via MVBs [24, 92] (**Figure 6**).

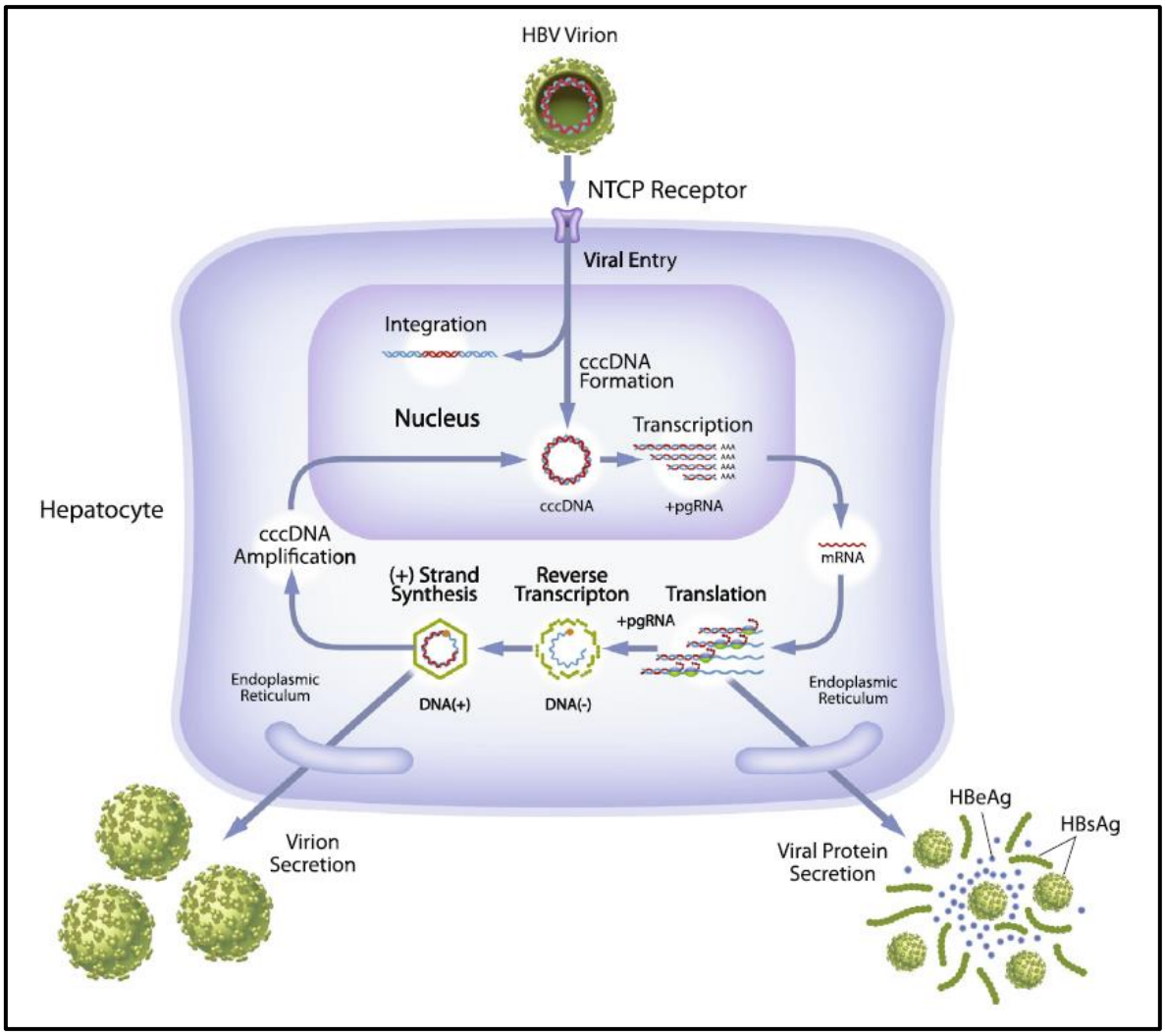


Figure 6. Schematic diagram of the HBV life cycle

Reprinted from Antiviral Research, Gish *et al*. 2015, Chronic hepatitis B: Virology, natural history, current management and a glimpse at future opportunities. Copyright (2015), with permission from Elsevier.

1.6. HBV Genotypes and Subgenotypes

HBV replicates at high rates using a viral polymerase that lacks proofreading ability during reverse transcription [93] and is therefore prone to mutagenesis under the influence of diverse and dynamic selection pressures; this has resulted in the evolution of HBV into a pool of quasispecies, genotypes and mutants [16]. These viral quasispecies possess varying replication fitness in different environments, allowing HBV to adapt to internal and external selection pressures, such as those from the host immune system and medical interventions like antiviral treatments and vaccination - granting HBV a significant survival advantage [36].

High sequence heterogeneity is a feature of HBV, and phylogenetic analysis based on an intergroup divergence of ≥7.5% over the complete genome and ≥4% over the *S* gene, has led to the division of HBV into nine genotypes, designated upper cases letters A-I and a putative tenth genotype, designated J [94, 95]. These different genotypes have a distinct geographical distribution (**Figure 7**). Sequence variability of between 4% and 7.5% over the complete genome and a high phylogenetic bootstrap support allows HBV genotypes to be further classified into subgenotypes, with distinct geographical distributions [94, 95]. Genotypes A, B, C, D and F can be divided into at least 35 subgenotypes [95, 96]. Clinical evidence indicates that HBV genotypes influence liver disease progression and response to antiviral therapy, with virological characteristics and clinical manifestations even differing among subgenotypes [7, 94].

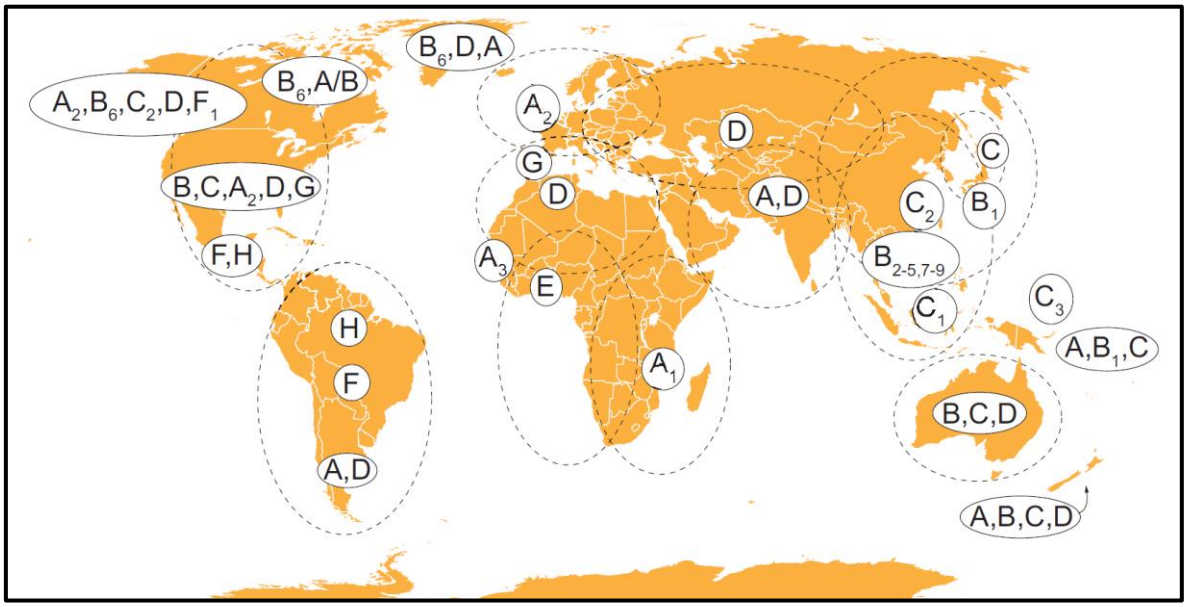


Figure 7. Geographical distribution of hepatitis B virus genotypes and subgenotypes

HBV genotypes have distinct geographical distributions. Genotype I and J are not shown as they have not been confirmed by the International Committee on Taxonomy of Viruses. Reprinted from the Journal of Hepatology, Locarnini *et al.* 2015. Strategies to control hepatitis B: Public policy, epidemiology, vaccine and drugs. Copyright (2015), with permission from Elsevier.

1.6.1. Genotype A

Genotype A is the predominant strain found in Africa, prevailing in central, eastern and southern Africa – whereas genotype D dominates in northern Africa and genotype E is common in western Africa. In regions where at least two genotypes circulate, co-infection has been reported [7]

1.6.1.1. Subgenotypes A1 and A2

The bulk of research relating to the clinical outcomes of HBV genotype in Africa has been conducted on genotype A, with the majority of African genotype A strains sequenced having been found to be subgenotype A1, which is mostly found in eastern and southern Africa, including South Africa [7]. Subgenotype A2 is the predominant genotype A strain circulating within Europe, but has also been detected in South Africans [7]. A study on southern African patients found that the mean age of infection was 6.5 years younger in those infected with genotype A compared to a non-A genotype. Those infected with subgenotype A1 are less frequently HBeAg positive, possess an increased chance of early seroconversion of HBeAg to antibodies against HBeAg [97], and have significantly lower levels of HBV DNA compared to those infected with subgenotype A2 or genotype D [98]. A 2005 study, in southern African patients with HCC or asymptomatic carriage, showed that subgenotype A1 exhibited a higher hepatocarcinogenic potential compared to subgenotype A2 and genotype D [99]. Compared to genotype D, infection with subgenotype A1 has also been found to cause elevated levels of liver inflammation as well as higher expression of apoptosis biomarkers in HBV-infected HCC patients [100].

In vitro characterisation of subgenotype A1 demonstrated decreased replication levels compared to A2 [101], as well intracellular accumulation of replicative intermediates and HBcAg, possibly contributing to liver necroinflammation [102]. This may play a role in the development of HCC, where Huh7 cells transfected with subgenotype A1 exhibit higher levels of ER stress and prolonged activation of the unfolded protein response compared to Huh7 cells transfected with subgenotype A2 or D3 [103].

1.6.2. Genotype D and Subgenotype D3

Genotype D is widely distributed throughout Northern Asia and Northern Africa, as well as parts of Europe and the United States. This genotype is associated with early seroconversion, a higher incidence of inactive carrier patients, as well as severe liver disease and HCC in younger patients, when compared to genotype A [104]. Patients infected with subgenotype D3 have shown evidence of persistent HBV infection, as well as low levels of HBV DNA and HBsAg [105].

1.6.3. The Role of HBsAg and HBeAg in Different Genotypes and Subgenotypes

Virological differences in HBV antigen expression intracellularly and extracellularly between genotypes have been documented both *in vitro* and *in vivo*. Studies also show that HBV antigens vary in their subcellular localisation between different genotypes; HBeAg [103] and HBcAg has been found in the cytoplasm, nuclear [106] and membrane compartments of the cell; HBsAg is generally found within the ER or Golgi compartments, with some studies showing expression of HBsAg within the cytoplasm, although this appears to be frequently associated with chronic HBV infection [84, 107-109]. Increased localisation of HBV antigens within the perinuclear space seems to indicate accumulation of antigens within the ER [87, 103], often resulting in ER stress, apoptosis and an increased risk of hepatocarcinogenesis [83, 84, 103, 109].

Sugiyama and colleagues observed higher extracellular HBsAg expression in subgenotype A2 compared to subgenotype A1 and genotype D, which expressed the lowest. However, they found that genotype D not only expressed extracellular HBeAg the highest, but also induced higher levels of ER stress [102]. A different study by Hassemer *et al.* found that genotype D HBsAg expression is higher than genotype A expression both intracellularly and extracellularly [87]. Additionally, M-HBs and L-HBs were expressed in higher proportions intracellularly versus extracellularly, with L-HBs generally existing in higher proportion to M-HBs.

An investigation conducted using the same replication competent plasmids used in the present study found that, when compared to genotype A, D3 replicated at low levels, evidenced by low HBsAg and HBV DNA expression. Subgenotype A1 expressed HBV DNA, HBeAg and HBsAg the highest when compared to subgenotypes A2 and D3. Research surrounding the virological differences between genotypes A and D is sparse and conflicting [87, 101, 102].

1.7. Rationale

Changes in HBsAg expression are shown to influence detection, viral pathogenicity and disease progression [44, 110]. Differences in the mode of expression of HBsAg may account for their differences in hepatocarcinogenic potential.

1.8. Aims and Objectives

The aim of this study was to compare the expression, subcellular localization and release of the S-HBs, M-HBs and L-HBs and their relative ratios *in vitro* for subgenotypes A1, A2 and D3, circulating in South Africa.

Following transfection of Huh7 cells with replication competent plasmids for subgenotypes A1, A2 or D3, the objectives of the study were to:

(1) Optimise subcellular fractionation and polyethylene glycol (PEG) precipitation methods used in the study for the detection of intracellular and extracellular HBsAg respectively
(2) Determine the intracellular expression of L-HBs, M-HBs, S-HBs in the nucleus, cytoplasm and membrane of the cell
(3) Determine the extracellular expression of HBV proteins L-HBs, M-HBs, S-HBs, and HBeAg

CHAPTER 2: MATERIALS AND METHODS

2.1. Ethics

An ethics waiver was obtained for the study from the University of the Witwatersrand Human Research Ethics Committee (Medical), Johannesburg, South Africa (Clearance Certificate Number: W-CJ-170308-2) (Appendix I: **Figure 31**, p91).

2.2. Materials

The following materials were used during this study:

(1) The following replication competent plasmids containing full-length HBV DNA were used in this study, provided by Dr. Nimisha Bhoola, Hepatitis Virus Diversity Research Unit, Department of Internal Medicine, School of Clinical Medicine, Faculty of Health Sciences, University of the Witwatersrand, Johannesburg, South Africa:
   (i) Wild-type subgenotype A1 1.28 mer plasmid (A1-WT)
   (ii) Wild-type subgenotype A2 1.28 mer plasmid (A2-WT)
   (iii) Wild-type subgenotype D3 1.28 mer plasmid (D3-WT)

(2) The following control plasmids used in this study were kindly donated by Professor Hans Will, Heinrich-Pette Institute for Experimental Virology and Immunology, University of Hamburg, Germany:
   (i) Wild-type subgenotype D3 1.28 mer replication competent plasmid containing a cytomegalovirus (CMV) promoter (D3-WT (CMV+)
   (ii) Plasmid expressing the GFP reporter gene (eGFP)
   (iii) Plasmid expressing the pCDNA™4/TO mammalian expression vector only (Invitrogen by Life Technologies Corporation, Thermo Fisher Scientific, Waltham, Massachusetts, USA).

(3) Human hepatocellular carcinoma (Huh7) cells were kindly donated by Prof. Charles M Rice, Centre for the Study of Hepatitis C, The Rockefeller University, New York, NY, USA.

(4) Subcellular Protein Fractionation Kit for Cultured Cells (Pierce Biotechnology, Thermo Fisher Scientific).

(5) Primary and secondary antibodies used in this study are listed in **Table 1** below. The mouse monoclonal antibody against the S region of HBsAg (mAbHB1) was kindly

donated by Dr. Dieter Glebe, Justus-Liebig University, Giessen, Germany). All secondary antibodies are conjugated to horseradish peroxidase (HRP) and recognise immunoglobulin G (IgG) heavy and light (H+L) chains.

(6) Murex HBsAg Version 3 (Diasorin S. p. A., Saluggia, Italy)

(7) ETI-EBK PLUS (Diasorin)

Table 1. Antibody information

Antibody	Proprietary Name	Target	Size of Target	Antibody Dilution	Supplier
Primary rat monoclonal anti-Hsp90 antibody	Anti-Hsp90 antibody [16F1]	Heat shock protein 90 (Hsp90) (cytoplasmic fraction)	90 kDa	1:100000	Abcam* (ab13494)
Primary rabbit monoclonal anti-Calreticulin antibody	Anti-Calreticulin antibody [EPR3924]	Endoplasmic reticulum (membrane fraction)	48 kDa	1:100000	Abcam (ab92516)
Primary mouse monoclonal anti-Nuclear Matrix Protein p84	Anti-Nuclear Matrix Protein p84 antibody [5E10]	Nuclear Matrix Protein p84 (soluble-nuclear fraction)	90 kDa	1:10000	Abcam (ab487)
Primary mouse monoclonal anti-Histone H3 antibody	Anti-Histone H3 antibody [1B1B2] - ChIP Grade	Histone H3 (chromatin-bound nuclear fraction)	15 kDa	1:100000	Abcam (ab195277)
Primary mouse monoclonal anti-Cytokeratin 18 antibody	Anti-Cytokeratin 18 antibody [CK-18]	Cytokeratin-18 (cytoskeletal fraction)	48 kDa	1:100000	Abcam (ab82254)
Primary mouse monoclonal anti-HBsAg antibody	Mouse monoclonal antibody against the S region of HBsAg (mAbHB1)	L-HBs, M-HBs and S-HBs	42 kDa, 36 kDa and 25 kDa	1:5000	-
Primary rabbit polyclonal anti-GFP antibody	Anti-GFP antibody	Green fluorescent protein (GFP)	27 kDa	1:25000	Abcam (ab6556)
Secondary goat anti-mouse antibody	Goat anti-mouse IgG (H+L)-(HRP) conjugate	Mouse primary antibody	-	1:5000	Bio-Rad**
Secondary goat anti-rabbit antibody	Goat anti-rabbit IgG (H+L)-HRP conjugate	Rabbit primary antibody	-	1:5000	Bio-Rad
Secondary goat anti-rat antibody	Goat anti-rat IgG (H+L)-HRP conjugate	Rat primary antibody	-	1:5000	Abcam (ab97057)

*Abcam plc., Cambridge, Massachusetts, USA **Bio-Rad Laboratories, Hercules, California, USA

2.3. Methodology

Figure 8 provides an overview of the flow of the methodology used in this study. 1.28 mer replication competent plasmids for subgenotypes A1, A2 and D3, previously shown to express HBV DNA and proteins [101], were used in this study. Plasmid DNA was extracted on a large scale and transiently transfected into cultured Huh7 cells. These cells were harvested and subcellularly fractionated to determine the intracellular expression of HBsAg using Western blotting. Extracellular expression of HBsAg was determined using an enzyme-linked immunosorbent assay (ELISA) and polyethylene (PEG) precipitation of supernatants and analysed using Western blotting. Extracellular expression of HBeAg was determined using ELISA.

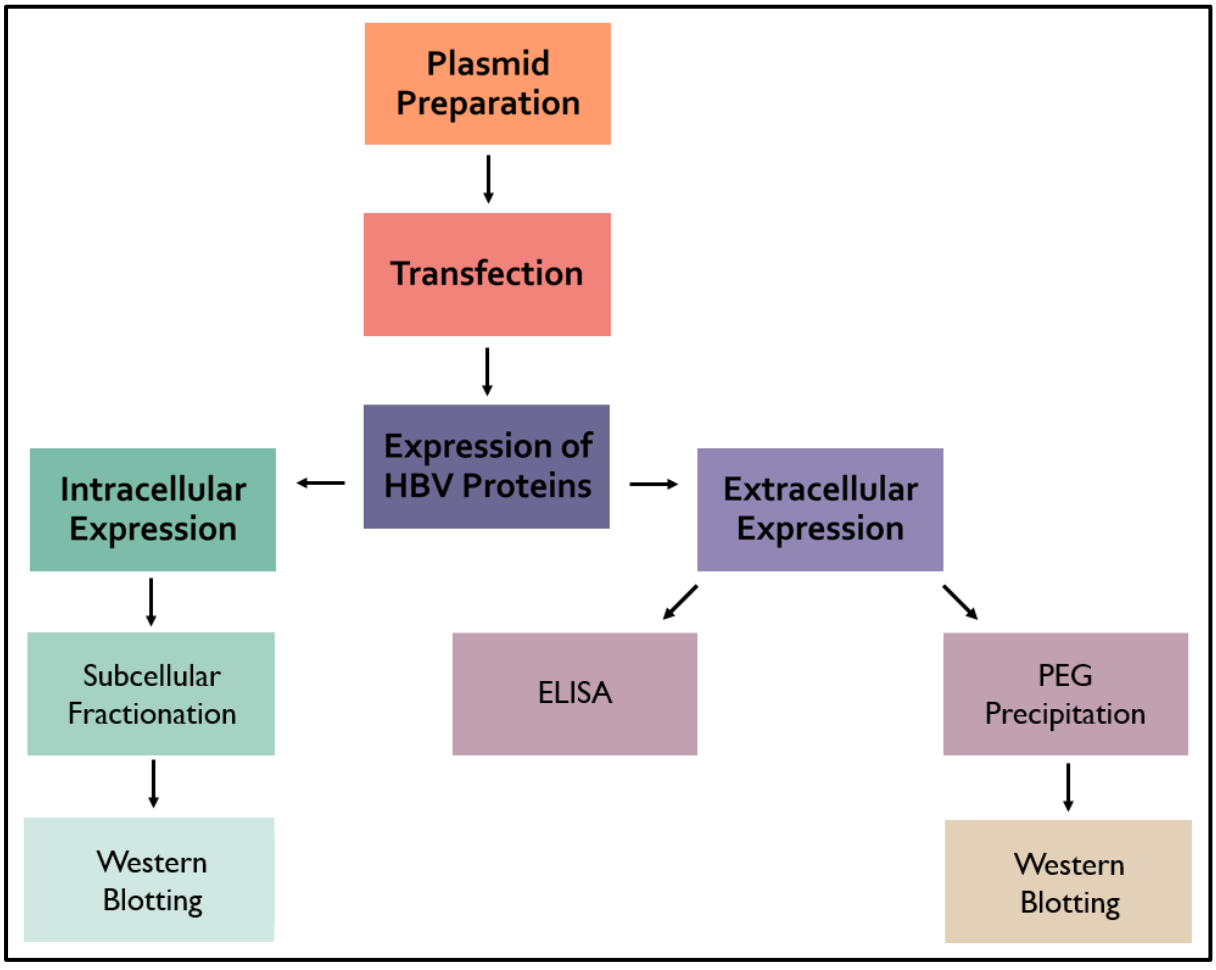


Figure 8. Flow diagram illustrating an overview of the methodology in this study

2.3.1. Plasmid Preparation

Figure 9 illustrates the methods used to prepare the 1.28 mer replication competent plasmids for transfections. Plasmid DNA was extracted from cultured *Escherichia coli (E. coli)* cells transformed with either one of the following: subgenotype A1, A2, D3, D3 (CMV+) replication competent plasmids, eGFP-expressing plasmid or pCDNA™4/TO-expressing plasmid. Restriction digestion was performed to confirm the size and orientation of the HBV DNA and sequencing done to confirm integrity of the HBV DNA.

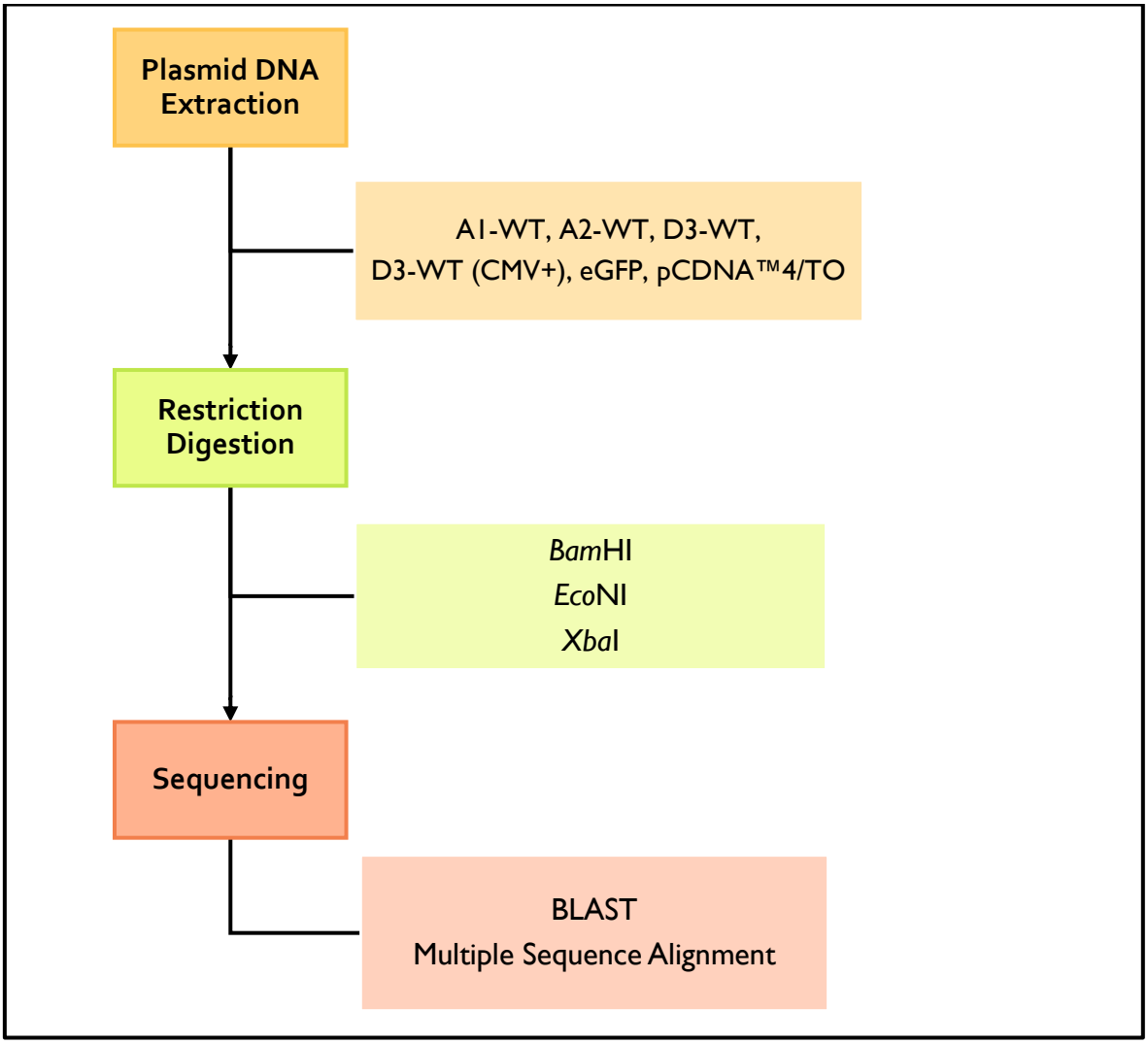


Figure 9. Flow diagram illustrating the methods used for preparation of 1.28 mer replication competent HBV plasmids

2.3.1.1. Plasmid DNA Extraction

2.3.1.1.1. Growth of bacterial colonies

A 2 µl glycerol stock aliquot, containing One Shot® TOP10 chemically competent *E. coli* cells (Invitrogen) transformed with either one of the various 1.28 mer HBV DNA replication competent plasmids or the control plasmids, was streaked on a 2X Yeast extract and Tryptone (YT) agar plate (Appendix IV, A9 and A10, p98), supplemented with 100 mg/ml ampicillin (Appendix IV, A2, p96) or 50 mg/ml kanamycin (Appendix IV, A3, p96), and incubated at 37 °C overnight. Except for the kanamycin-resistant eGFP control plasmid, all plasmids used were ampicillin-resistant. Agar plates supplemented with either antibiotic ensured bacterial cultures resistant to either antibiotic would only grow under antibiotic selection. For the negative control, 2X YT agar plates containing either 100 mg/ml ampicillin or 50 mg/ml kanamycin were incubated overnight at 37 °C without glycerol stock.

2.3.1.1.2. Small-scale inoculation of medium

A colony for each of the experimental and control plasmids was inoculated in 5 ml 2X YT medium (Appendix IV, A11, p98) supplemented with either 5 µl 100 mg/ml ampicillin or 50 mg/ml kanamycin and allowed to incubate at 37 °C for 8 hours while shaking constantly at 200 rpm. The negative control included 5 ml 2X YT medium supplemented with either 5 µl 100 mg/ml ampicillin or 50 mg/ml kanamycin and allowed to incubate in the absence of a bacterial colony.

2.3.1.1.3. Large-scale inoculation of medium

A 3 ml aliquot of the bacterial culture was inoculated into 300 ml Luria-Bertani (LB) medium (Appendix IV, A4, p96) supplemented with either 300 µl 100 mg/ml ampicillin or 50 mg/ml kanamycin, incubated at 37 °C for 16 hours and shaking constantly at 200 rpm. The negative control included 10 ml LB medium supplemented with either 10 µl 100 mg/ml ampicillin or 50 mg/ml kanamycin, incubated in the absence of bacterial inoculation.

2.3.1.1.4. Plasmid DNA extraction

Purified plasmid DNA was prepared on a large-scale using the Plasmid DNA Purification NucleoBond® Xtra Maxi EF (Macherey-Nagel GmbH & Co. KG, Düren,

Germany) plasmid DNA extraction kit, following the manufacturer's protocol with a modification in the dehydration step.

Bacterial cells were harvested from the LB culture by centrifugation at 6000 x g for 15 min at 4 °C using an Eppendorf 5804 R refrigerated centrifuge (Eppendorf, Barkhausenweg, Hamburg), and the supernatant discarded. The bacterial pellet was resuspended in 12 ml Resuspension Buffer RES-EF containing RNase A (Appendix IV, A8, p97) and pipetted up and down until there were no visible clumps. The suspension was mixed with 12 ml Lysis Buffer LYS-EF by gently inverting the tube five times and incubated at room temperature for 5 min. A NucleoBond® Xtra Column Filter placed within the NucleoBond® Xtra Column was set over a 500 ml conical flask, equilibrated with 35 ml Equilibration Buffer EQU-EF and allowed to empty by gravity flow.

The lysed bacterial suspension was then neutralised with the addition of 12 ml Neutralisation Buffer NEU-EF and the tube inverted gently until the crude lysate became a colourless and low-viscosity homogenate, followed by incubation on ice for 5 min. To ensure a homogenous suspension, the tube was inverted three times before the lysate was poured into the prepared filter, which simultaneously cleared and loaded the lysate onto the surrounding column while being allowed to drain by gravity flow. The filter and column were washed with 10 ml Filter Wash Buffer FIL-EF and emptied by gravity flow, after which the filter was discarded. Next, the column was washed with 90 ml Wash Buffer ENDO-EF, allowed to empty, and finally washed with 45 ml Wash Buffer WASH-EF, emptied by gravity flow and the flow-through discarded.

Plasmid DNA was collected into a clean 50 ml polypropylene tube by eluting the column with 15 ml Elution Buffer ELU-EF, the column allowed to drain by gravity flow and subsequently discarded. The eluted plasmid DNA was precipitated via the addition of 10.5 ml 100% (v/v) isopropanol (Saarchem (Pty) Ltd. By Merck Chemicals & Laboratory Supplies (Pty) Ltd., Wadeville, Gauteng, South Africa), the suspension thoroughly vortexed and centrifuged at 15000 x g for 30 min at 4 °C, and the supernatant discarded. The resulting pellet was dehydrated by briefly vortexing with 5 ml endotoxin-free 70% (v/v) ethanol (EtOH) and centrifuged at 15000 x g for 5 min at room temperature, after which the supernatant was gently removed, and the pellet

allowed to dry overnight at room temperature. The dried DNA pellet was then reconstituted in 300 µl 10 mM tris(hydroxymethyl)aminomethane (Tris) pH 7.5 (Appendix IV, A5, p97) incubated at 37 °C for 30 min while shaking at 200 rpm. Dissolved plasmid DNA was transferred to a sterile 1.5 ml microcentrifuge tube and incubated at 37 °C for 30 min while shaking vigorously at 600 rpm to ensure complete homogenization of the suspension, following which the plasmid DNA was stored at -20 °C until used.

The yield and purity of the extracted plasmid DNA was determined by UV spectrophotometry using a NanoDrop 1000 UV/VIS Microvolume Spectrophotometer and analysed using the Nanodrop 1000 UV/VIS version 3.7 software (Thermo Fisher Scientific), by determining the optical density at an absorbance of 260 and 280 nm. Plasmid DNA with an A_{260}/A_{280} ratio of ≥ 1.8 was considered pure DNA. Agarose gel electrophoresis was used to determine the integrity of the extracted plasmid DNA (for a detailed protocol, please refer to Appendix III, A, p94).

2.3.1.2. Restriction Digestion

2.3.1.2.1. Restriction digestion of plasmid DNA

To confirm the size and orientation of the extracted HBV DNA, single digests were performed using *Bam*HI, *Eco*NI and *Xba*I restriction enzymes (Fermentas Molecular Biology Tools, Thermo Fisher Scientific). **Table 2** summarises the reaction conditions used in this protocol. Restriction digestion reaction tubes were briefly vortexed and centrifuged, then incubated at 37 °C for 3 hours. The reaction was stopped by addition of 3 µl Blue/Orange 6X Loading Dye (Promega Corporation, Madison, Wisconsin, USA). The size and orientation of the 1.28 mer HBV DNA was confirmed using agarose gel electrophoresis (please refer to Appendix III, A, p94).

Table 2. Restriction digestion reaction set-up used to confirm size and orientation of HBV DNA

Concentration	Reagent	Volume (µl)		
		Restriction Digestion Reaction		
	Nuclease-Free Water	7.0	7.0	7.0
10 X	Buffer *Bam*HI	1.0	-	-
10 X	Buffer R	-	1.0	-
10 X	Buffer Tango	-	-	1.0
10 U/µl	Restriction Enzyme: *Bam*HI	1.0	-	-
10 U/µl	Restriction Enzyme: *Eco*NI	-	1.0	-
10 U/µl	Restriction Enzyme: *Xba*I	-	-	1.0
1 µg	Plasmid DNA	1.0	1.0	1.0

Nuclease-free water and restriction enzyme buffers were purchased from Thermo Fisher Scientific.

2.3.1.2.2. Expected results

Table 3 summarises the expected results of each restriction digestion reaction for the 1.28 mer HBV DNA replication competent plasmids containing wild-type HBV subgenotype either A1, A2 or D3.

Table 3. Expected fragment sizes following restriction digestion of 1.28 mer HBV plasmid DNA

Restriction Enzyme	Restriction Enzyme Recognition Site	Restriction Enzyme Recognition Site Positions			Fragment Sites (bp)		
		Subgenotype					
		A1	A2	D3	A1	A2	D3
*Bam*HI	HBV	488	28	488	8235	1372 1850 5013	806 912 1504 5013
			1400	1400			
				2904			
	pCDNA™4/TO	-	-	-			
*Eco*NI	HBV	537	536	536	881 1104 1238 5012	881 1104 1238 5012	8195
		1641	1640				
		2879	2878				
	pCDNA™4/TO	-	-	-			
*Xba*I	HBV	247	246	247	786 1644 5805	2430 5805	151 951 1328 5805
		2684		1990			
				2140			
	pCDNA™4/TO	1059	1059	1059			

2.3.1.3. Sequencing and Bioinformatics

2.3.1.3.1. Sequencing

Sequencing of the purified plasmid DNA was done by the Central DNA Sequencing Facility, University of Stellenbosch (Stellenbosch, Western Cape, South Africa) to confirm the presence and orientation of the 1.28 mer HBV in the plasmid DNA. **Table 4** shows the primers that were used for sequencing.

Table 4. Sequencing primers (700 bp) used to confirm the presence and orientation of HBV DNA within each plasmid

Primer Name	Primer Sequence	Vector or HBV Primer	Primer Binding Site	Region Covered of HBV	Size of Sequencing Fragment (bp)
Post-*Bgl*II	5'-CCG ATA CAG AGC TGA GGC-3'	HBV	2036-2042	1298-1998	700
pCR-BGH3.1R	5'-TAG AAG GCA CAG TCG AGC-3'	Vector	1089-1106	1064-1764	700
2497F	5'-TTC CTT GGA CTC ATA AGG TG-3'	HBV	2497-2516	2556-315	700
3188F	5'-AGT CAG GAA GGC AGC CTA C-3'	HBV	3188-3206	3196-275	700
591F	5'-ATT GCA CCT GTA TTC CCA TCC-3'	HBV	591-611	634-1334	700
TO-F	5'-GGT TCC GCG CAC ATT TCC-3'	Vector	5039-5056	1064-1864	700
1040F	5'-TGG TTA CCC TGC CTT AAT GCC TT-'3	HBV	1038 - 1060	1083-1073	700

Table adapted from Bhoola, *et al.,* 2014.

2.3.1.3.2. Bioinformatics analysis

FinchTV version 1.4.0., a free software developed by Geospiza Inc., (downloaded from: https://finchtv.software.informer.com/1.4/), was used to analyse the integrity of the sequences using the DNA chromatogram function. Following automatic sequence alignment using the Nucleotide BLAST sequence analysis tool (available on the NCBI website at: https://blast.ncbi.nlm.nih.gov/Blast.cgi), the sequences were manually aligned and edited using GeneDoc, Multiple Sequence Alignment Editor and Shading Utility version 2.6.002, also freely available. Lastly, all the sequences were aligned using MEGA 7.0.26 (available from: https://www.megasoftware.net/).

2.3.2. Transient Transfection of Huh7 Cells

Figure 10 illustrates an overview of the methods used for transient transfection of Huh7 cells with the various 1.28 mer replication competent plasmids.

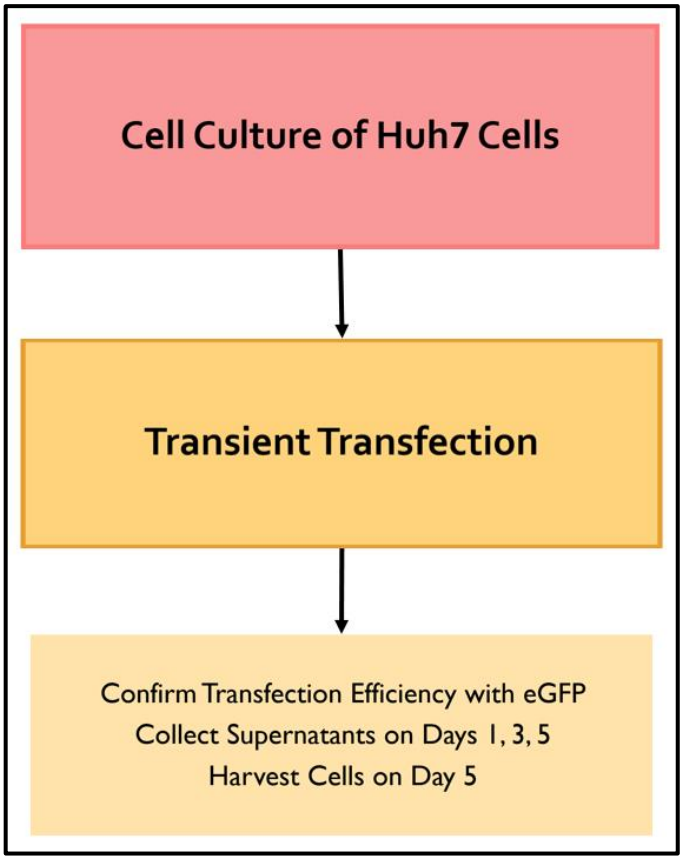


Figure 10. Flow diagram illustrating the methodology established for cell culture and transient transfection of Huh7 cells.

2.3.2.1. Cell Culture of Huh7 Cells

Huh7 cells were cultured in culture flasks containing complete growth Dulbecco's Modified Eagle's Medium (DMEM) (1X) + GlutaMAX (Gibco™ by Life Technologies, Thermo Fisher Scientific) supplemented with 10% (v/v) foetal bovine serum (FBS) (Gibco™), 2% (v/v) Penicillin-Streptomycin (10000 U/ml) (Gibco™) and 1% (v/v) 100X Minimum Essential Medium Non-Essential Amino Acids (MEM NEAA) (Gibco™) (Appendix IV, B1, p98). Cells were maintained in a humidified incubator at 37 °C containing 5% (v/v) CO_2 and passaged upon reaching ~70% confluency by detaching the cells with 0.25% Trypsin-EDTA (1X) (Gibco™) for 5 min, and the reaction stopped by addition of complete growth DMEM. Prior to transient transfection, cells were tested for contamination using the LookOut™ Mycoplasma PCR Detection Kit (Sigma-Aldrich, Merck (Pty) Ltd, St. Louis, USA) (for the detailed mycoplasma detection protocol, please refer to Appendix III, B, p94).

2.3.2.2. Transient Transfection of Huh7 Cells

Twenty-four hours prior to transfection, cultured Huh7 cells at ~70% confluency were counted using a haemocytometer and either 6 x 10^5 cells or 1.2 x 10^6 cells were plated on a either a 6 cm or 10 cm culture dish, respectively, then placed in a humidified incubator at 37 °C containing 5% (v/v) CO_2. The next day, cells were transfected with DNA for either A1-WT 1.28 mer, A2-WT 1.28 mer, D3-WT 1.28 mer, D3-WT (CMV+) 1.28 mer, eGFP or the pCDNA4/TO vector, complexed with 45 µl TransIT®-LT1 Transfection Reagent (Mirus Bio Corporation, Madison, Wisconsin, USA), in triplicate, and allowed to incubate at 37 °C in a humidified incubator containing 5% (v/v) CO_2. Cells in the 6 cm dish and 10 cm dish were transfected with 7.5 µg and 10 µg DNA, respectively.

Supernatants from each sample were collected on days 1, 3 and 5, and replaced with fresh complete growth DMEM on days 1 and 3 post-transfection. Transfection efficiency was estimated day 1 post-transfection by calculating the number of cells that were successfully transfected with eGFP using the FLoid™ Cell Imaging Station (Thermo Fisher Scientific), with fluorescent and brightfield images captured using the FLoid™ Cell Imaging Station Software. Supernatants were aliquoted into 2 ml microcentrifuge tubes and stored at -70 °C for downstream ELISA and polyethylene glycol (PEG) precipitation.

Transiently transfected Huh7 cells were harvested 5 days post-transfection by trypsinization for 5 min at 37 °C in a humidified incubator containing 5% (v/v) CO_2, following which the cell suspension was transferred to a 1.5 ml microcentrifuge tube and centrifuged at 500 x g at 4 °C for 5 min using a Sigma 1-14K refrigerated microcentrifuge (Sigma Laborzentrifugen GmbH, Osterode, Germany). The supernatant was discarded, and the cells were washed with 1 ml ice-cold phosphate buffered saline (PBS) (Appendix IV, B2, p98) at 500 x g at 4 °C for 5 min. The supernatant was carefully discarded to leave the cell pellet as dry as possible and the pellet immediately stored at -70 °C until further used for subcellular fractionation or whole cell lysis.

2.3.3. Expression of HBV Proteins

2.3.3.1. Intracellular Expression of HBV Proteins

Figure 11 illustrates an overview of the methods used to determine the intracellular expression of S-HBs, M-HBs, L-HBs within transiently transfected Huh7 cells.

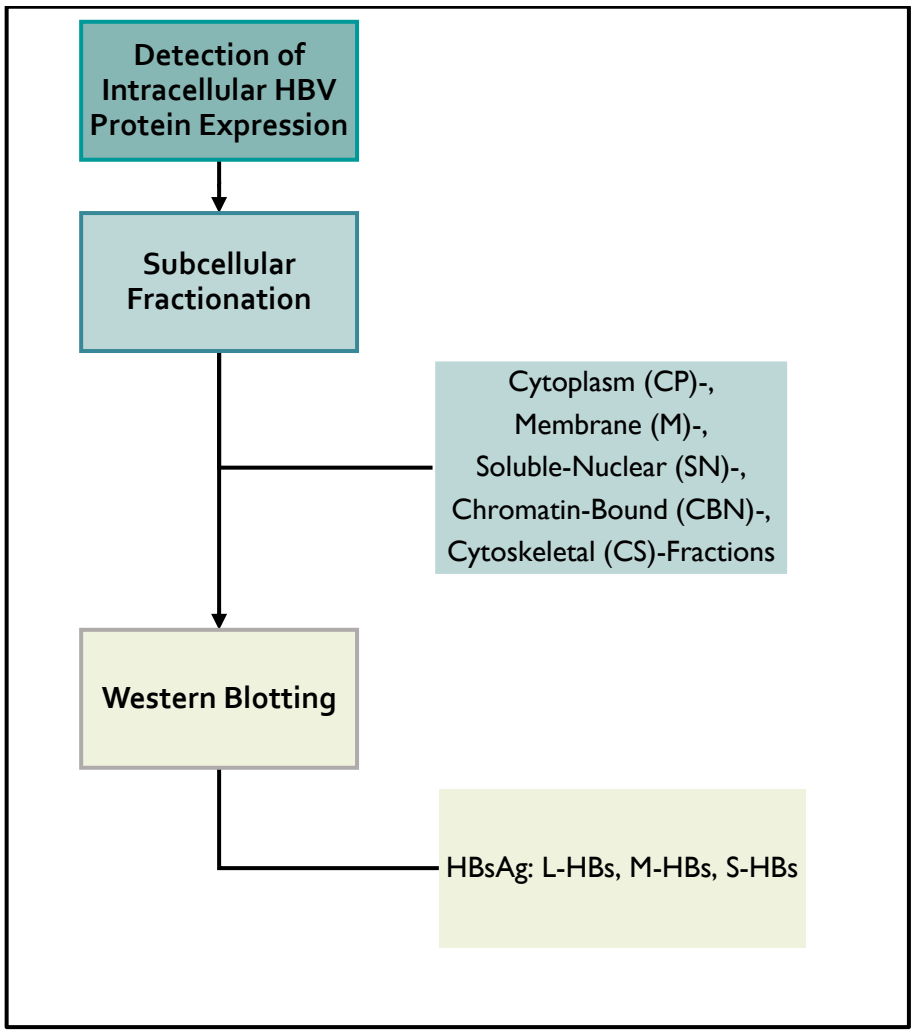


Figure 11. Flow diagram illustrating the methods used to quantify the extracellular expression of HBsAg

2.3.3.1.1. Subcellular Fractionation

Subcellular fractionation was conducted using the Subcellular Protein Fractionation Kit for Cultured Cells (Thermo Fisher Scientific). **Figure 12** provides a summary of the subcellular fractionation protocol used in this study.

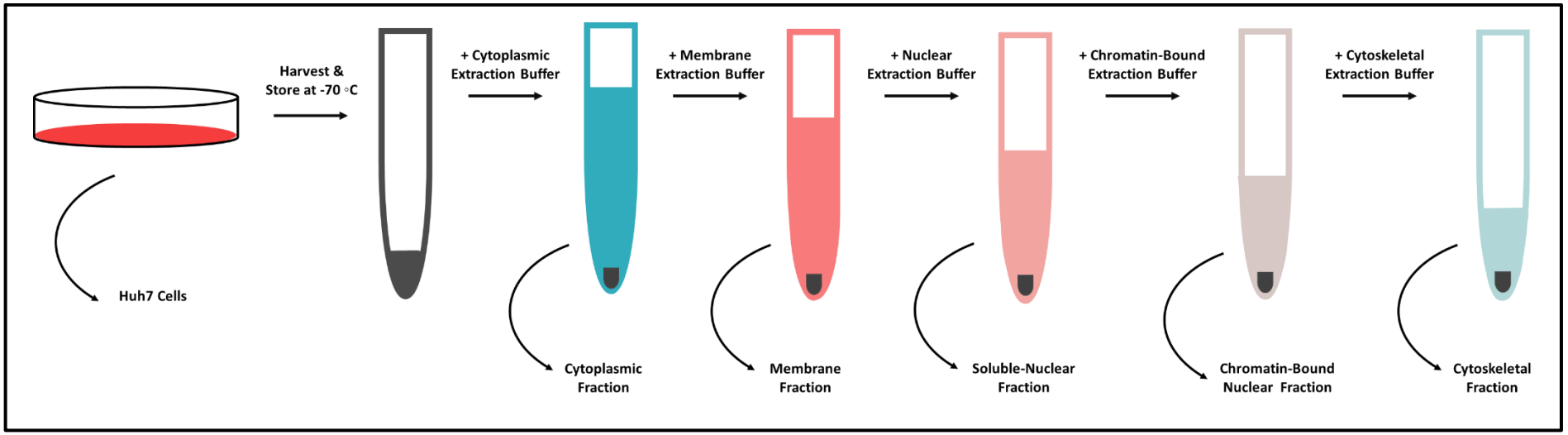


Figure 12. Schematic illustration of subcellular fractionation protocol used in this study

The manufacturer's protocol was modified to achieve optimal purity of the extracted fractions. Buffer volumes were scaled according to the estimated packed cell volume (PCV) of each Huh7 pellet; with the volume of the cytoplasmic (CEB) : membrane (MEB) : nuclear (NEB) : chromatin-bound nuclear (CBEB): pellet (PEB) extraction buffers maintained at a volume of 100 : 100 : 50 : 50 : 50 µl respectively, prepared per 10 µl PCV. All buffers and samples were kept on ice throughout, and all incubations were conducted at 4°C while gently mixing on a horizontal shaker, unless otherwise noted. Samples were vortexed on the highest setting at each vortex step.

Frozen Huh7 pellets were defrosted on ice for 30 min, after which the pellet was initially lysed by gentle resuspension in cold CEB (Appendix IV, C1, p99), selectively permeabilising the cell membrane to release the soluble cytoplasmic contents. The suspension was incubated at 4 °C for 10 min, centrifuged at 500 x g at 4 °C for 5 min and the supernatant containing the cytoplasmic extract (CPE) was immediately collected.

The resulting pellet was gently resuspended in cold MEB (Appendix IV, C2, p99), which solubilises the plasma, mitochondria, ER and Golgi membranes, but does not dissolve the nuclear membrane. The suspension vortexed for 5 seconds and incubated at 4 °C for 10 min, then centrifuged at 3000 x g at 4 °C for 5 min and the membrane extract (ME) collected.

Cold NEB was then gently mixed with the pellet (Appendix IV, C3, p99), lysing pelleted intact nuclei to release the soluble-nuclear extract (SNE) containing nuclear envelope and soluble nucleoplasmic proteins. The suspension was vortexed for 15 seconds and incubated at 4 °C for 30 min, centrifuged at 5000 x g at 4 °C for 5 min and the SNE collected.

The pellet was carefully resuspended in CBEB (Appendix IV, C4, p99), which digests nucleic acids and shears chromatin to release chromatin-bound proteins. The suspension was vortexed for 15 seconds and incubated at room temperature for 15 min without any shaking, then vortexed again for 15 seconds, centrifuged at 16000 x g at 4 °C for 5 min and the chromatin-bound nuclear extract (CBNE) collected.

The remaining insoluble pellet was mixed with room temperature PEB (Appendix IV, C5, p99) which isolates cytoskeletal proteins. The suspension was vortexed for 15 seconds,

incubated at room temperature for 20 min without shaking and centrifuged at 16000 x g at 4 °C for 5 min, followed by collection of the cytoplasmic extract (CPE).

Extracted fractions were mixed with an appropriate volume of 4X Laemmli Buffer (Appendix IV, D5, p101,), heated at 95 °C for 5 min and stored at -20 °C until used for downstream Western blotting analysis. A 50µl aliquot of each fraction was reserved for protein quantification.

2.3.3.1.2. Whole Cell Lysis

Frozen Huh7 pellets were defrosted on ice for 30 min and the cells disrupted by gently flicking the tube. The pellet was resuspended in 100 µl SDS Total Cell Lysis Buffer Working Solution (Appendix IV, C8, p100), briefly vortexed to lyse the cells, and incubated at 99 °C for 5 min. Samples were briefly centrifuged to collect condensation and then sonicated three times for 5 min each using a Eumax Memory Quick Ultrasonic Cleaner (Kwun Wah International Limited, Hong Kong).

Whole cell lysates were mixed with an appropriate volume of 4X Laemmli Buffer (Appendix IV, D4, p36), heated at 95 °C for 5 min and stored at -20 °C until used for downstream Western blotting analysis. A 20 µl aliquot of each lysate was reserved and diluted with 30 µl PBS (Appendix IV, B2, p34) for protein quantification.

2.3.3.1.3. Protein Quantification

Protein concentration of subcellular fractions and whole cell lysates was determined using the Pierce™ BCA Protein Assay Kit (Thermo Fisher Scientific) according to the manufacturer's microplate procedure.

An aliquot of 25 µl of prepared bovine serum albumin (BSA) standards (each at a concentration of 2000-, 1500-, 1000-, 750-, 500-, 250-, 125-, 25-, 0 µg/ml) and 25 µl of each sample of unknown concentration were pipetted on to a 96-well microplate, in duplicate. Two hundred microlitres of BCA working reagent (Appendix IV, C9, p100) was then added to each well and thoroughly mixed on an orbital shaker at 200 rpm for 30 seconds. The plate was then wrapped in aluminium foil and incubated at 37 °C for 30 min, following which the plate was cooled to room temperature for 10 min. The absorbance of the standards and unknown samples were measured at 562 nm using the Thermo

Scientific™ MultiSkan™ FC Microplate Photometer (Thermo Fisher Scientific). The measured absorbance of each BSA standard was plotted against their known concentration to generate a standard curve, allowing for the extrapolation of each unknown sample concentration.

2.3.3.1.4. Western Blotting

Sodium Dodecyl Sulphate Polyacrylamide Gel Electrophoresis to Resolve Subcellular Fractions

A 5 µl aliquot of Precision Plus Protein™ WesternC™ Standards (Bio-Rad) (Appendix V, **Figure 36**, p108) was used as a reference. An aliquot of 10 µg of whole cell lysate or 12 µg of each fraction were loaded on to the prepared 12% (v/v) SDS-PAGE gel (Appendix IV, D10, p101). The electrophoresis module was placed in a Mini-PROTEAN® Tetra Cell System (Bio-Rad) filled with 1X SDS Running Buffer (Appendix IV, D12, p102) and the samples allowed to run through the stacking gel at 80 V for ~30 min. The samples were then separated according to molecular weight while running through the separating gel at 100 V for ~95 min.

Transfer of Proteins from the SDS-PAGE Gel to the Nitrocellulose Membrane

The nitrocellulose membrane, filter paper and sponges were pre-soaked in 1X Wet Transfer Buffer (Appendix IV, D22, p104) prior to assembling the "transfer sandwich". The transfer sandwich was assembled as illustrated in **Figure 13**, from the black side to the clear side of the cassette: sponge, filter paper, gel, nitrocellulose membrane, filter, sponge. Any bubbles between the gel and membrane were removed by gently rolling a glass pipette over the filter paper prior to tightly closing the cassette. The cassette was placed in the Mini Trans-Blot® module (Bio-Rad), with the resolved gel facing the cathode. The transfer module was then placed Mini-PROTEAN® Tetra Cell filled with 1X Wet Transfer Buffer and the transfer conducted at 60 V for 75 min.

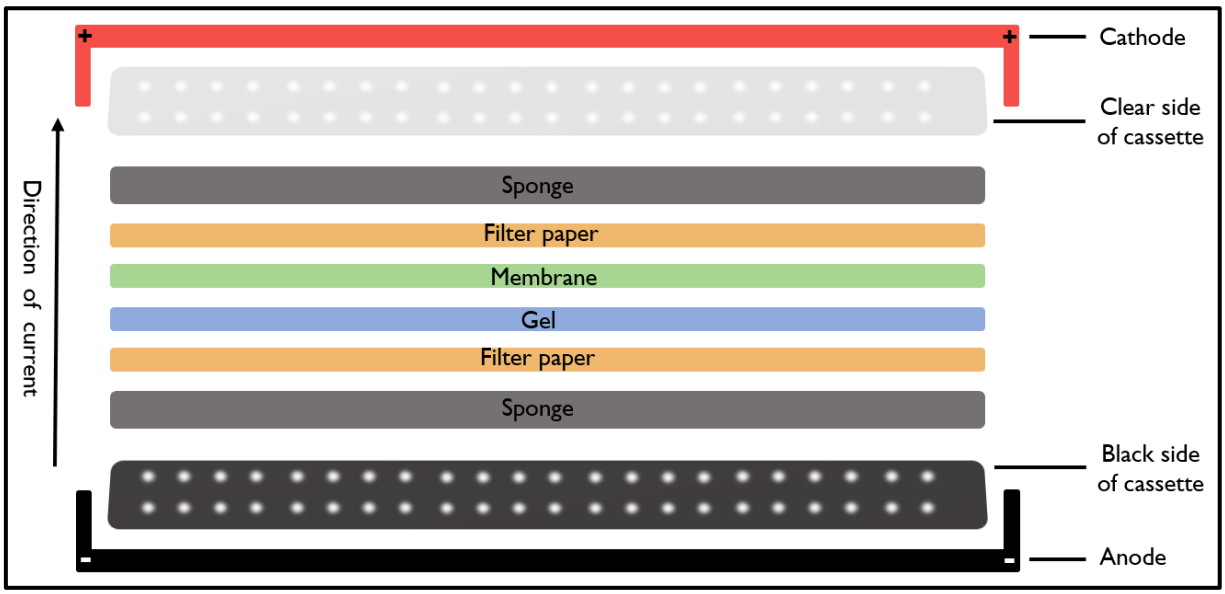


Figure 13. Schematic diagram illustrating the assembly of the Western blot "transfer sandwich"

Efficiency of the transfer was determined by staining the nitrocellulose membrane with 25 ml Ponceau Stain (Appendix IV, D8, p101) for 5 min while shaking continuously, after which the membrane was washed with 50 ml Milli-Q water for 10 min shaking continuously. Colorimetric detection for the successful transfer of proteins was captured using the SYNGENE G:BOX Chemi XRG gel doc system, and GeneSys V1.5.9.0 software for fluorescence and chemiluminescence (SYNGENE, Synoptics Group, Cambridge, UK).

Immunodetection

Following confirmation of successful transfer, the membrane was blocked in 25 ml 5% (w/v) Blocking Buffer (Appendix IV, D3, pD3100) at room temperature for 1 hour while shaking continuously. The membrane was then incubated, overnight at 4 °C while gently shaking in primary antibody (please refer to **Table 1**) diluted in 25 ml Blocking Buffer.

The next day, the primary antibody was removed, and the membrane washed three times with 25 ml TBS-T (Appendix IV, D16, p103) at 10 min for each wash, while shaking continuously. The nitrocellulose membrane was then incubated, at room temperature for 1 hour while gently shaking, with 25 ml Blocking Buffer containing 1:10000 Precision Protein™ StrepTactin-HRP conjugate (Bio-Rad) and the appropriate secondary antibody (please refer to **Table 1**).

Finally, the membrane was washed with TBS-T for 10 min, three times and 600 µl SuperSignal® West Dura Extended Duration Substrate working solution (Appendix IV, D13, p102) was added dropwise across the membrane to develop the protein signal of interest. The membrane was placed between two overhead projector sheets and enhanced chemiluminescent detection of bound proteins was captured with the SYNGENE G:BOX Chemi XRG gel doc system, and GeneSys software.

Intoxication of Nitrocellulose Membrane

Following successful detection of the proteins of interest, HRP conjugated to the secondary antibody was quenched in 25 ml Stripping Buffer (Appendix IV, D14, p102) at room temperature for 1 hour, and washed with TBS-T for 10 min, three times. The stripped membrane was either re-probed with a new primary antibody or stored at 4 °C in TBS-T.

Western Blot Quantification

Western blot densitometry was conducted using Image Studio Lite version 5.2, a freely available software designed by LI-COR for Western blot quantification and analysis (available from: https://www.licor.com/bio/products/software/image_studio_lite/).

2.3.3.2. Extracellular Expression of HBsAg and HBeAg

Figure 14 illustrates the methods used to determine the expression and quantification of extracellular HBsAg and HBeAg expression, using Western blotting and ELISA, respectively.

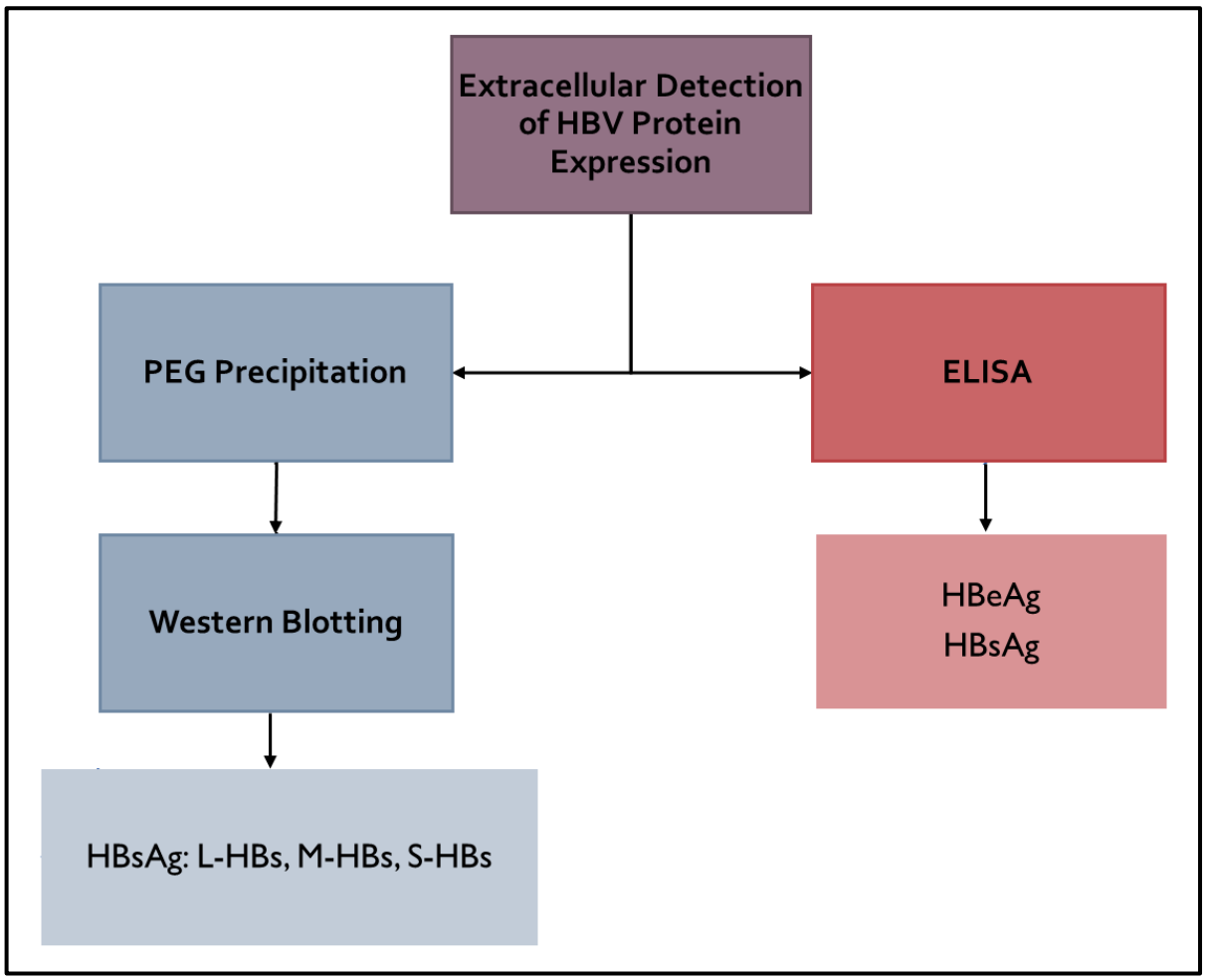


Figure 14. Flow diagram illustrating the methodology employed to quantify extracellular expression of HBsAg and HBeAg.

2.3.3.2.1. Enzyme-Linked Immunosorbent Assay (ELISA)

HBeAg ELISA

The ETI-EBK PLUS HBeAg ELISA kit provides a direct, non-competitive "sandwich" immunoassay that involves the capture of HBeAg between antibodies; i.e., the formation of an antibody-antigen-antibody complex. Microwells precoated with multiple mouse monoclonal antibodies bind to analyte containing HBeAg, and an HRP-conjugated enzyme tracer also containing mouse monoclonal HBeAg antibody allows for the detection of captured HBeAg.

Cell culture supernatants previously stored at -70 °C were thawed on ice until fluid and diluted 1:100 with DMEM (1X) + GlutaMax™. The contents of the kit were brought to room temperature prior to use. No reagents were dispensed into the blank well until addition of the chromogen, and reagents were consistently dispensed in the same order and at the

same pace. **Figure 38** (Appendix VI, p110) illustrates the manufacturer's recommended plate layout used in this protocol.

A 50 µl aliquot of Incubation Buffer was added to all wells, followed by addition of 100 µl either Calibrator, Control, or sample into designated wells. The Calibrator, which contains human sera non-reactive for HBeAg, was added in triplicate. The Negative and Positive controls – containing human sera non-reactive for HBeAg or sera containing recombinant HBeAg expressed in *E. coli,* respectively – were loaded in singlicate. Samples were loaded in duplicate. The plate was covered in a protective bag to prevent evaporation, gently tapped to release any bubbles trapped in the reaction wells and incubated at 37 °C for 2 hours.

Using the Thermo Scientific™ Wellwash™ Microplate Washer (Thermo Fisher Scientific), the liquid was aspirated, and each well rinsed with 300 µl Wash Buffer (Appendix IV, E7, p105). This was repeated four times with a 30 second soak period between each cycle to remove excess sample. After completion of this wash step, the plate was inverted and gently tapped to ensure removal of residual Wash Buffer. Immediately, 100 µl Working Enzyme Tracer Solution (Appendix IV, E9, p105) was added to each well, the plate covered and gently tapped, and samples incubated at 37 °C for 1 hour.

The wash step was repeated as described above to remove excess enzyme tracer. A 100 µl aliquot of Chromogen/Substrate, which reacts with bound HRP, was dispensed into all wells, including the blank. The plate was covered, placed in a dark area and incubated at room temperature for 30 min. One hundred microliters Stop Solution was added to each well and the absorbance measured at 450/630 nm within 1 hour. The Stop Solution contains sulphuric acid, which potently inactivates HRP by lowering the pH of the reaction and preventing any further chromogenic development. Samples non-reactive for HBeAg remained colourless, while samples positive for HBeAg appear blue prior addition of the Stop Solution, and yellow after.

<u>HBsAg ELISA</u>

The Murex HBsAg Version 3 ELISA kit is a direct, non-competitive assay which utilises mouse monoclonal capture antibodies containing specific for different epitopes on the "a" determinant of HBsAg. Microwells precoated with multiple mouse monoclonal antibodies

bind to analyte containing HBsAg, and an HRP-conjugated enzyme tracer containing goat anti-HBsAg allows for the detection of captured HBsAg.

Cell culture supernatants previously stored at -70 °C were thawed on ice until fluid and diluted 1:100 with DMEM (1X) + GlutaMax™. The contents of the kit were brought to room temperature prior to use. **Figure 39** (Appendix VI, p111) illustrates the manufacturer's recommended plate layout used in this protocol.

A 25 µl aliquot of Sample Diluent was added to each well, followed by 75 µl of sample. The Negative Control, containing human sera non-reactive for HBsAg, was added in duplicate as 75 µl aliquots. The Positive Control, containing human sera reactive for HBsAg, was added in a single 75 µl aliquot. The plate was covered an incubated at 37 °C for 1 hour.

Fifty microliters Conjugate, containing HRP-conjugated goat anti-HBsAg, was added to each well and the plate gently tapped to mix the reagents prior to incubation at 37 °C for 30 min. Using the Thermo Scientific™ Wellwash™ Microplate Washer, the liquid was aspirated, and each well rinsed with 500 µl Wash Fluid (Appendix IV, E8, p105). This was repeated four times with a 30 second soak period between each cycle to remove excess sample. After completion of this wash step, the plate was inverted and gently tapped to ensure removal of residual Wash Fluid. Immediately, 100 µl Substrate Solution (Appendix IV, E6, p105) was added to each well, the plate covered and gently tapped, and samples incubated at 37 °C for 30 min.

Fifty microliters Stop Solution was added to each well and the absorbance measured at 450/630 nm within 15 min. Samples non-reactive for HBsAg remained pink, while samples positive for HBsAg appeared purple prior to the addition of the Stop Solution, and orange thereafter.

2.3.3.2.2. Polyethylene Glycol (PEG) Precipitation

This protocol was developed and optimised to achieve highly concentrated viral protein precipitates which provide distinct bands and low background when analysed using Western blotting.

Cell culture supernatants previously stored at -70 °C were thawed on ice until fluid. A 1.875 ml aliquot 37% (w/v) PEG 8000 solution (Appendix IV, E4, p104) was added per 6 ml supernatant in a 15 ml polypropylene tube, vortexed briefly, and gently mixed at 4 °C overnight on a horizontal shaker.

The following day, samples were aliquoted into 2 ml microcentrifuge tubes and centrifuged at 18000 x g at 4 °C for 1 hour using a Sigma 1-14K refrigerated microcentrifuge. The supernatant was carefully discarded, and the translucent pellet thoroughly resuspended in 500 µl ice-cold PBS (Appendix IV, B2, p34), which allows for the washing and removal of most proteins found abundantly in cell culture supernatant that would interfere with downstream analysis, such as FBS. The samples were pooled together and centrifuged at 18000 x g at 4 °C for 5 min, the supernatant discarded, and each pellet carefully resuspended in 150 µl HEPES Resuspension Buffer (Appendix IV, E5, p104). If the pellet was particularly viscous and difficult to resuspend, HEPES Resuspension Buffer was added to the pellet (without mixing), and the pellet allowed to dissolve at 4 °C overnight.

Samples were sonicated three times at 4 °C for 5 min each using a Eumax Memory Quick Ultrasonic Cleaner to ensure a homogenous solution. Failure to thoroughly homogenise the suspension will result in particulate that interferes with protein quantification. Samples were then mixed with an appropriate volume of 4X Laemmli Buffer (Appendix IV, D4, p100), heated at 95 °C for 5 min and stored at -20 °C until used for downstream Western blotting analysis. A 20 µl aliquot of each sample was reserved and diluted with 30 µl PBS (Appendix IV, B2, p34) for protein quantification.

2.3.3.2.3. Protein Quantification

Precipitate concentration was quantified using samples the Pierce™ BCA Protein Assay Kit, as per the protocol previously described in section 2.3.3.1.3, p35.

2.3.3.2.4. Western Blotting

Samples containing viral proteins extracted from during PEG precipitation were analysed using Western blotting, as per the protocol previously described in section 2.3.3.1.4, p36. A 10 µg aliquot whole cell lysate (used as a positive control) and 12 µg of each sample were loaded on to the prepared 12% (v/v) SDS-PAGE gel. A 5 µl aliquot of Precision Plus

Protein™ WesternC™ Standards was used as a reference for day 1 post-transfection samples, and Thermo Scientific™ Pierce™ Prestained Protein Molecular Weight Marker (Thermo Fisher Scientific) (Appendix V, **Figure 37**, p109) was used for day 3 and 5 post-transfection samples.

2.3.4. Statistical Analysis

Statistical analysis was completed using the Microsoft Excel Data Analysis tool equipped with the Analysis ToolPak. A one-way ANOVA was used as a robust test to determine if there was a statistically significant difference in observations between two or more independent groups. The Scheffe comparison method was conducted as a post-hoc analysis to determine which groups specifically were significantly different. Probability (P) < 0.05 was regarded as statistically significant.

CHAPTER 3: RESULTS

3.1. Plasmid Preparation

3.1.1. Restriction Digestion

Following extraction of A1-WT, A2-WT, D3-WT and pCDNA™4/TO plasmid DNA from transformed *E. coli* cells, restriction digestion was conducted to confirm the size and orientation of the extracted HBV DNA, using either one of the following restriction enzymes: *Bam*HI, *Eco*NI or *Xba*I (**Figure 15**). Digested fragments were of the predicted size, as predicted and shown in **Table 3** above.

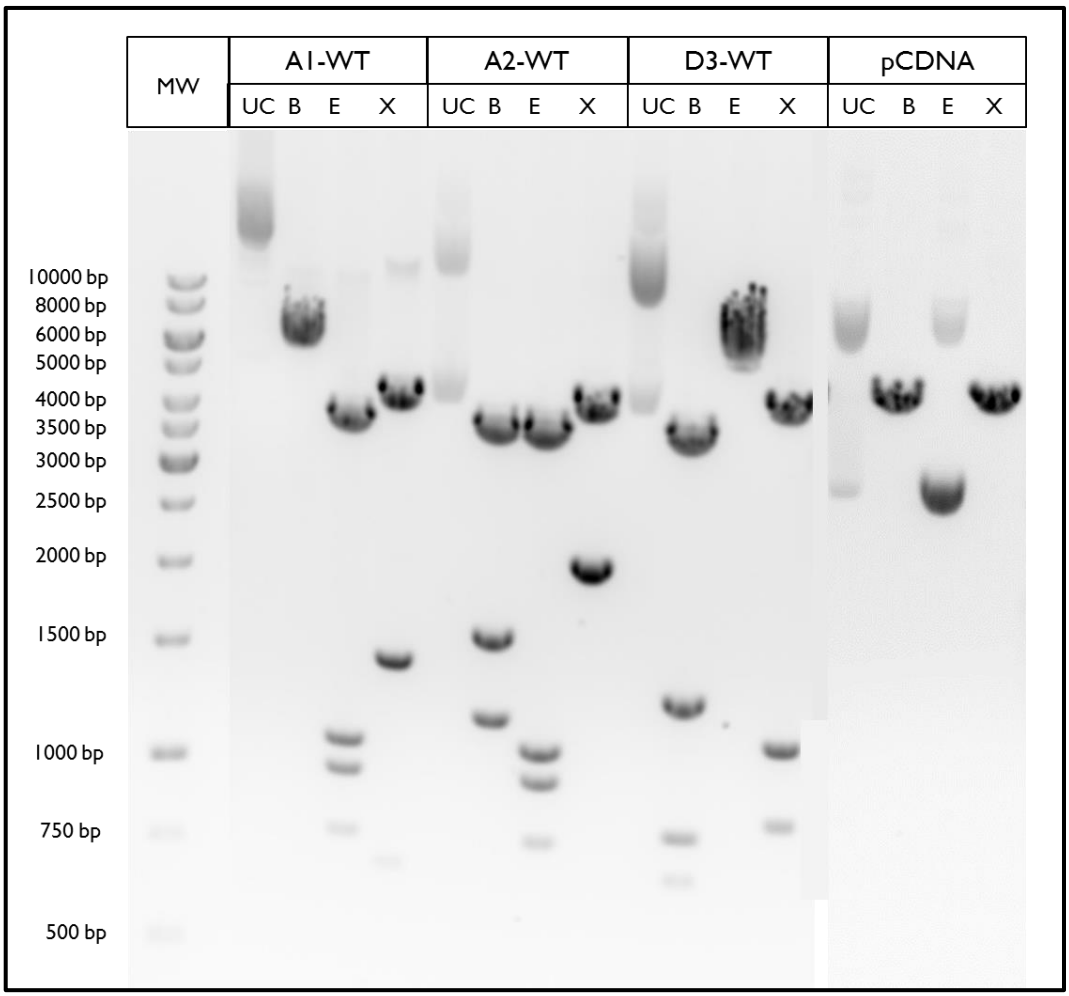


Figure 15. Agarose gel electrophoresis of A1-WT, A2-WT, D3-WT and pCDNA™4/TO DNA restriction digest

Gel electrophoresis image of A1-WT, A2-WT, D3-WT and pDCNA™4/TO restriction digest fragments. Restriction enzymes used were *Bam*HI **(B)**, *Eco*NI **(E)**, and *Xba*I **(X)**. DNA with no enzyme added was used as a control **(UC)**. Fragments were the expected size predicted from the DNA sequences. A1-WT full length DNA was 8235 bp; *Bam*HI fragments: 1372 bp, 1850 bp, 5013 bp; *Eco*NI fragments: 881 bp, 1104 bp, 1238 bp, 5012 bp; *Xba*I fragments: 2430 bp, 5805 bp. A2-WT full length DNA was 8235 bp; *Bam*HI fragments: 1372 bp, 1850 bp, 5013 bp; *Eco*NI fragments: 881 bp, 1104 bp, 1238 bp, 5012 bp; *Xba*I

fragments: 2430 bp, 5805 bp. D3-WT full length DNA is 8195 bp; *Bam*HI fragments: 806 bp, 912 bp, 1504 bp, 5013 bp; *Eco*NI cut D3-WT only once, producing a single fragment of 8195 bp; *Xba*I fragments: 151 bp, 951 bp, 1328 bp and 5805 bp. The pDCNA™4/TO mammalian expression vector contains *Bam*HI and *Xba*I restriction sites and was therefore cut once by each of these enzymes to produce a fragment of 5078 bp; digestion with *Eco*NI results in an uncut fragment. **MW**, O'GeneRuler™ 1 kb DNA Ladder. This image was a composite; although all lanes are from a single gel with the same molecular marker, a section between the marker and A1-WT, as well as a section between D3-WT and pCDNA was removed to provide an accurate representation.

3.2. Transient Transfection of Huh7 Cells

3.2.1. Mycoplasma Detection

The LookOut™ Mycoplasma PCR Detection Kit was used to confirm that Huh7 cell cultures used in this study were free from *Mycoplasma* and *Acholeplasma* contamination, prior to transient transfection. Test reaction tubes were pre-coated with internal control DNA to indicate a successfully performed PCR reaction. PCR products from cell culture supernatants and the negative control indicate successful amplification of internal control DNA as a distinct band at ~481 bp. PCR products from cell culture supernatant matched that of the negative control (**Figure 16**).

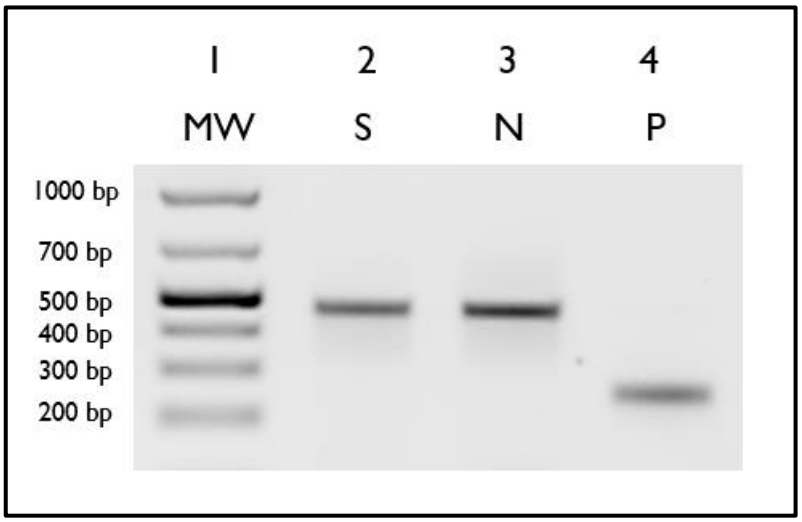


Figure 16. Agarose gel electrophoresis of PCR products for *Mycoplasma* detection

PCR products from cell culture supernatant **(S)**, negative control DNA **(N)** and a positive control **(P)** containing *Mycoplasm orale* DNA fragments, were run on a 0.8% agarose gel. PCR products from cell culture supernatants and the negative control indicates successful amplification of internal control DNA as a distinct band at ~481 bp. PCR products from the sample is matched against the negative control, confirming the absence of *Mycoplasm* and *Acholeplasm* contamination from the cell cultures. **MW**, O'GeneRuler™ 1 kb Plus DNA Ladder.

3.2.2. Measurement of Transfection Efficiency with eGFP

Huh7 cells were transiently transfected with an eGFP-expressing plasmid to determine the efficiency of the transfection. On day 1 post-transfection, the number of eGFP-expressing cells was compared to the number of Huh7 cells in a given field of view (**Figure 17**). Transient transfection was considered successful as the number of eGFP-expressing cells was greater than 70%.

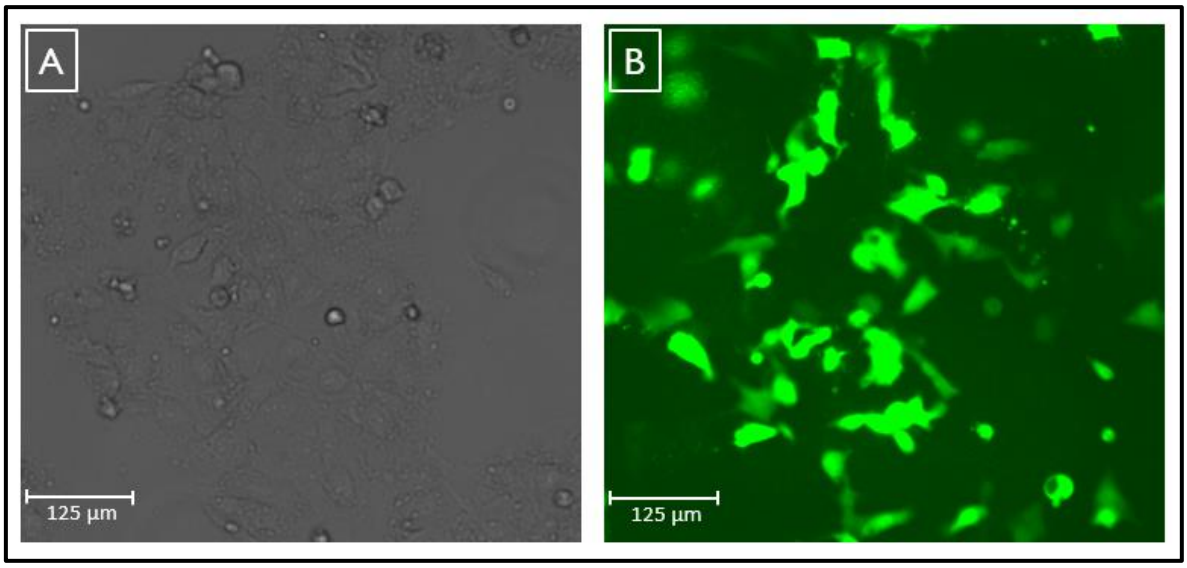


Figure 17. Representative photomicrographs of Huh7 cells transfected with eGFP

Comparison of bright field images of Huh7 cells **(A)** transiently transfected with an eGFP-expressing plasmid to fluorescent images **(B)**. The number of green-fluorescing cells versus non-fluorescing cells give a measure of transfection efficiency of ≥70%. Brightfield and fluorescence microscopy, 40x magnification, images captured with the FLoid™ Cell Imaging Station.

3.3. Expression of HBV Proteins

3.3.1. Subcellular Fractionation Optimisation

The Subcellular Protein Fractionation Kit for Cultured Cells was used in this study to fractionate Huh7 cell pellets into cytoplasmic, membrane, soluble-nuclear, chromatin-bound nuclear and cytoskeletal fractions. The Ponceau stain in **Figure 18** below shows successfully extracted proteins and compares the whole cell lysate to the extracted subcellular fractions. The cytoplasmic, membrane and soluble-nuclear fractions contain mostly higher molecular weight proteins, while the chromatin-bound nuclear and cytoskeletal fractions contain proteins of a lower molecular weight. Each subcellular fraction was visibly distinct with equivalent bands in the whole cell lysate.

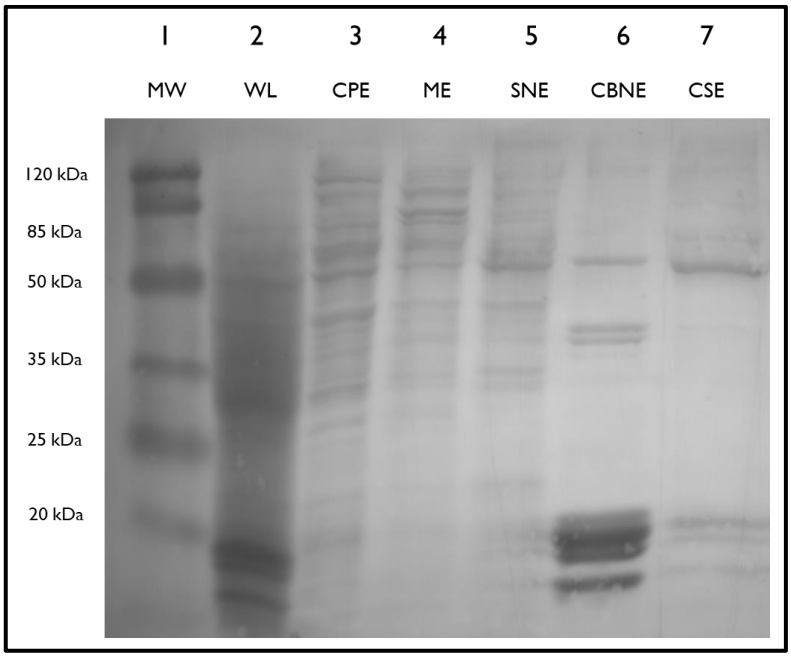


Figure 18. Ponceau S stains of whole lysate and subcellular fractions extracted from Huh7 cells

Huh7 whole cell lysate **(WL)** (lane 2) and subcellular fractions (lanes 3 -7) extracted using the Subcellular Protein Fractionation Kit for Cultured Cells, was separated using SDS-PAGE and transferred on to nitrocellulose membrane. The membrane was stained with Ponceau S stain. 10 µg whole lysate and 8 µg subcellular fractions were loaded. **CPE**, cytoplasmic extract; **ME**, membrane extract; **SNE**, soluble-nuclear extract; **CBNE**, chromatin-bound nuclear extract; **CSE**, cytoskeletal extract. Each subcellular fraction was visibly distinct from the other and its equivalent bands were found in the whole cell lysate. Whole cell lysate provided a range of proteins from 250 kDa to 10 kDa; CPE, ME and SNE mostly contained proteins of high molecular weights, compared to the CBNE and CSE containing proteins of lower molecular weights. **MW**, Thermo Scientific™ Pierce™ Prestained Protein Molecular Weight Marker. Images included are representative.

The manufacturer's standard protocol recommended fractionation of fresh cell pellets; however, the use of fresh Huh7 cell pellets was not feasible because of time constraints and the large volume of samples used. Thus, Huh7 cell pellets were harvested and stored at -70 °C prior to use.

Figure 19 compares the purity of subcellular fractions extracted from fresh Huh7 pellets versus Huh7 pellets previously stored at -70 °C. Western blotting analysis using antibodies targeted towards fraction-specific organelles confirmed the purity of each fraction, as well as confirmed that the proteins contained within each fraction were correctly representative. Freshly harvested Huh7 cells produced almost completely pure fractions (**A**), while fractions extracted from defrosted Huh7 cells (**B**) were not pure, with the exception of the soluble-nuclear fraction. The cytoskeletal fraction was particularly cross-contaminated – evidenced by the presence of Cytokeratin 18 in all fractions. There was also slight contamination between the cytoplasmic and membrane fractions, as indicated by the expression of the cytoplasmic-specific marker Hsp90 and membrane-specific marker Calreticulin between the two fractions. Contaminated fractions are highlighted with boxes in the figure.

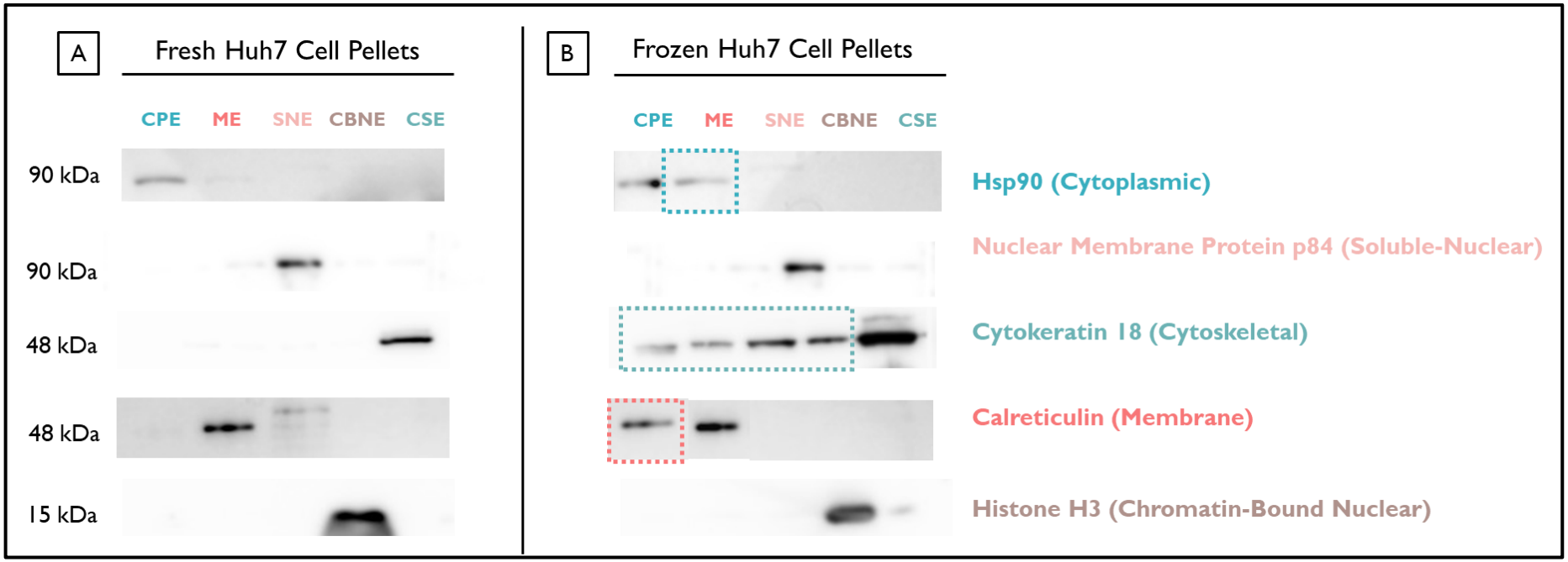


Figure 19. Composite Western blot image comparing subcellular fractions extracted from freshly harvested Huh7 cells versus Huh7 cells previously stored at -70 °C

The purity of subcellular fractions extracted from Huh7 cells was validated using Western blotting against fraction-specific housekeeping proteins; **CPE**, cytoplasmic extract, stained; **ME**, membrane extract; **SNE**, soluble-nuclear extract; **CBNE**, chromatin-bound nuclear extract; **CSE**, cytoskeletal extract. Subcellular fractions extracted from fresh Huh7 cell pellets were pure **(A)**. Dotted boxes highlight cross-contamination between fractions, indicated by the presence of fraction-specific housekeeping proteins in other fractions. With regards to subcellular fractions extracted from defrosted Huh7 cells **(B)** there was slight cross-contamination between the cytoplasmic and membrane fractions, and heavy contamination of cytoskeletal proteins in all fractions. The cytoplasmic fraction was detected using rat monoclonal anti-Hsp90; the membrane fraction detected using rabbit monoclonal anti-Calreticulin; the soluble-nuclear fraction detected using mouse monoclonal anti-Nuclear Matrix Protein p84; the chromatin-bound nuclear fraction detected using mouse monoclonal anti-Histone H3; the cytoskeletal fraction detected using mouse monoclonal anti-Cytokeratin 18.

As the other fractions were notably contaminated with cytoskeletal proteins, the standard protocol used in this study required further optimisation to improve the purity of the cytoskeletal fraction extracted from defrosted Huh7 cells. **Table 5** summarises the tested modifications and their outcomes:

(1) Additional 500 µl PBS wash steps between extractions (**B**) or doubling the buffer volume (**C**) did not visibly improve fraction purity and resulted in lower protein yield

(2) Doubling centrifugation time did not improve purity (**D**)

(3) Doubling the incubation time of the extraction buffer improved purity of the cytoskeletal fraction the most effectively (**E**)

Table 5. Summary of modifications tested to improve purity of the cytoskeletal fraction extracted from Huh7 cells previously stored at -70 °C

Condition		Anti-Cytokeratin 18 (48 kDa)
		CPE ME SNE CBNE CSE
A.	Standard Protocol	
B.	PBS Wash	
C.	Double Buffer Volume	
D.	Double Centrifugation Time	
E.	Double Buffer Incubation Time	

Doubling the incubation time of the cytoskeletal extraction buffer yielded the purest cytoskeletal fraction, therefore this step was included in the subcellular fractionation protocol used for this study. Maintaining cells in ideal conditions during culture, harvesting and defrosting, as well as improvement of the proper extraction technique during subcellular fractionation helped minimise unavoidable cell lysis and

subsequent cross-contamination of fractions that occurred during the freeze-thaw process.

Figure 20 represents subcellular fractions extracted from defrosted Huh7 cells using the optimised protocol; the small band in the cytoplasmic fraction when stained with the membrane-specific Calreticulin marker (boxed) indicates light cross-contamination of membrane proteins within the cytoplasmic fraction. Cross-contamination was not observed in fractions extracted from fresh Huh7 cell pellets, therefore it can be speculated that membrane cross-contamination was a consequence of the freeze-thaw process. This cross-contamination did not affect downstream Western blotting analysis of HBV proteins.

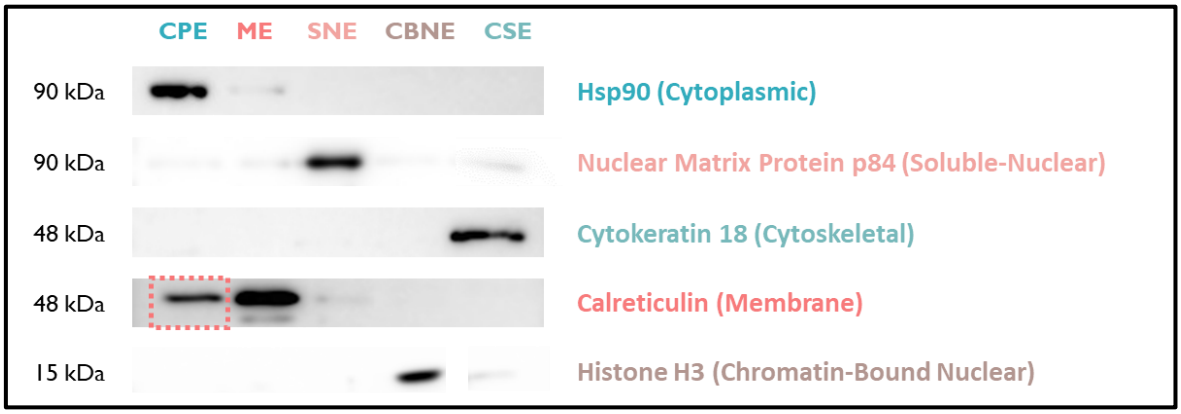


Figure 20. Composite Western blot image of Huh7 subcellular fractions validated with fraction-specific housekeeping proteins

The purity of subcellular fractions extracted from Huh7 cells was validated using Western blotting against fraction-specific housekeeping proteins; **CPE**, cytoplasmic extract (rat monoclonal anti-Hsp90); **ME**, membrane extract (rabbit monoclonal anti-Calreticulin); **SNE**, soluble-nuclear extract (mouse monoclonal anti-Nuclear Matrix Protein p84); **CBNE**, chromatin-bound nuclear extract (mouse monoclonal anti-Histone H3); **CSE**, cytoskeletal extract (mouse monoclonal anti-Cytokeratin 18).

3.3.2. Detection of Intracellular HBsAg

Following successful optimisation of the subcellular fractionation protocol, subcellular fractionation was performed on Huh7 cells transfected with 1.28 mer replication competent plasmids. Western blot densitometry analysis (section 2.3.3.1.4, p36) was carried out to compare intracellular expression of S-HBs, M-HBs and L-HBs between Huh7 cells transfected with one of the following: subgenotypes A1, A2 or D3.

Variable expression of each of these three antigens between the three subgenotypes required varying exposure and saturation limits of each antigen during chemiluminescent detection. This made it difficult to compare all antigen forms of HBsAg for all subgenotypes at the same exposure; M-HBs especially required a longer exposure time, however, at the point where M-HBs could be analysed, S-HBs and L-HBs was over-exposed – as evidenced in **Figure 21**. The densitometry analysis software automatically detects band saturation and does not generate a numerical value for over-saturated bands. For example, although this was visibly observed, it cannot be concluded quantitatively that A1-WT M-HBs expression was lower than that of D3-WT S-HBs, because the software considered D3-WT S-HBs over-saturated. Therefore, to allow for comparison across subgenotypes, each HBsAg form was analysed independently at the exposure just prior to the saturation point.

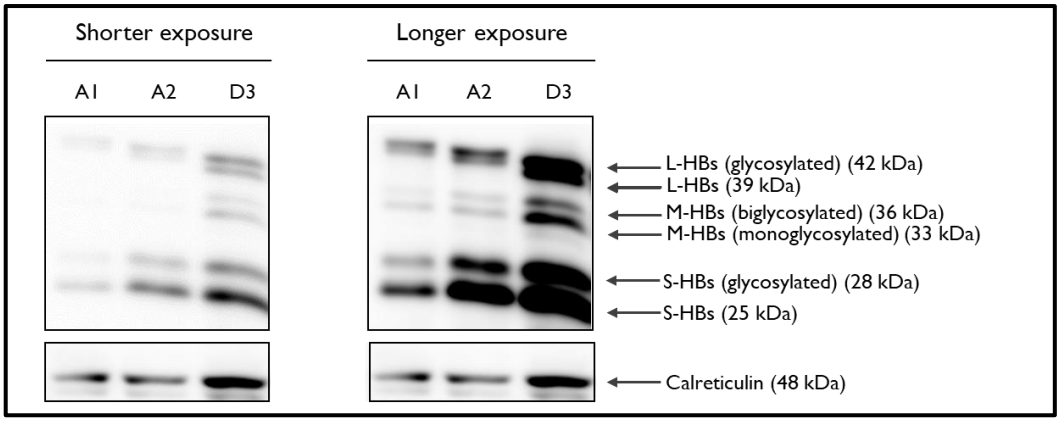


Figure 21. Western blot image of intracellular HBsAg expression in HBV subgenotypes A1, A2 and D3, over short and long exposure times

Membrane fractions extracted from Huh7 cells transfected with wild type HBV subgenotypes A1, A2 or D3 were analysed for hepatitis B surface antigen (HBsAg) expression. Western blot densitometry analysis of all three forms of HBsAg could not be performed at the same exposure, as some bands reached their saturation limit before other bands were sufficiently expressed.

3.3.3. Quantification of Intracellular HBsAg Expression

Pure subcellular fractions enriched for HBsAg were extracted, providing the opportunity to determine localisation of HBsAg within the cell. HBsAg expression was present exclusively in the membrane fraction (**Figure 22, B**) (boxed), with no HBsAg detected in the cytoplasmic- (**A**), soluble-nuclear- (**C**), chromatin-bound nuclear- (**D**) or cytoskeletal- (**E**) fractions. Measured band densities for HBsAg were normalised to the housekeeping protein for the respective fraction used as a loading control, and further normalised to D3-WT whole lysate used as a positive control. S-HBs, M-HBs and L-HBs have two forms; S-HBs and L-HBs each have glycosylated and nonglycosylated forms; M-HBs has a monoglycosylated and biglycosylated form. Each form for S-HBs and M-HBs was calculated separately and summed to provide a total value for S-HBs and M-HBs. Both forms of L-HBs were analysed as one band because of their co-migration and close proximity on the Western blot.

HBsAg expression was highest in the membrane fraction extracted from D3-WT, where S-HBs, monoglycosylated M-HBs and L-HBs were particularly highly expressed, as evidenced by the saturated bands. A2-WT HBsAg was expressed the second highest, with the nonglycosylated S-HBs expressed higher than all other forms, medium L-HBs expression and low M-HBs expression. A1-WT HBsAg was expressed the lowest, where nonglycosylated S-HBs was the highest HBsAg form expressed, followed by L-HBs and low M-HBs expression. The nonglycosylated and glycosylated forms of L-HBs appear to be expressed at approximately equal amounts in all subgenotypes, whereas the monoglycosylated form of M-HBs is expressed slightly higher and the nonglycosylated form of S-HBs expressed much higher than its glycosylated form.

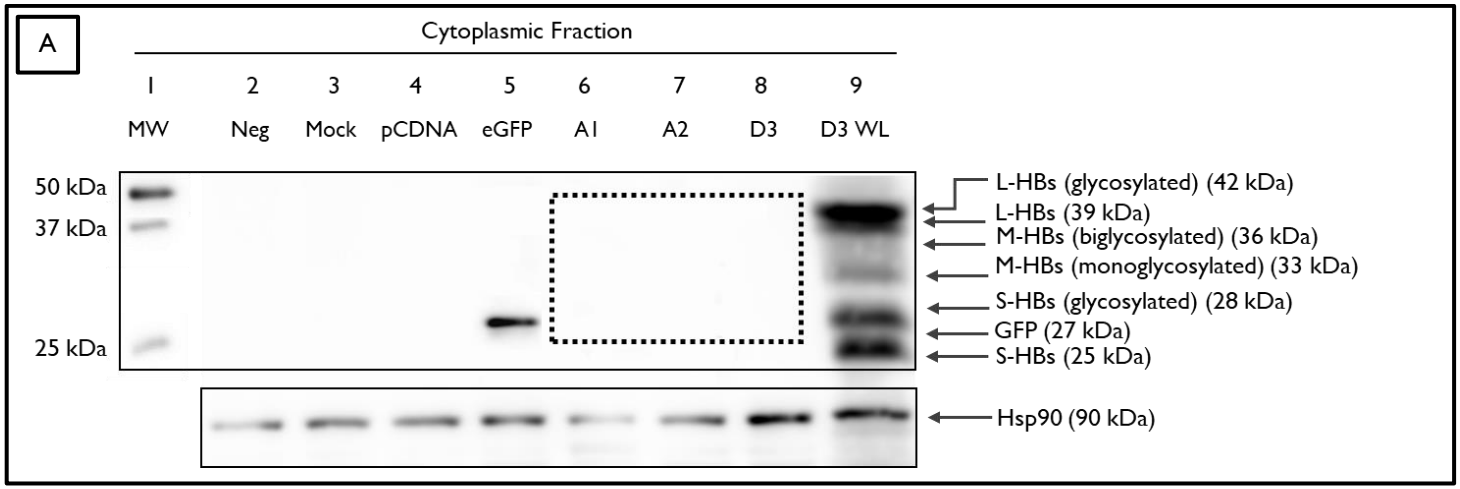


Figure 22. Composite Western blot images of HBsAg expression in subcellular fractions for HBV subgenotypes A1, A2 and D3

Subcellular fractions extracted from Huh7 cells transfected with wild type HBV subgenotypes A1, A2, D3 (lanes 6 – 9) were analysed for HBsAg expression. Samples were separated using SDS-PAGE and transferred on to nitrocellulose membrane. 10 µg D3-WT whole cell lysate harvested on day 5 post-transfection **(D3 WL)** was used as a positive control, and 12 µg of each sample was loaded. Each fraction was identified with a housekeeping protein antibody specific to that fraction; cytoplasmic fraction (rat monoclonal anti-Hsp90), soluble-nuclear fraction (mouse monoclonal anti-Matrix Protein p84), cytoskeletal fraction (mouse monoclonal-Cytokeratin 18), membrane fraction (rabbit monoclonal anti-Calreticulin), and the chromatin-bound nuclear fraction (mouse monoclonal anti-Histone H3). GFP was detected using a rabbit polyclonal anti-GFP antibody, and HBsAg detected using mouse monoclonal anti-HB1 (mAbHB1). All primary antibodies were detected using either secondary goat anti-mouse IgG (H+L)-HRP antibody, goat anti-rabbit IgG (H+L)-HRP antibody or goat anti-rat IgG (H+L)-HRP antibody. Precision Protein™ StrepTactin-HRP conjugate was used to detect Precision Plus Protein WesternC™ Standards, and enhanced chemiluminescent detection was achieved with SuperSignal® West Dura Extended Duration Substrate. Lanes 2 – 5 were negative controls that included negative (Huh7 cells only), negative mock (Huh7 cells treated with transfection reagent only), pCDNA™4/TO and eGFP fractions. GFP (lane 5) was used to measure transfection efficiency and was localised in the cytoplasmic fraction **(A)**. HBsAg was exclusively localised to the membrane fraction **(B**, continued on next page**)** and consists of S-HBs, M-HBs and L-HBs, with each antigen form expressing distinct double bands differentiating nonglycosylated or glycosylated forms. Dotted boxes indicate where HBsAg expression would be expected. **MW**, Precision Plus Protein™ WesternC™ Standards. Images included are representative.

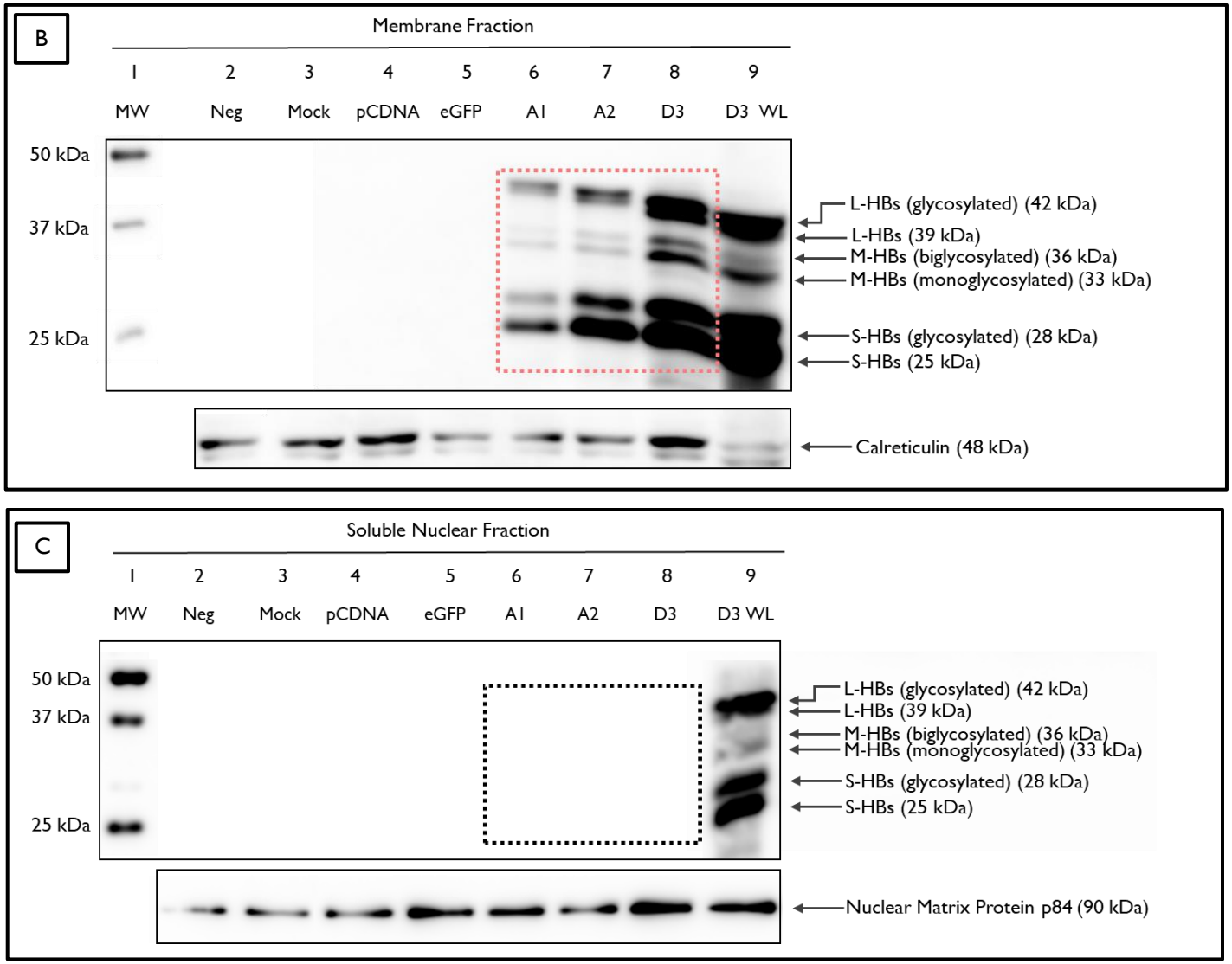


Figure 22 *(continued)*

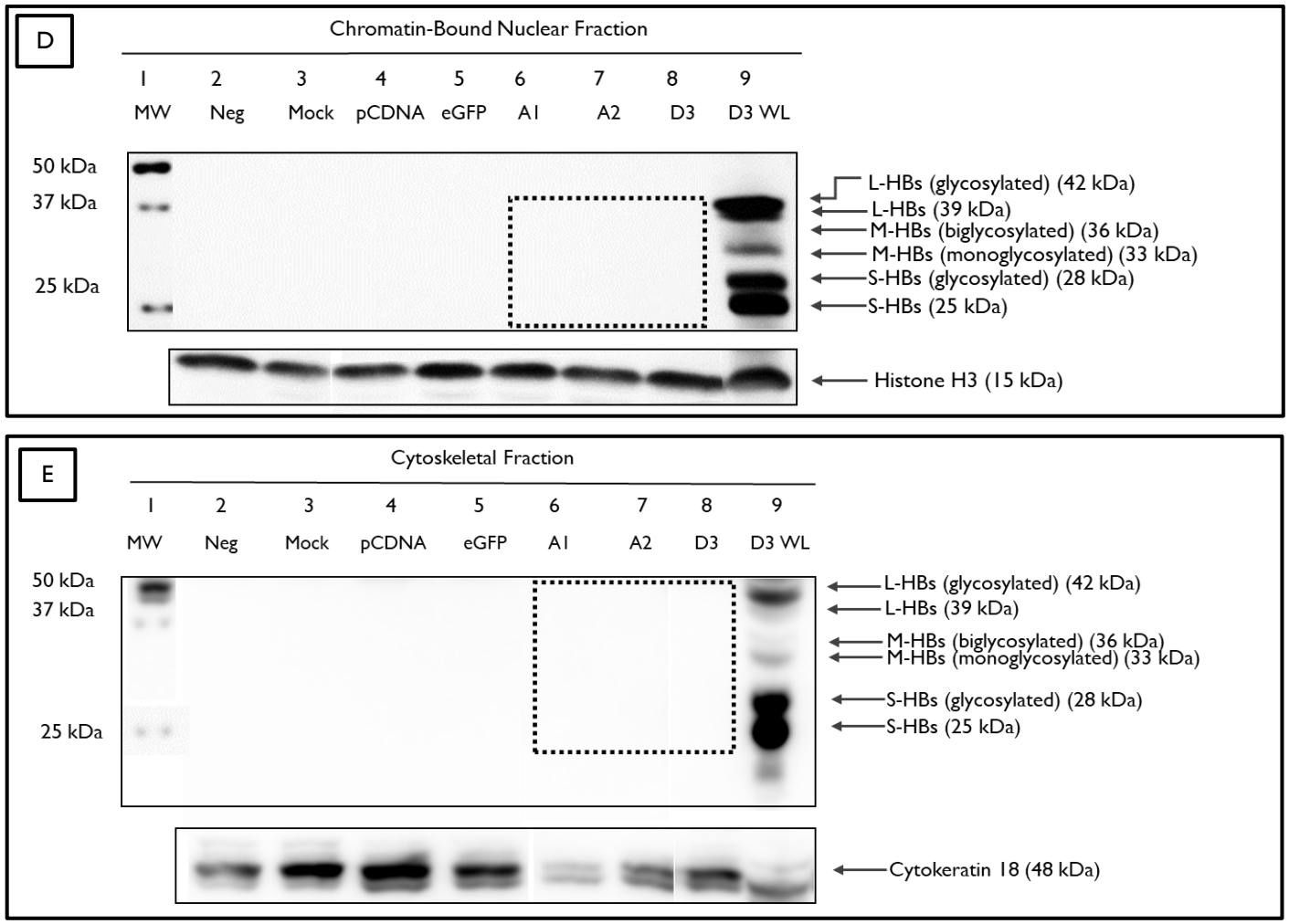


Figure 22 *(continued)*

As discussed earlier, the different exposure times necessary for viewing the expression of the individual proteins (S-HBs, M-HBs and L-HBs) did not allow us to measure the relative expression of each protein within each subgenotype (**Figure 21**). However, because the same exposure time used for each protein was the same across all subgenotypes, **Figure 23** compares the relative expression of each protein for subgenotypes A1, A2 and D3. HBsAg (L-HBs, M-HBs and S-HBs) expression was significantly higher in D3-WT compared to A1-WT, whereas only M-HBs and L-HBs was significantly higher in D3-WT compared to A2-WT. A1-WT and A2-WT express similar levels of M-HBs and L-HBs, but S-HBs expression in A2-WT was significantly higher than A1-WT

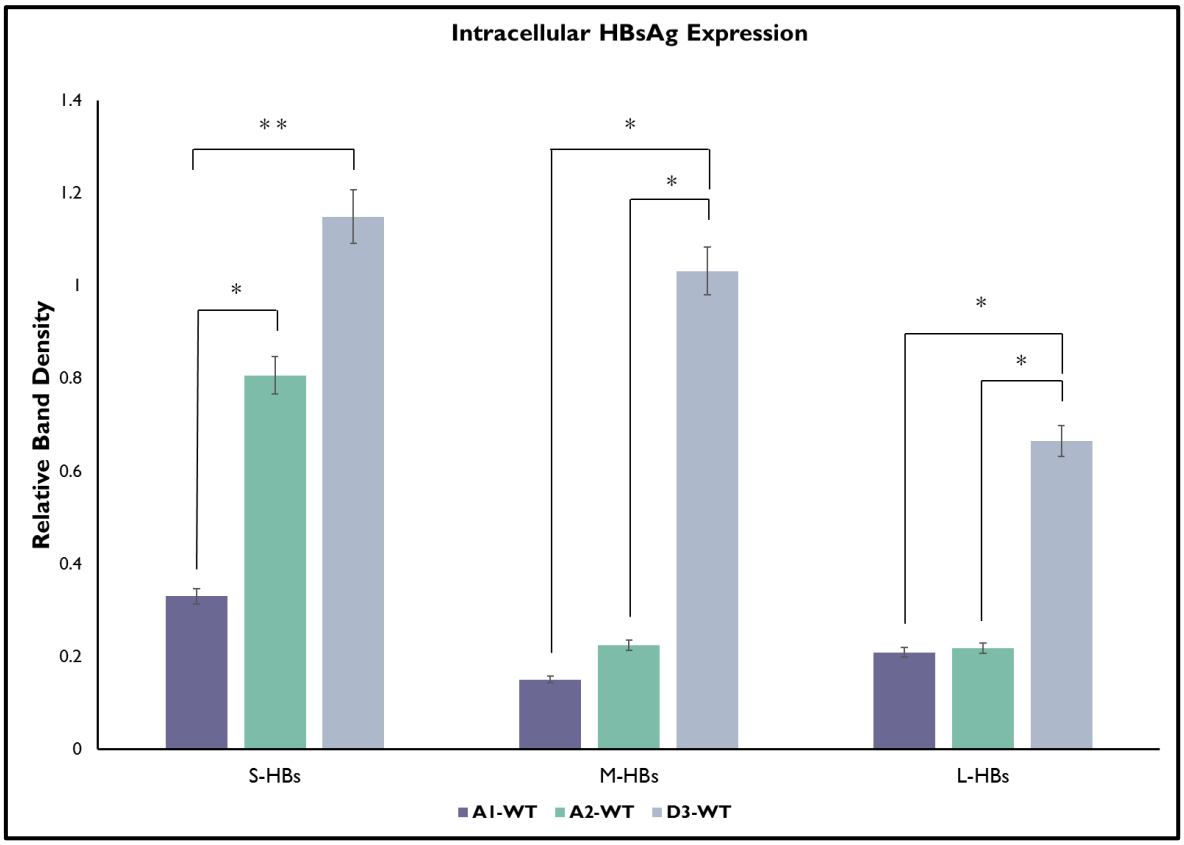


Figure 23. Semi-quantitative analysis of intracellular HBsAg expression in A1-WT, A2-WT and D3-WT

Image Studio Lite was used to quantify the expression of S-HBs, M-HBs and L-HBs within the membrane fraction of either A1-WT, A2-WT or D3-WT transfected Huh7 cells. D3-WT expressed HBsAg significantly higher than A1-WT and A2-WT. A1-WT and A2-WT were only comparable in expression of S-HBs. n=3; error bars represent a 5% difference from the absolute value; *$p < 0.05$ significance between joined groups; **$p < 0.05$ significance between all groups.

Whole cell lysates extracted from Huh7 cells transiently transfected with either A1-WT, A2-WT or D3-WT were used as a positive control to ensure that the patterns of HBsAg expression observed in the subcellular fractions aligned with those found in the whole lysate. We found that whole lysate does not produce the clean, distinct bands seen in the membrane subcellular fraction, but the overall trend of HBsAg expression between the subgenotypes remains the same – i.e. D3-WT expresses HBsAg the highest, followed by A2-WT and lastly A1-WT (**Figure 24**).

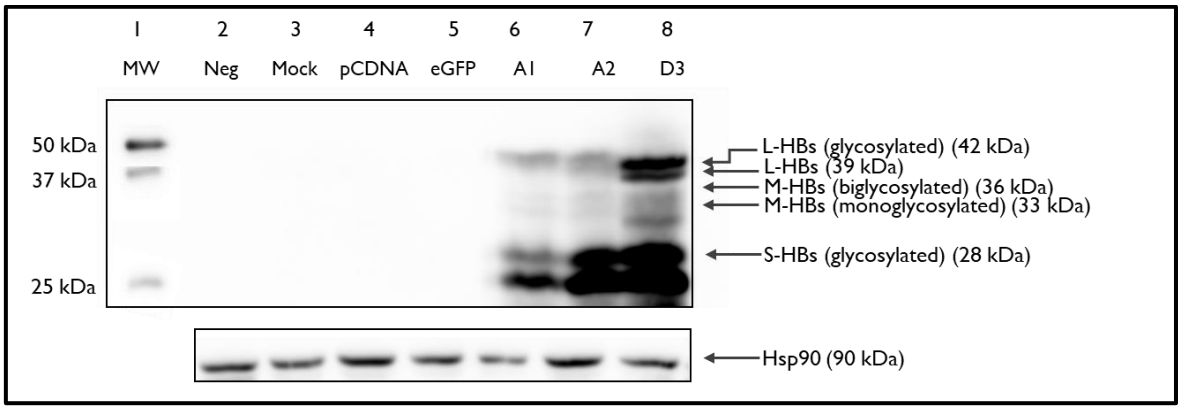


Figure 24. Composite Western blot images of HBsAg expression within whole cell lysates of Huh7 cells transfected with either HBV subgenotypes A1, A2, or D3

Whole cell lysates extracted from Huh7 cells transfected with wild type HBV subgenotypes A1, A2, D3 (lanes 6 – 8) were analysed for HBsAg expression. Samples were separated using SDS-PAGE and transferred on to nitrocellulose membrane. 10 µg of each sample was loaded. Rat monoclonal anti-Hsp90 was used as a loading control, and HBsAg detected using mouse monoclonal anti-HB1. Primary antibodies were detected using either secondary goat anti-mouse IgG (H+L)-HRP antibody or goat anti-rat IgG (H+L)-HRP antibody. Precision Protein™ StrepTactin-HRP conjugate was used to detect Precision Plus Protein WesternC™ Standards, and enhanced chemiluminescent detection was achieved with SuperSignal® West Dura Extended Duration Substrate. Lanes 2 – 5 were negative controls that included negative (Huh7 cells only), negative mock (Huh7 cells treated with transfection reagent only), pCDNA™4/TO and eGFP. **MW**, Precision Plus Protein™ WesternC™ Standards. Images included are representative.

3.4. Quantification of Extracellular HBeAg and HBsAg Expression

3.4.1. ELISA

Supernatants containing extracellularly expressed HBeAg and HBsAg were collected on days 1, 3 and 5 post-transfection and quantitatively analysed using ELISA. Samples were considered negative if absorbance measurements fell below the cut-off value stipulated in the manufacturer's guidelines. Negative controls (not shown) included negative, negative mock, pCDNA™4/TO and eGFP. Measurements were normalised to D3-WT (CMV+) HBeAg expression measured on day 5 post-transfection.

3.4.1.1. HBeAg

The ETI-EBK PLUS HBeAg ELISA kit was used to quantify extracellular HBeAg expression in A1-WT, A2-WT and D3-WT (**Figure 25**). ELISA results reveal HBeAg expression in D3-WT (CMV+) was significantly higher than A1-WT, A2-WT and D3-WT on Day 3, however A1-WT and D3-WT (CMV+) HBeAg expression was significantly higher than both A2-WT and D3-WT on day 5. HBeAg was significantly higher on each consecutive day for all subgenotypes.

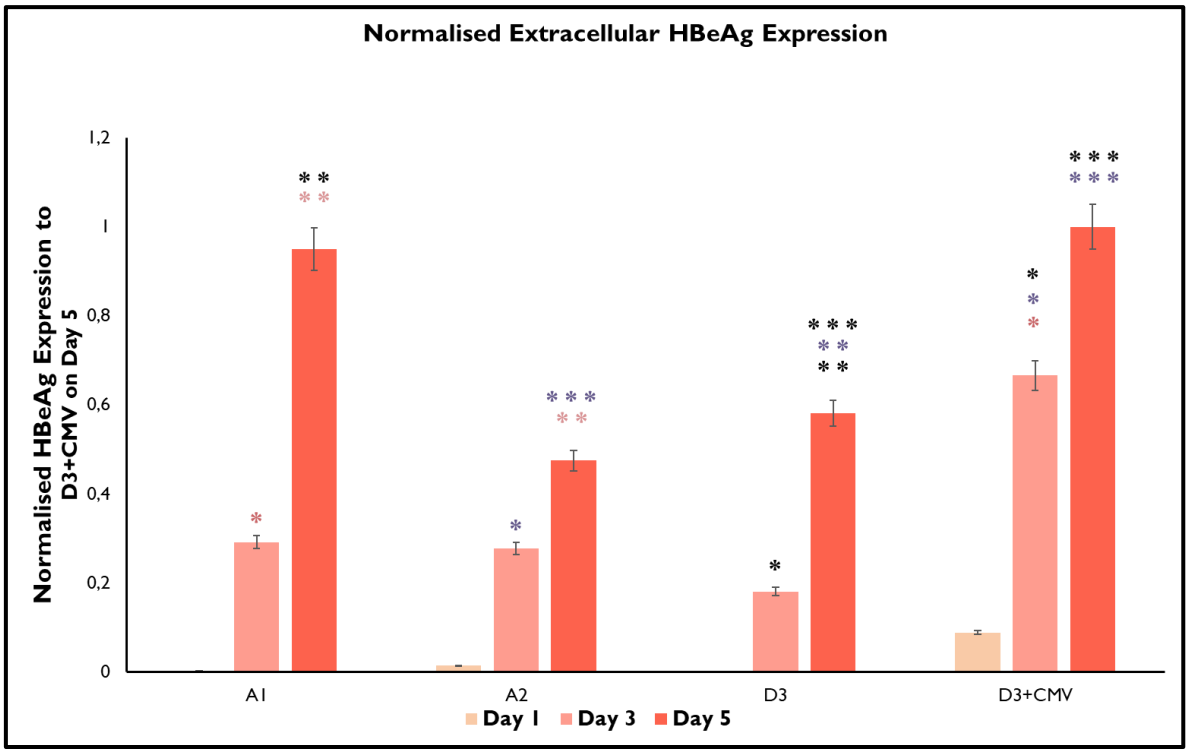


Figure 25. Normalised HBeAg expression in cell culture supernatant of transfected Huh7 cells

Histogram illustrating the mean extracellular HBeAg expression in cell culture supernatants from Huh7 cells transfected with either A1-WT, A2-WT or D3-WT plasmids, measured by ELISA. Measurements were normalised to D3-WT (CMV+) HBeAg expression on day 5 post-transfection. HBeAg expression in D3-WT (CMV+) was significantly higher than A1-WT, A2-WT and D3-WT on Day 3, however A1-WT and D3-WT (CMV+) HBeAg expression was significantly higher than both A2-WT and D3-WT on day 5. n=3; error bars represent a 5% difference from the absolute value; *p < 0.05 significance; the corresponding colour and number of asterisks indicate which days and plasmid constructs showed significantly different expression levels.

3.4.1.2. HBsAg

The Murex HBsAg Version 3 ELISA detected the lowest HBsAg expression on day 1, with significantly higher HBsAg expression in D3-WT (CMV+) compared to A1-WT, A2-WT and D3-WT on day 3. Day 5 generated the highest HBsAg expression in all three subgenotypes, with A1-WT having significantly the highest HBsAg expression compared to A2-WT and D3-WT (**Figure 26**). HBsAg expression increased significantly on each consecutive day for all subgenotypes, except for D3-WT between days 3 and 5.

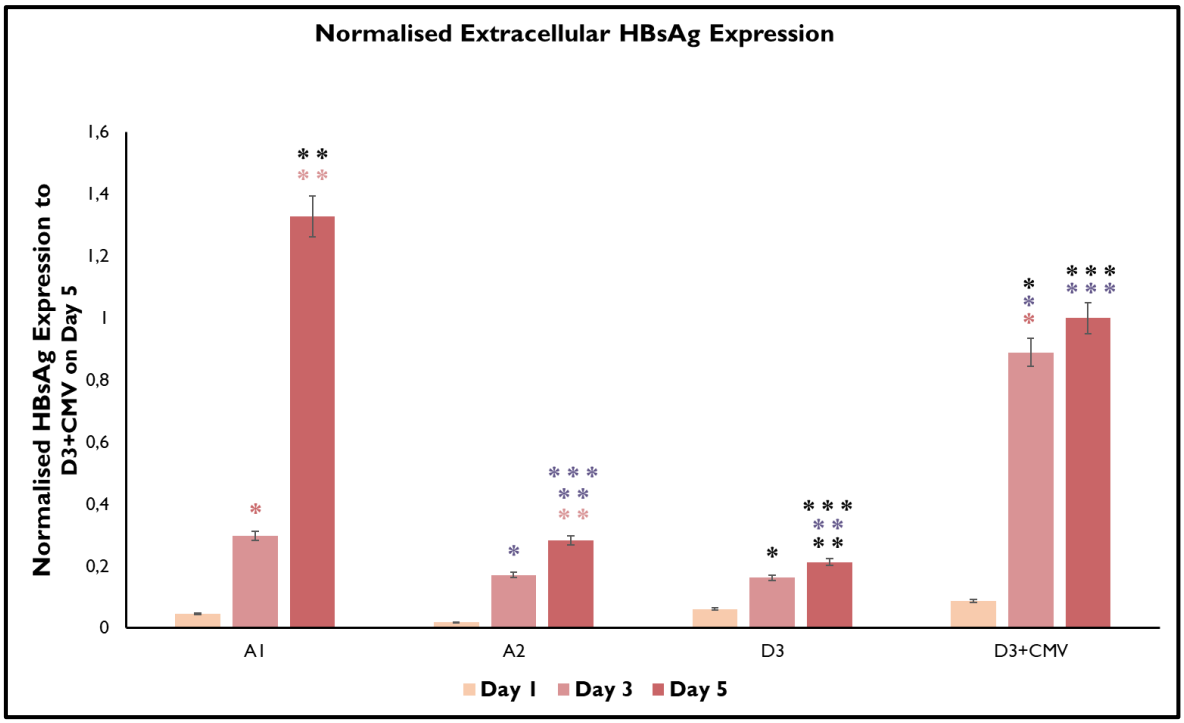


Figure 26. Normalised HBsAg expression in cell culture supernatant of transfected Huh7 cells

Histogram illustrating the mean extracellular HBsAg expression in cell culture supernatants from Huh7 cells transfected with either A1-WT, A2-WT or D3-WT plasmids, measured by ELISA. Measurements were normalised to D3-WT (CMV+) expression on day 5 post-transfection. HBsAg expression in A1-WT was significantly higher than A2-WT and D3-WT on day 1. n=3; error bars represent a 5% difference from the absolute value; *p < 0.05 significance; the corresponding colour and number of asterisks indicate which days and plasmid constructs showed significantly different expression levels.

3.4.2. PEG Precipitation

3.4.2.1. PEG Precipitation Optimisation

To perform Western blotting analysis on the expression of extracellular HBsAg, a precipitation protocol was developed to extract HBV viral proteins in the cell culture supernatants collected from Huh7 cells transiently transfected with one of the following: A1-WT, A2-WT or D3-WT 1.28 mer plasmids.

Optimisation was carried out using supernatants collected on day 5 post-transfection from the cell culture of Huh7 cells transiently transfected with the A1-WT 1.28 mer plasmid. Western blotting was performed as described in section 2.3.3.2.4, p36, and the mouse monoclonal antibody against the S region of HBsAg (mAbHB1) (**Table 1**) was used to detect HBsAg expression in PEG precipitates. **Table 6** on the next page provides a summary of the optimisation process, with asterisks (*) indicating the expression of the various forms of HBsAg.

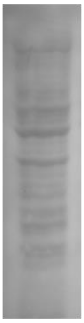
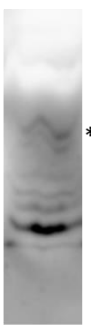
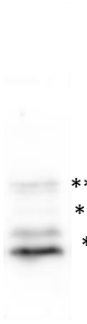
Firstly, supernatants were mixed with 37% (w/v) PEG overnight and resultant precipitates resuspended in HEPES Resuspension buffer. Western blot analysis revealed successful detection of HBsAg with high background, bands were visibly distorted, and viral protein yields were too low (**C**).

Further review of the literature suggested that using a PEG solution containing a greater than 8% PEG concentration would result in aggregate formation of serum proteins present in supernatant, interfering with viral protein precipitation and analysis. PBS wash steps were also recommended. Tested modifications produced the following results:

(1) Precipitation using a 7% (w/v) PEG solution still produced distorted bands (**A**).
(2) Precipitation using a 7% (w/v) PEG solution and an additional PBS wash resulted in most proteins being washed away, and slightly visible HBsAg-positive bands (**B**).
(3) Precipitation using a 37% (w/v) PEG solution and an additional PBS wash minimised background and produced HBsAg-positive bands suitable for Western blot analysis (**D**).

Ponceau stains showed the efficiency of the protein extraction, as well as the presence of serum protein aggregates which caused the distorted banding (indicated within dotted boxes in **Table 6**). PBS washes removed most serum aggregates to produce clean precipitates. After confirming that a 37% (w/v) PEG solution with an additional PBS wash produced suitable bands for Western blotting analysis, larger volumes of supernatant were precipitated to successfully increase yield (**E**). This resulted in bands which revealed expression of all 3 forms of HBsAg, although the bands appeared slightly irregular. Samples were then sonicated to properly homogenise precipitates within the resuspension buffer, improving the appearance of the bands similar to those observed in cell lysate (**F**). **Table 6** below provides a summary of the optimisation process.

Table 6. Summary of polyethylene glycol (PEG) precipitation optimisation for Western blotting analysis of cell culture supernatants containing HBV viral proteins

Condition	A	B	C	D	E	F
	7% PEG only	7% PEG + PBS wash	37% PEG only	37% PEG + PBS wash	37% PEG + PBS wash	37% PEG + PBS wash + sonication
Volume of Supernatant	850 µl	850 µl	850 µl	850 µl	1700 µl	1700 µl
Ponceau S Stain						
Anti-HBsAg						

Dotted boxes indicate aggregated serum proteins.
*S-HBs
** M-HBs
*** L-HBs

3.4.2.2. Western Blotting to Detect Extracellular HBsAg

PEG precipitation was used to extract extracellular HBsAg secreted into the cell culture supernatants of Huh7 cells transiently transfected with one of the following: A1-WT, A2-WT or D3-WT 1.28 mer plasmids. Supernatants collected on day 1, 3 and 5 post-transfection were precipitated and run in duplicate for Western blotting analysis. Measured band densities were normalised to HBsAg expression for A1-WT on Day 5; however, no loading control (such as housekeeping proteins used to control for intracellular expression) was included because of the difficulty in finding a protein that is constitutively expressed extracellularly. Negative controls included negative, negative mock, pCDNA™4/TO and eGFP. Precision Protein™ StrepTactin-HRP conjugate was used to detect Precision Plus Protein WesternC™ Standards, and enhanced chemiluminescent detection was achieved with SuperSignal® West Dura Extended Duration Substrate.

Qualitative analysis of bands (**Figure 27**) shows that S-HBs was already expressed on day 1 post-transfection for subgenotypes A1 and A2, although the expression was minimal. On day 3 post-transfection, all three forms of HBsAg were expressed in all subgenotypes; A1-WT expressed HBsAg the highest followed by D3-WT, with A2-WT expressing the lowest. On day 5 post-transfection, HBsAg was expressed the highest across all subgenotypes. Western blot densitometry analysis (**Figure 28**) revealed that A1-WT exhibited the highest HBsAg expression, once again followed by D3-WT and lastly A2-WT. On both days 3 and 5, the nonglycosylated S-HBs and monoglycosylated form of M-HBs were expressed in higher proportion to their further glycosylated counterparts. Furthermore, M-HBs was expressed much lower by A2-WT transfected cells relative to subgenotypes A1 and D3.

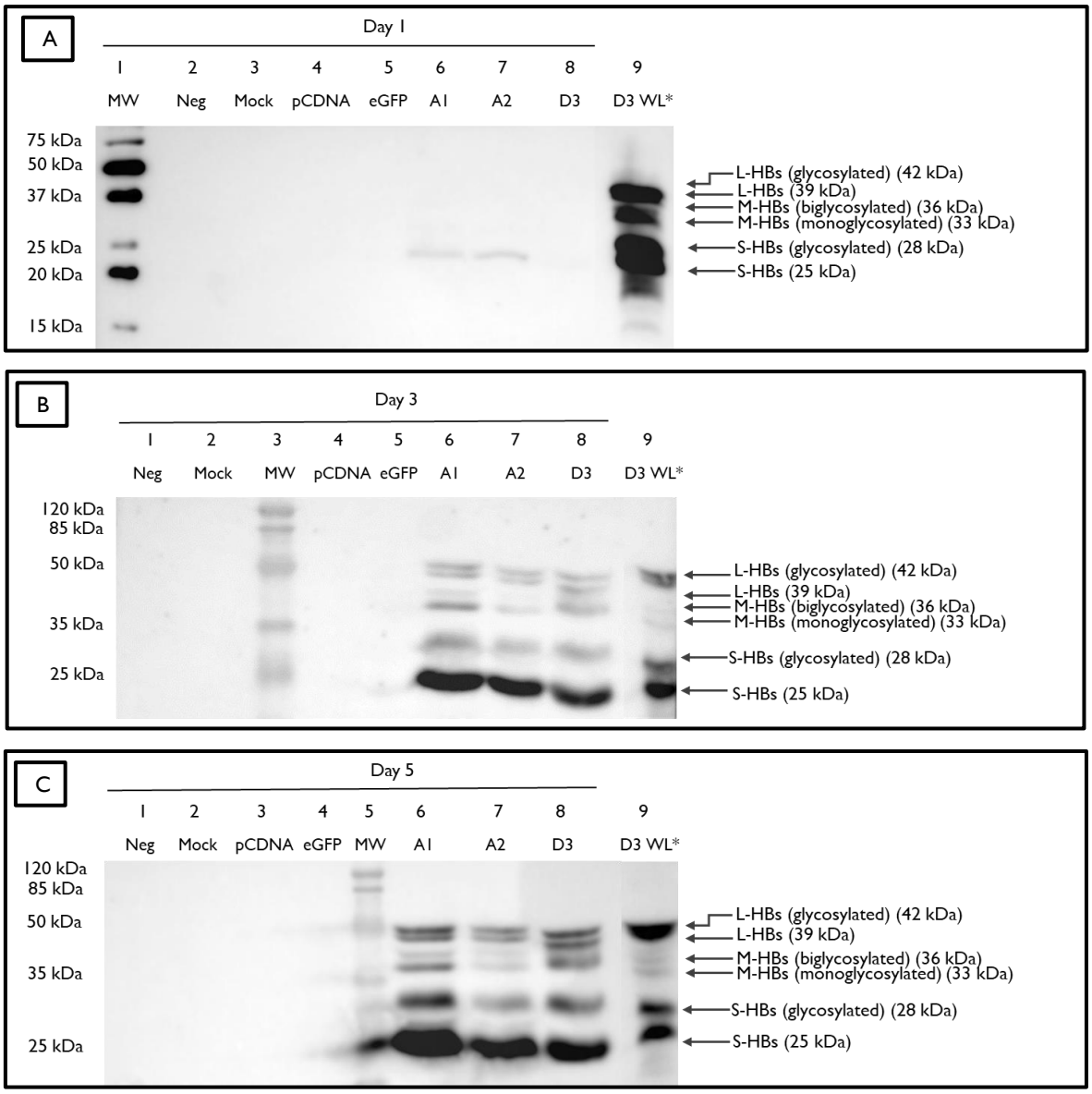


Figure 27. Western blot image of extracellular HBsAg expression in HBV subgenotypes A1, A2 and D3

Extracellular HBsAg was extracted using PEG precipitation of cell culture supernatants from Huh7 cells transiently transfected with wild type HBV subgenotypes A1, A2 or D3, collected on days 1, 3 and 5 post-transfection. Samples were separated using SDS-PAGE and transferred on to nitrocellulose membrane. 10 µg D3-WT whole cell lysate harvested on day 5 post-transfection **(D3 WL*)** (lane 9) was used as a positive control, and 12 µg of each sample was loaded. HBsAg consists of small- (S-HBs), middle- (M-HBs) and large- (L-HBs) HBsAg, with each expressing distinct double bands indicating nonglycosylated or glycosylated forms. Subgenotype A1 consistently expressed HBsAg higher than A2-WT or D3-WT, and A2-WT consistently expressed HBsAg the lowest. The non-glycosylated form of S-HBs and monoglycosylated form of M-HBs were expressed higher than their larger, further glycosylated counterparts; however, HBsAg was detected using primary mouse monoclonal anti-HB1 and secondary goat anti-mouse IgG (H+L)-HRP antibody. *indicates D3-WT whole lysate was harvested on day 5 post-transfection. **MW**, Precision Plus Protein™ WesternC™ Standards for day 1; **MW**, Thermo Scientific™ Pierce™ Prestained Protein Molecular Weight Marker for days 3 and 5. Images included are representative.

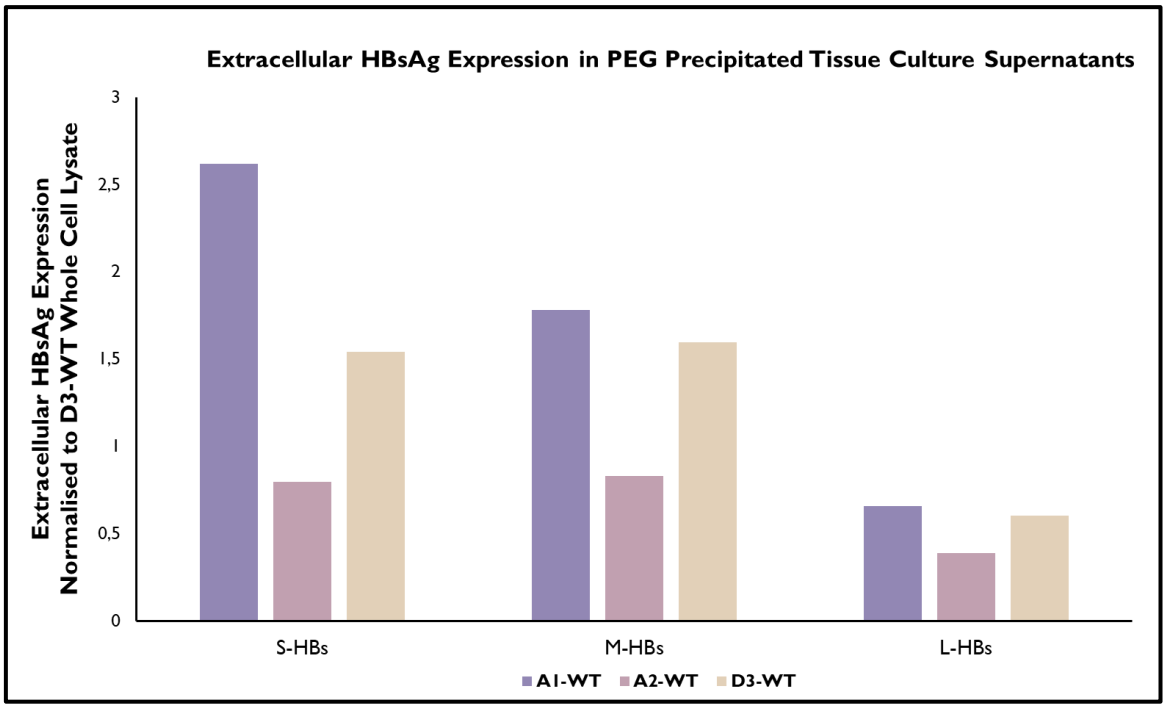


Figure 28. Semi-quantitative analysis of extracellular HBsAg expression in A1-WT, A2-WT and D3-WT on day 5 post-transfection

Image Studio Lite was used to quantify the extracellular expression of HBsAg precipitated from cell culture supernatants of Huh7 cells transiently transfected with A1-WT, A2-WT or D3-WT, collected on day 5 post-transfection. All measurements were normalised to HBsAg expression in D3 whole lysate harvested on day 5 post-transfection. Extracellular expression in A1-WT was consistently higher than A2-WT and D3-WT for all forms of HBsAg. Expression was only comparable between subgenotypes, and not within subgenotypes; n=2.

3.5. Comparison of Intracellular and Extracellular HBsAg Expression

Intracellular and extracellular HBsAg expression was measured on day 5 post-transfection within the membrane fraction and cell culture supernatants of Huh7 cells transfected with one of the following wild type HBV subgenotypes: A1, A2 or D3. Western blot densitometry analysis reveals variable intracellular and extracellular HBsAg expression between A1-WT, A2-WT and D3-WT. Resulting from the varying saturation limits between subgenotypes, HBsAg expression was quantified independently for each subgenotype, allowing for accurate representation of the proportions of S-HBs, M-HBs and L-HBs. The nonglycosylated S-HBs form and monoglycosylated M-HBs form were consistently expressed higher than their glycosylated and biglycosylated counterparts, respectively.

Figure 29 shows that, both intracellularly and extracellularly, S-HBs constitutes the largest proportion of HBsAg, followed by L-HBs and M-HBs. With regards to intracellular HBsAg expression, there was a consistent pattern between all three subgenotypes; namely that S-HBs contributes to at least 60% of HBsAg expression, followed by L-HBs, and M-HBs expressing the least.

In comparison to intracellular S-HBs HBsAg expression, the proportion of S-HBs appeared to increase extracellularly in all subgenotypes, consisting of at least 70% S-HBs. A1-WT and A2-WT expressed all forms of extracellular HBsAg in similar proportions to each other, with S-HBs constituting approximately 80% of HBsAg. D3-WT expressed extracellular S-HBs in lower proportions compared to A1-WT and A2-WT, but M-HBs and L-HBs expression was slightly higher, each contributing approximately 15% to HBsAg expression; notably, extracellular expression of M-HBs and L-HBs in D3-WT was of similar proportions.

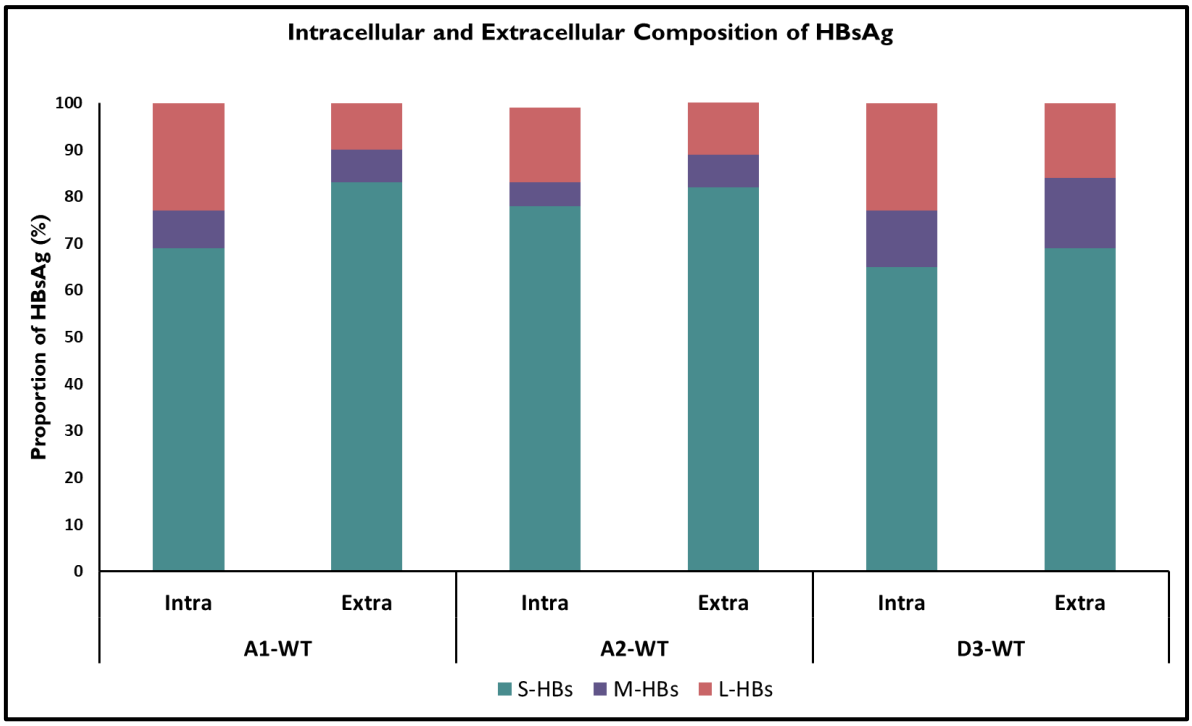


Figure 29. Comparison of intracellular and extracellular S-HBs, M-HBs and L-HBs expression in wild type HBV subgenotypes A1, A2 and D3

Histogram representing the proportion of S-HBs, M-HBs and L-HBs expression in the membrane fraction and PEG precipitated tissue culture supernatants harvested from Huh7 cells 5 days post-transfection with either wild type subgenotypes A1, A2 or D3. In all three subgenotypes S-HBs was expressed in the highest proportion, and extracellular expression was higher compared to intracellular S-HBs expression. Intracellular L-HBs expression was similar between A1-WTand D3-WT, and both were higher than intracellular A2-WT L-HBs expression. However, M-HBs and L-HBs expression shifted towards similar expression between A1-WT and A2-WT when measured extracellularly; M-HBs and L-HBs were expressed in nearly equal proportion in D3-WT extracellularly. Intracellular analysis was based on quantification of 3 independent Western blots (n=3), and extracellular analysis was based on quantification of 2 independent Western blots (n=2). Statistical analysis was not performed as differences between the proportions of S-HBs, M-HBs and L-HBs appeared minor.

Figure 30 provides a further comparison of the ratio of glycosylated S-HBs to nonglycosylated S-HBs, and biglycosylated M-HBs to nonglycosylated M-HBs, both intracellularly and extracellularly for subgenotypes A1, A2 and D3. Intracellular quantification was based on the expression of HBsAg in the membrane fraction of Huh7 cells harvested on day 5 post-transfection, and extracellular quantication was based on the expression of HBsAg in PEG precipitated tissue culture supernatants harvested on day 5 post transfection. The different forms of L-HBs was not included because of their close co-migration on the Western blot, however when referring back to **Figure 22 B and Figure 27 B** and **C**, it was evident that the proportion of nonglycosylated L-HBs and glycosylated L-HBs were more or less equal. In all subgenotypes, the glycosylated

form of S-HBs and the biglycosylated form of M-HBs was expressed lower than their smaller nonglycosylated and monglycosylated forms, respectively. Moreover, the same pattern of expression was noted extracellularly, but glycosylated S-HBs and biglycosylated M-HBs were expressed much lower in subgenotypes A1 and D3. The expression of biglycosylated M-HBs in A2-WT appeared to instead increase extracellularly.

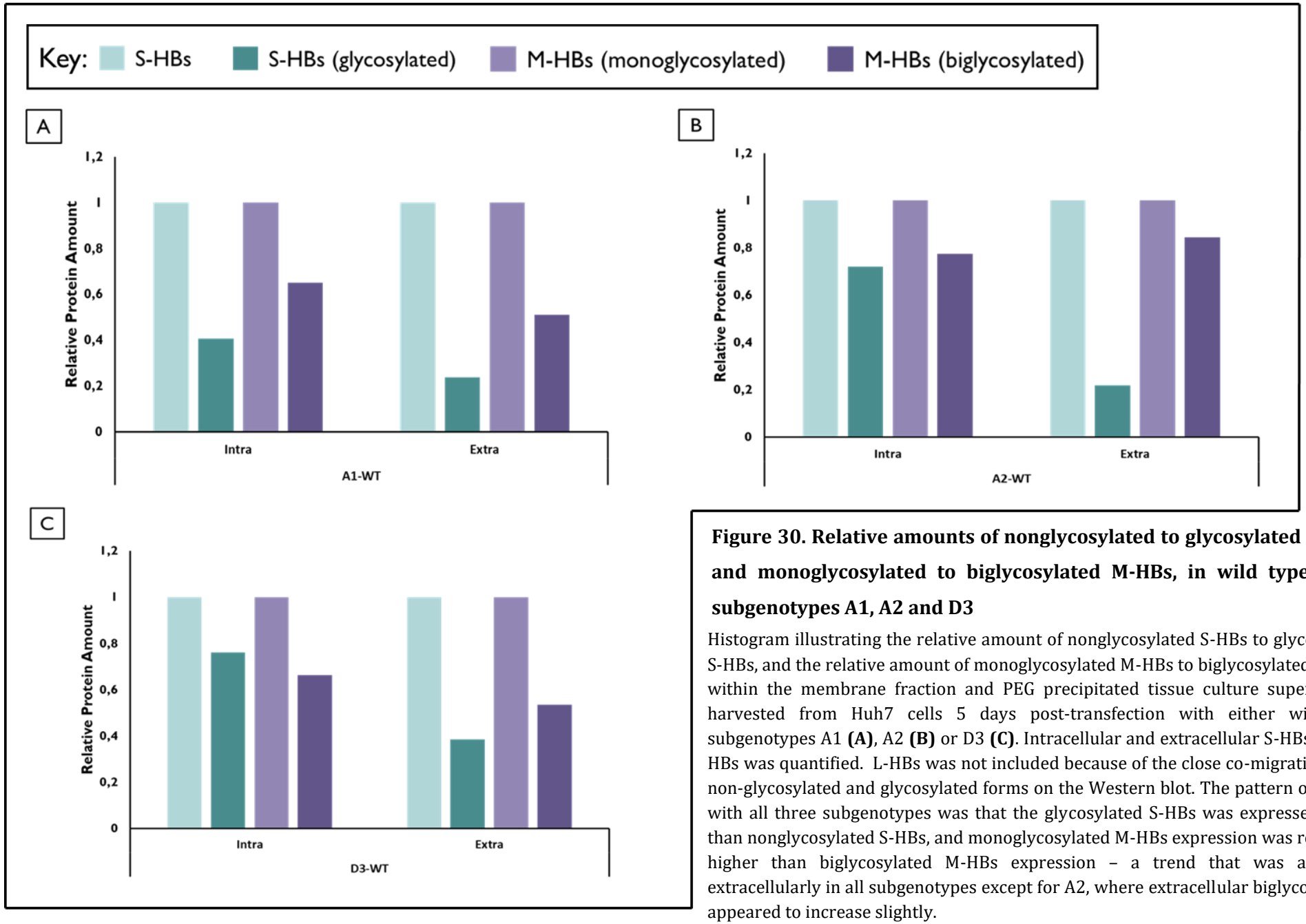


Figure 30. Relative amounts of nonglycosylated to glycosylated S-HBs and monoglycosylated to biglycosylated M-HBs, in wild type HBV subgenotypes A1, A2 and D3

Histogram illustrating the relative amount of nonglycosylated S-HBs to glycosylated S-HBs, and the relative amount of monoglycosylated M-HBs to biglycosylated M-HBs, within the membrane fraction and PEG precipitated tissue culture supernatants harvested from Huh7 cells 5 days post-transfection with either wild type subgenotypes A1 **(A)**, A2 **(B)** or D3 **(C)**. Intracellular and extracellular S-HBs and M-HBs was quantified. L-HBs was not included because of the close co-migration of its non-glycosylated and glycosylated forms on the Western blot. The pattern observed with all three subgenotypes was that the glycosylated S-HBs was expressed lower than nonglycosylated S-HBs, and monoglycosylated M-HBs expression was relatively higher than biglycosylated M-HBs expression – a trend that was amplified extracellularly in all subgenotypes except for A2, where extracellular biglycosylation appeared to increase slightly.

CHAPTER 4: DISCUSSION

Hepatitis B virus infection is hyperendemic to southern Africa, with genotype A and D predominating [7, 94]. The genotype or subgenotype can account for the differences in clinical outcomes and response to treatment [7, 111], with studies showing differences in the expression of HBsAg and HBeAg between genotypes/subgenotypes [7, 87, 101]. Subgenotype A1 is the predominant HBV strain circulating in South Africa, and has been noted to be particularly hepatocarcinogenic [7]. The aim of this study was to compare the intracellular and extracellular expression of HBV antigens HBsAg and HBeAg between the subgenotypes circulating in South Africa, following subcellular fractionation.

The appearance of HBsAg in serum is one of the first viral indicators of HBV infection, and is clinically used as an indicator of viral replication[112]. In the past 15 years HBsAg seroprevalence has been used to predict and monitor outcomes in acute HBV infection, as well as track disease progression and treatment response in chronic patients [62]. Investigating the differences in HBsAg expression between different HBV strains may therefore have important diagnostic implications.

4.1. Optimisation of Subcellular Fractionation and PEG Precipitation

Subcellular fractionation is a useful technique allowing for the separation of complex cells into purified compartments whose properties and constituents can be accurately analysed and quantified. Utilising inherent qualities attributed to proteins, such as size and density, cells are partitioned into fractions, mainly: nuclear, membrane and cytoplasmic [113, 114]. A common limitation in the acquiring of pure fractions is the difficulty in achieving the "ideal homogenate" – a suspension enriched for its individual cellular components and free from those of other fractions [115]. This is problematic since cellular compartments share similar properties and will generally co-fractionate to some extent [113].

Subcellular compartments are prone to cross-contamination with the cytoskeletal fraction, as organelles tend to remain associated with cytoskeletal elements [115]. This cross-contamination was observed in the present study, where defrosted Huh7 cell pellets exhibited notable cross-contamination with cytoskeletal proteins, and vice

versa, in all extracted fractions. Thus, a few modifications were tested to improve fraction purity, with an increase in Cytoskeletal Extraction Buffer incubation time improving the isolation of the cytoskeletal fraction. It was also observed that there was cross-contamination of the membrane fraction within the cytoplasmic fraction, only present in Huh7 cells that were previously frozen at -70 °C and defrosted. This occurrence can be attributed to the freeze-thaw process, where the integrity of cellular membranes is often compromised by the formation of ice-crystals. Maintenance of cells under ideal culture, harvesting and fractionation conditions (i.e. gentle washing of cells, keeping samples on ice, dexterity of technique when extracting supernatants containing individual fractions) greatly improved the overall purity and yield of fractions.

A protocol for the precipitation of HBV viral proteins from tissue culture supernatants was also developed and optimised. Initial precipitations of supernatants harvested from the culture of Huh7 cells transfected with A1-WT, on day 5 post-transfection, using a 37% PEG solution yielded extractions containing high volumes of aggregated serum proteins that interfered with the migration of the HBV proteins of interest. A lower concentration PEG solution of 7% was then used with little success and continued formation of serum aggregates. A PBS wash step was introduced, which proved to remove most of the excess serum, and cleared the 37% PEG extractions enough to proceed with optimisation. We then sought to improve the yield of the precipitates by doubling the volume of supernatants used while maintaining the previous volume of buffers used. This was successful, and further sonification of the precipitated pellets thoroughly homogenised the pellet within the resuspension buffer, providing clear and distinct bands of the similar quality expected from cell lysates. The established PEG protocol used was cheap and efficient, and provided quality precipitates suitable for downstream Western blotting analysis.

4.2. Subcellular Localisation of Intracellular HBsAg

Determining the subcellular localisation of HBsAg may provide insight into the factors influencing its assembly and secretion. Previous studies show that the variable localisation of HBV antigens within different compartments of the cell may be indicative of the disease status. For this reason, we sought to investigate the

distribution of HBsAg within Huh7 cells transiently transfected with one of the following subgenotypes: A1, A2 or D3, to determine if variations in subcellular localisation may contribute to differences in pathogenesis between subgenotypes.

Following subcellular fractionation of transiently transfected Huh7 cells, fractions were analysed using Western blotting and HBsAg detected using a mouse monoclonal antibody targeted towards the S-domain – hence all forms of HBsAg were collectively targeted, with no distinction between subviral particles or virions. It was observed that HBsAg was exclusively retained within the membrane fraction, with no detection the cytoplasm or remaining fractions. This was expected, as HBsAg is assembled within the ER, where subviral particles are secreted from the cell via the constitutive pathway of vesicular transport, while virions and filamentous subviral particles are secreted via the ESCRT endosomal pathway [47, 48]. Failure to detect HBsAg in the cytoplasmic fraction is in agreement with other studies that show cytoplasmic localisation of HBsAg to be generally associated with chronic HBV infection [84, 107-109], while the present study can only model acute HBV infection.

The membrane fraction isolated during subcellular fractionation was expected to contain the ER, Golgi and endosomes; however, it would have been interesting if it were possible to further fractionate these compartments to determine the expression of the various forms of HBsAg within the secretory pathway. It would be expected that HBV virions and L-HBs would show expression within the endosomes, while S-HBs and M-HBs would express higher localisation within the ER and Golgi compartments. Previous work with immunofluorescence shows that HBsAg and L-HBs do not co-localise in similar proportions within the ER and endosomal pathway [87].

4.3. The Composition of Intracellular and Extracellular HBsAg Differs Between Genotypes

Western blotting analysis was performed to determine the intracellular and extracellular expression of HBsAg between Huh7 cells transiently transfected with either subgenotype A1-WT, A2-WT or D3-WT. Intracellular HBsAg was analysed within the membrane fraction of transfected Huh7 cells harvested on day 5 post-transfection. Extracellular expression of HBsAg was analysed in PEG precipitated tissue culture

supernatants also collected on day 5 post-transfection. An ELISA was also conducted on tissue culture supernatants to determine the change in HBsAg expression over days 1, 3 and 5 post-transfection.

Western blotting analysis provided the opportunity to determine the proportion of S-HBs, M-HBs and L-HBs expression. There was an observed difference in HBsAg expression between subgenotypes A1-WT, A2-WT and D3-WT, with further distinctions in the proportions of S-HBs, M-HBs and L-HBs [47]. S-HBs was always expressed the highest as expected, as it constitutes the highest percentage in spherical and viral particles [62, 87]. L-HBs was expressed the second highest, with M-HBs being expressed the least. This pattern is expected, as both S-HBs and L-HBs play important roles within the HBV life cycle, while M-HBs seems to be dispensable [62].

Intracellularly, A1-WT presented with the lowest HBsAg expression compared to A2-WT and D3-WT, which was the highest. This may indicate that A1-WT replicates at a lower rate compared to A2-WT and D3-WT, or that A1-WT possibly secretes HBsAg out of the cell more efficiently. Additionally, A1-WT and D3-WT were found to express L-HBs in similar proportions, although A1-WT expressed a higher proportion of S-HBs. The ratio of S-HBs to L-HBs is important for successful virion secretion, as high L-HBs expression seems to be associated with retention of HBsAg within the ER of infected hepatocytes [81].

Genotype D has been noted to express HBsAg higher intracellularly [87], as well as displaying a higher S-HBs secretion efficiency compared to genotype A; however, increased L-HBs production in genotype D has a pronounced negative regulatory effect on S-HBs [116]. L-HBs has previously been shown to inhibit S-HBs secretion in a dose dependent manner [117]. Inhibition of S-HBs secretion may result in retention of HBsAg intracellularly leading to an ER stress response and liver disease pathogenesis, which may account for the increased severity and incidence of liver disease in patients infected with genotype D [104].

Extracellularly, HBsAg ELISA and PEG precipitated supernatants reveal that A1-WT expresses HBsAg the highest. This observation may support possibility that A1-WT

possesses the ability to secrete HBsAg with higher efficiency[116]. If HBsAg can be equated to viral loads, the data supports that subgenotype A1-WT has higher replicative potential compared to subgenotype A2-WT. While this may contradict previous research describing the low replicative activity of A1-WT, high levels of HBeAg and HBsAg secretion may confer an immune escape mechanism, allowing the HBV infection to progress towards chronicity. Furthermore, A1-WT and A2-WT express S-HBs, M-HBs and L-HBs at similar proportions extracellularly, and display elevated levels of S-HBs to a final proportion of approximately 80% of HBsAg. Indeed, M-HBs and L-HBs is expected to only represent approximately 20% of all HBsAg-containing particles [50].

Conversely, subgenotype D3-WT was found to express HBsAg the lowest extracellularly when measured with ELISA, and still lower than A1-WT when analysed with Western blotting. D3-WT was also noted to have lower proportions of S-HBs intracellularly and extracellularly, compared to A1-WT and A2-WT. As discussed earlier, the higher proportion of L-HBs may be causing retention of HBsAg intracellularly in subgenotype D3-WT.

4.4. Glycosylation of HBsAg Differs Between Genotypes

An interesting observation noted in the present study was the variation in the glycosylation of S-HBs, M-HBs and L-HBs intracellularly and extracellularly, between subgenotypes A1-WT, A2-WT and D3-WT.

The major HBV antigenic epitope, the "a" determinant, includes the N-glycosylation site at asparagine residue 146 where all forms of HBsAg are N-glycosylated. This N-glycosylation site is extremely conserved but only functional approximately half the time[118]. N-glycosylation is essential for numerous protein functions, including protein folding, sorting, secretion, quality control and degradation; the surface proteins of enveloped viruses are frequently N-glycosylated to improve stability and function in particle assembly and viral infectivity [119].

Interestingly, many enveloped viruses heavily glycosylate their surface proteins to mask themselves from the immune system and evade neutralising antibodies [119] –

HBV is no exception. Elevated levels of N-glycosylation have been associated with immune escape mutants [120-122]. Mutational analysis studies show that N-glycosylation is crucial for the secretion of HBV virions, but not subviral particles [122, 123].

Although the ratio of nonglycosylated S-HBs to glycosylated S-HBs, and monoglycosylated M-HBs to biglycosylated M-HBs is expected to be approximately 1:1 [118], Western blot analyses in this study show otherwise. Nonglycosylated S-HBs and monoglycosylated M-HBs was generally higher than their further glycosylated counterparts. There was also a visible reduction in glycosylated S-HBs and biglycosylated M-HBs extracellularly compared to intracellularly in A1-WT and D3-WT. Notably, A2-WT expressed increased biglycosylated M-HBs extracellularly versus intracellularly, but also appeared to express glycosylated S-HBs and L-HBs higher compared to A1-WT. This may confer an immune escape adaptation in subgenotype A2-WT, especially when considering the presence of B cell and T cell epitopes on the PreS1 and PreS2 domains.

The ratio of nonglycosylated L-HBs to glycosylated L-HBs could not be quantified due to their close proximity and co-migration on the Western blot, thus the ratio had to be estimated via close visual inspection of the Western blot. Throughout this study it was observed that the ratio of nonglycosylated to glycosylated L-HBs was approximately 1:1, with the exception of A2-WT discussed earlier. The careful balance of this ratio has two implications; firstly, it may be possible that glycosylation of L-HBs modifies its ability to bind to endosomal components within the ESCRT secretory pathway; and studies show that reduction in N-glycosylation inhibits virion secretion but not subviral particle secretion[123]. Secondly, hyperglycosylation of L-HBs could result in the masking of the myristoylated domain required for binding to the NTCP, thus reducing viral infectivity. Hyperglycosylated mutants expressing a high density of glycans on the surface their virions show exhibited impaired infectivity [118].

4.5. Extracellular Expression of HBeAg Differs Between Genotypes

HBeAg is clinically used as an indicator of HBV infectivity, disease severity and treatment response [42], and is an especially important biomarker used in the monitoring of chronic HBV infection [111]. Normally, HBeAg seroconversion is a sign of good prognosis, and is associated with clearance of HBcAg and HBV DNA from serum, as well as establishment of normal liver histology [44]. In the context of this study, quantification of HBeAg using ELISA was used as an indicator of viral replication.

A1-WT was found to express HBeAg the highest extracellularly, in agreement with data previously generated in the same lab[103]. Subgenotype A1-WT has been described as demonstrating low replicative potential compared to subgenotypes A2-WT and D3-WT [101], however the high HBeAg expression observed in this study appear to indicate that A1-WT replicates the highest compared to the other subgenotypes. However, it is possible that HBeAg levels are not directly proportional to viral replication for subgenotype A1.

With regards to subgenotype A2-WT, HBeAg appeared to enter the secretory pathway earlier than A1-WT or D3-WT, as evidence by the slight expression on day 1 post transfection. However, A2-WT continued to express HBeAg lower than A1-WT for the remaining days. Individuals infected with subgenotype A2-WT have been shown to remain HBeAg positive for a longer duration compared to those infected with A1-WT, which may be a result of lower HBeAg expression levels and a reduced host immune response to clear HBeAg. This may also account for the increased potential of A2-WT to establish chronic infection [96]. Additionally, a reduced immune response resulting from the lower levels of HBeAg and HBsAg expression in subgenotype A2-WT compared to A1-WT may account for the lower hepatocarcinogenic potential of A2-WT [96].

Subgenotype D3-WT was shown to express extracellular HBeAg lower than both subgenotypes A1-WT and A2-WT. *In vitro* studies [103] as well as patient data [124] confirm HBeAg expression in genotype D to generally be low; genotype D has been shown to have lower frequencies of HBeAg positivity as well as earlier HBeAg

seroconversion, which generally indicates a higher risk progression towards chronic infection [124].

4.6. ER Stress and HBV-associated Hepatocarcinogenesis

The ER is a complex tubular structure that forms an interconnected network with almost every membrane-bound organelle, including the Golgi, endosomes, mitochondria and the plasma membrane [125]. The rough ER containing ribosomes is involved in the production, folding and glycosylation of membrane proteins [126], while the smooth ER lacking ribosomes plays a role in numerous metabolic processes including the synthesis of cholesterol, carbohydrate metabolism and intracellular calcium regulation [127]. The most important function of the ER is to ensure the proper folding and modification of proteins maintained under strict quality control processes [128], which ensures that only correctly synthesised proteins are exported to the Golgi [129]. Viral infection results in the synthesis of immense volumes of viral proteins which overload the ER, compromising quality control processes and resulting in the aggregation of misfolded or unfolded proteins within the ER and induction of the ER stress response [83]. During productive HBV infection, an enormous amount of HBV surface proteins is synthesised and processed within the ER, often resulting in disruption of ER homeostasis and subsequent ER stress. HBV viral proteins accumulate within the ER, causing the ER to hypertrophy and resulting the formation of the histopathological condition termed ground-glass hepatocytes [82]. Chronic ER stress under disease states such as chronic HBV infection can induce liver necroinflammation and cirrhosis [83].

Excess production of HBV surface antigens as well as generation of misfolded forms of the M-HBs and L-HBs can induce ER stress pathways that initiate the unfolded protein response and cause carcinogenic oxidative stress. A 1985 study by Chisari and colleagues found that transgenic mice used as models for the chronic HBV carrier state overexpressed L-HBs, resulting in abnormal liver growth and damage, accompanied by liver repair and eventual progression towards HCC [45, 130].

Previous research shows that subgenotype A1-WT induced the unfolded protein response which was also prolonged over a greater period of time and induced higher

levels of apoptosis compared to subgenotypes A2-WT and D3-WT [103]. In the present study, extracellular HBeAg and HBsAg expression in subgenotype A1-WT was the highest compared to A2-WT and D3-WT, which may indicate overload of HBV viral proteins within the ER and a subsequent stress response. Chronic infection with subgenotype A1-WT and a resulting prolonged ER stress response with accumulating liver injury may explain the increased hepatocarcinogenic potential of subgenotype A1-WT compared to subgenotypes A2-WT and D3-WT.

4.7. Limitations and Future Studies

A limitation to the present study is the use of a commercial subcellular fractionation kit. The high price of the kit as well as the propriety nature of the buffers prevented extensive modification of the protocol and made it difficult to determine the influence of each buffer on the proteins of interest, if any at all. Future studies of this nature would be more practical using a manual subcellular fractionation protocol. Future studies would also benefit from the use of freshly harvested cell pellets, as this would more closely match *in vivo* conditions; also, the true extent of the influence the freeze-thaw process has on cells is not completely known and cannot be reliably controlled for.

During this study there was difficulty in acquiring Western blotting antibodies that would effectively detect HBeAg, which hindered investigation into the subcellular localisation of HBeAg within the different subgenotypes. Additionally, D3-WT (CMV+) was intended to be used as a control throughout all parts of this study, however when using the S-domain specific antibody (mAbHB1) there was decreased reactivity for HBsAg from D3-WT (CMV+) transfected cells, thus this control was not included during Western blotting analysis. Difficulty in detecting genotype D using Western blotting has been observed elsewhere [87], and may indicate an underlying issue in the detection of genotype D strains.

Regarding comparison of HBsAg expression intracellularly and extracellularly, it was difficult to find a protein that could be used as a loading control both intracellularly and extracellularly. Using a protein that is constitutively expressed at similar levels both inside and outside the cell would have allowed for a more definitive comparison of each

subgenotype and their secretion efficiencies of HBsAg. Also, apoptosis of cells in culture – either as a natural consequence of HBV infection or resulting from cell culture conditions – may provide an inaccurate representation of intracellular versus extracellular expression of HBV viral proteins.

Comparative analysis of the different HBV genotypes is often based on data collected from HBV-infected individuals, which presents a scenario influenced by the complex interplay between the virus and the immune response [87]. The present study uses an *in vitro* approach that standardises conditions and allows for comparative analyses between genotypes to be primarily based on the genetic differences of each genotype. We can gain insight on the production, morphogenesis, subcellular localisation and secretion of HBV particles, free from the influence of physiological factors associated with a host response. Conversely, because HBV viral particles are strongly immunogenic, it is important to correlate the differences in particle expression to the response elicited by the immune system, as it is the immune-mediated response that is largely responsible for liver necroinflammation and hepatocarcinogenesis [111]. Thus, future *in vitro* studies of this nature would benefit from an immune component, where genotypes are compared simultaneously in an environment free from immune mediators, as well as under conditions that mimic a host immune response. We could then model a more realistic environment and would be able to determine whether variations in the expression of HBeAg and HBsAg, and the relative proportions and glycosylation patterns of S-HBs, M-HBs and L-HBs do actually confer immunomodulatory adaptions.

Notably, there was a discrepancy in HBsAg expression of subgenotype A2-WT when measured with ELISA compared to measurement of PEG precipitated supernatants analysed using Western Blotting. PEG precipitated HBsAg appears to be lowest for A2-WT, whereas ELISA measurements show A2-WT expression to be higher than that of D3-WT. Considering that the ELISA kit is often used reliably as a diagnostic tool, the drop in HBsAg expression most likely lies with the PEG precipitation and Western blotting. It may be that a proportion of A2-WT HBsAg is not completely enriched during PEG precipitation, or that A1-WT and D3-WT express HBsAg in a manner that causes preferential enrichment when using PEG. Further investigation is required but was

limited because of time constraints. However, the HBsAg ELISA is specific towards the "a" determinant epitope expressed on all HBsAg particles, and therefore cannot differentiate between virions and subviral particles, nor the proportion of S-HBs, M-HBs and L-HBs in these particles (120). PEG precipitation accompanied by downstream Western blotting analysis was useful with respect to a more comprehensive characterisation of HBsAg expression. In light of this, confirmatory experiments where various techniques are used to measure the same outcome would also be useful. Qualitative studies such as immunofluorescence in conjunction with quantitative techniques such as flow cytometry or even an automated Western blotting analysis would provide more robust comparative analyses.

CHAPTER 5: CONCLUSION

HBsAg and HBeAg are virological markers with important diagnostic and clinical significance. HBsAg is of particular interest, as clearance of HBsAg is now considered the goal of a functional HBV cure [131]. This study contributes towards knowledge surrounding acute HBV infection, as well as the successful establishment of productive HBV transfection *in vitro*.

The present study aimed to comparatively analyse the expression of HBsAg between the different strains of HBV predominantly circulating in South Africa, following subcellular fractionation. To achieve this, Huh7 cells were transiently transfected with either subgenotypes A1-WT, A2-WT or D3-WT, and on day 5 post-transfection were then fractionated into cytoplasmic-, membrane-, soluble-nuclear-, chromatin-bound nuclear- and cytoskeletal- fractions. HBsAg was found to be exclusively localised within the membrane fraction, and subgenotype D3-WT expressed HBsAg the highest, followed by subgenotype A2-WT and lastly subgenotype A1-WT. Supernatants were also collected from these transiently transfected Huh7 cells on days 1, 3 and 5, and extracellular HBsAg expression was analysed using ELISA as well as Western blotting. Subgenotype A1-WT was observed to express HBsAg the highest extracellularly. Expression of HBeAg extracellularly was measured using ELISA, and subgenotype A1-WT was found to also express HBeAg the highest compared to A2-WT and D3-WT.

High levels of HBeAg and HBsAg associated with infection with subgenotype A1 could create an immunomodulatory environment which allows this HBV strain to circumvent the host immune response and establish chronic infection. Consequently, chronic infection could result in prolonged ER stress and hepatic injury, conferring an increased hepatocarcinogenic potential to subgenotype A1-WT.

Finally, Western blotting analysis of intracellular and extracellular HBsAg revealed notable differences in the expression of the different forms of HBsAg, namely S-HBs, M-HBs and L-HBs. As far as we are aware, this is the first study to comparatively analyse the proportion and glycosylation of HBsAg in subgenotypes A1, A2 and D3. Variations in the proportion and glycosylation of S-HBs, M-HBs and L-HBs were observed, and differences in HBsAg expression may influence the host immune response as well as

the progression of HBV infection from acute to chronic, towards an increased risk of HCC. This study contributes to the body of evidence surrounding the natural history of HBV infection, which is essential for HBV diagnosis, disease management and the development of therapeutics.

REFERENCES

1. Organization WH. Hepatitis B Fact Sheet 2018. Available from: https://www.who.int/news-room/fact-sheets/detail/hepatitis-b.

2. Polaris Observatory C. Global prevalence, treatment, and prevention of hepatitis B virus infection in 2016: a modelling study. The Lancet gastroenterology & hepatology. 2018;3(6):383-403.

3. Bray F, Ferlay J, Soerjomataram I, Siegel RL, Torre LA, Jemal A. Global cancer statistics 2018: GLOBOCAN estimates of incidence and mortality worldwide for 36 cancers in 185 countries. CA: a cancer journal for clinicians. 2018;68(6):394-424.

4. Han GR, Cao MK, Zhao W, Jiang HX, Wang CM, Bai SF, et al. A prospective and open-label study for the efficacy and safety of telbivudine in pregnancy for the prevention of perinatal transmission of hepatitis B virus infection. J Hepatol. 2011;55(6):1215-21.

5. Chu CJ, Hussain M, Lok AS. Hepatitis B virus genotype B is associated with earlier HBeAg seroconversion compared with hepatitis B virus genotype C. Gastroenterology. 2002;122(7):1756-62.

6. Kao JH, Chen PJ, Lai MY, Chen DS. Clinical and virological aspects of blood donors infected with hepatitis B virus genotypes B and C. Journal of clinical microbiology. 2002;40(1):22-5.

7. Kramvis A, Kew MC. Epidemiology of hepatitis B virus in Africa, its genotypes and clinical associations of genotypes. Hepatology research : the official journal of the Japan Society of Hepatology. 2007;37(s1):S9-S19.

8. Spearman CW, Sonderup MW. Preventing hepatitis B and hepatocellular carcinoma in South Africa: The case for a birth-dose vaccine. South African medical journal. 2014;104(9):610-2.

9. Baig S. Gender disparity in infections of Hepatitis B virus. Journal of the College of Physicians and Surgeons--Pakistan : JCPSP. 2009;19(9):598-600.

10. Jang SY, Jang SI, Bae HC, Shin J, Park EC. Sex differences associated with hepatitis B virus surface antigen seropositivity unwareness in hepatitis B virus surface antigen-positive adults: 2007-2012 Korea National Health and Nutrition Examination Survey. Journal of preventive medicine and public health. 2015;48(2):74-83.

11. Blumberg BS. Sex differences in response to hepatitis B virus. I. History. Arthritis and rheumatism. 1979;22(11):1261-6.

12. Mason WS, Gerlich, WH, Taylor JM, Kann M, Mizokami T, Loeb D, Sureau C, Magnius L, Norder H. ICTV 9th Report 2011. Available from: https://talk.ictvonline.org/ictv-reports/ictv_9th_report/reverse-transcribing-dna-and-rna-viruses-2011/w/rt_viruses/155/hepadnaviridae.

13. Liang TJ. Hepatitis B: the virus and disease. Hepatology. 2009;49(5 Suppl):S13-21.

14. Lauber C, Seitz S, Mattei S, Suh A, Beck J, Herstein J, et al. Deciphering the origin and evolution of hepatitis B viruses by means of a family of non-enveloped fish viruses. Cell host & microbe. 2017;22(3):387-99.

15. Muhlemann B, Jones TC, Damgaard PB, Allentoft ME, Shevnina I, Logvin A, et al. Ancient hepatitis B viruses from the Bronze Age to the Medieval period. Nature. 2018;557(7705):418-23.

16. Valaydon ZS, Locarnini SA. The virological aspects of hepatitis B. Best practice & research clinical gastroenterology. 2017;31(3):257-64.

17. Kidd-Ljunggren K, Holmberg A, Blackberg J, Lindqvist B. High levels of hepatitis B virus DNA in body fluids from chronic carriers. The journal of hospital infection. 2006;64(4):352-7.

18. Dane DS, Cameron CH, Briggs M. Virus-like particles in serum of patients with Australia-antigen-associated hepatitis. Lancet. 1970;1(7649):695-8.

19. Komiya Y, Katayama K, Yugi H, Mizui M, Matsukura H, Tomoguri T, et al. Minimum infectious dose of hepatitis B virus in chimpanzees and difference in the dynamics of viremia between genotype A and genotype C. Transfusion. 2008;48(2):286-94.

20. Vasilios Papastergiou RL, Douglas MacDonald, Emmanuel A. Tsochatzis. Global epidemiology of hepatitis B virus (HBV) infection. Current hepatology reports. 2015;4(3):171-8.

21. McMahon BJ, Alward WL, Hall DB, Heyward WL, Bender TR, Francis DP, et al. Acute hepatitis B virus infection: relation of age to the clinical expression of disease and subsequent development of the carrier state. The Journal of infectious diseases. 1985;151(4):599-603.

22. Araujo NM, Waizbort R, Kay A. Hepatitis B virus infection from an evolutionary point of view: how viral, host, and environmental factors shape genotypes and subgenotypes. Infection, genetics and evolution : journal of molecular epidemiology and evolutionary genetics in infectious diseases. 2011;11(6):1199-207.

23. Bond WW, Favero MS, Petersen NJ, Gravelle CR, Ebert JW, Maynard JE. Survival of hepatitis B virus after drying and storage for one week. Lancet. 1981;1(8219):550-1.

24. Seeger C, Mason WS. Molecular biology of hepatitis B virus infection. Virology. 2015;479-480:672-86.
25. Raffetti E, Fattovich G, Donato F. Incidence of hepatocellular carcinoma in untreated subjects with chronic hepatitis B: a systematic review and meta-analysis. Liver international : official journal of the International Association for the Study of the Liver. 2016;36(9):1239-51.
26. Varbobitis I, Papatheodoridis GV. The assessment of hepatocellular carcinoma risk in patients with chronic hepatitis B under antiviral therapy. Clinical and molecular hepatology. 2016;22(3):319-26.
27. Blumberg BS, Gerstley BJ, Hungerford DA, London WT, Sutnick AI. A serum antigen (Australia antigen) in Down's syndrome, leukemia, and hepatitis. Annals of internal medicine. 1967;66(5):924-31.
28. Bruss V. Hepatitis B virus morphogenesis. World journal of gastroenterology. 2007;13(1):65-73.
29. Landers TA, Greenberg HB, Robinson WS. Structure of hepatitis B Dane particle DNA and nature of the endogenous DNA polymerase reaction. Journal of virology. 1977;23(2):368-76.
30. Kaplan PM, Greenman RL, Gerin JL, Purcell RH, Robinson WS. DNA polymerase associated with human hepatitis B antigen. Journal of virology. 1973;12(5):995-1005.
31. Summers J, O'Connell A, Millman I. Genome of hepatitis B virus: restriction enzyme cleavage and structure of DNA extracted from Dane particles. Proceedings of the National Academy of Sciences of the United States of America. 1975;72(11):4597-601.
32. Tiollais P, Pourcel C, Dejean A. The hepatitis B virus. Nature. 1985;317(6037):489-95.
33. Clark DN, Hu J. Unveiling the roles of HBV polymerase for new antiviral strategies. Future virology. 2015;10(3):283-95.
34. Hatton T, Zhou S, Standring DN. RNA- and DNA-binding activities in hepatitis B virus capsid protein: a model for their roles in viral replication. Journal of virology. 1992;66(9):5232-41.
35. Stanaway JD, Flaxman AD, Naghavi M, Fitzmaurice C, Vos T, Abubakar I, et al. The global burden of viral hepatitis from 1990 to 2013: findings from the Global Burden of Disease Study 2013. Lancet. 2016;388(10049):1081-8.
36. Caballero A, Tabernero D, Buti M, Rodriguez-Frias F. Hepatitis B virus: The challenge of an ancient virus with multiple faces and a remarkable replication strategy. Antiviral research. 2018;158:34-44.
37. Garcia PD, Ou JH, Rutter WJ, Walter P. Targeting of the hepatitis B virus precore protein to the endoplasmic reticulum membrane: after signal peptide cleavage translocation can be aborted and the product released into the cytoplasm. The Journal of cell biology. 1988;106(4):1093-104.
38. Chang C, Enders G, Sprengel R, Peters N, Varmus HE, Ganem D. Expression of the precore region of an avian hepatitis B virus is not required for viral replication. Journal of virology. 1987;61(10):3322-5.
39. Chen HS, Kew MC, Hornbuckle WE, Tennant BC, Cote PJ, Gerin JL, et al. The precore gene of the woodchuck hepatitis virus genome is not essential for viral replication in the natural host. Journal of virology. 1992;66(9):5682-4.
40. Miyakawa Y, Okamoto H, Mayumi M. The molecular basis of hepatitis B e antigen (HBeAg)-negative infections. Journal of viral hepatitis. 1997;4(1):1-8.
41. Revill P, Yuen L, Walsh R, Perrault M, Locarnini S, Kramvis A. Bioinformatic analysis of the hepadnavirus e-antigen and its precursor identifies remarkable sequence conservation in all orthohepadnaviruses. Journal of medical virology. 2010;82(1):104-15.
42. Milich D, Liang TJ. Exploring the biological basis of hepatitis B e antigen in hepatitis B virus infection. Hepatology. 2003;38(5):1075-86.
43. Milich DR, Jones JE, Hughes JL, Price J, Raney AK, McLachlan A. Is a function of the secreted hepatitis B e antigen to induce immunologic tolerance in utero? Proceedings of the National Academy of Sciences of the United States of America. 1990;87(17):6599-603.
44. Brunetto MR, Giarin MM, Oliveri F, Chiaberge E, Baldi M, Alfarano A, et al. Wild-type and e antigen-minus hepatitis B viruses and course of chronic hepatitis. Proceedings of the National Academy of Sciences of the United States of America. 1991;88(10):4186-90.
45. Bouchard MJ, Navas-Martin S. Hepatitis B and C virus hepatocarcinogenesis: lessons learned and future challenges. Cancer letters. 2011;305(2):123-43.
46. Bouchard MJ, Schneider RJ. The enigmatic X gene of hepatitis B virus. Journal of virology. 2004;78(23):12725-34.
47. Bruss V, Ganem D. Mutational analysis of hepatitis B surface antigen particle assembly and secretion. Journal of virology. 1991;65(7):3813-20.
48. Bruss V, Ganem D. The role of envelope proteins in hepatitis B virus assembly. Proceedings of the National Academy of Sciences of the United States of America. 1991;88(3):1059-63.
49. Jiang B, Himmelsbach K, Ren H, Boller K, Hildt E. Subviral hepatitis B virus filaments, like infectious viral particles, are released via multivesicular bodies. Journal of virology. 2015;90(7):3330-41.

50. Heermann KH, Goldmann U, Schwartz W, Seyffarth T, Baumgarten H, Gerlich WH. Large surface proteins of hepatitis B virus containing the pre-s sequence. Journal of virology. 1984;52(2):396-402.
51. De Falco S, Ruvo M, Verdoliva A, Scarallo A, Raimondo D, Raucci A, et al. N-terminal myristylation of HBV preS1 domain enhances receptor recognition. The journal of peptide research : official journal of the American Peptide Society. 2001;57(5):390-400.
52. Cao J, Zhang J, Lu Y, Luo S, Zhang J, Zhu P. Cryo-EM structure of native spherical subviral particles isolated from HBV carriers. Virus research. 2019;259:90-6.
53. Ferrari C, Penna A, Bertoletti A, Cavalli A, Valli A, Schianchi C, et al. The preS1 antigen of hepatitis B virus is highly immunogenic at the T cell level in man. The Journal of clinical investigation. 1989;84(4):1314-9.
54. Milich DR. Genetic and molecular basis for T- and B-cell recognition of hepatitis B viral antigens. Immunological reviews. 1987;99:71-103.
55. Berting A, Hahnen J, Kroger M, Gerlich WH. Computer-aided studies on the spatial structure of the small hepatitis B surface protein. Intervirology. 1995;38(1-2):8-15.
56. Eble BE, MacRae DR, Lingappa VR, Ganem D. Multiple topogenic sequences determine the transmembrane orientation of the hepatitis B surface antigen. Molecular and cellular biology. 1987;7(10):3591-601.
57. Peterson DL, Nath N, Gavilanes F. Structure of hepatitis B surface antigen. Correlation of subtype with amino acid sequence and location of the carbohydrate moiety. The Journal of biological chemistry. 1982;257(17):10414-20.
58. Sun Y, Wang S, Yi Y, Zhang J, Duan Z, Yuan K, et al. The hepatitis B surface antigen binding protein: an immunoglobulin G constant region-like protein that interacts with HBV envelop proteins and mediates HBV entry. Frontiers in cellular and infection microbiology. 2018;8(338).
59. Schulze A, Schieck A, Ni Y, Mier W, Urban S. Fine mapping of pre-S sequence requirements for hepatitis b virus large envelope protein-mediated receptor interaction. Journal of virology. 2010;84(4):1989.
60. Gerlich WH, Heermann KH, Lu X. Functions of hepatitis B surface proteins. Archives of virology supplementum. 1992;4:129-32.
61. Eble BE, Lingappa VR, Ganem D. The N-terminal (pre-S2) domain of a hepatitis B virus surface glycoprotein is translocated across membranes by downstream signal sequences. Journal of virology. 1990;64(3):1414-9.
62. Cornberg M, Wong VW, Locarnini S, Brunetto M, Janssen HLA, Chan HL. The role of quantitative hepatitis B surface antigen revisited. Journal of hepatology. 2017;66(2):398-411.
63. Fernholz D, Stemler M, Brunetto M, Bonino F, Will H. Replicating and virion secreting hepatitis B mutant virus unable to produce preS2 protein. Journal of hepatololgy. 1991;13 Suppl 4:S102-4.
64. Bruss V, Vieluf K. Functions of the internal pre-S domain of the large surface protein in hepatitis B virus particle morphogenesis. Journal of virology. 1995;69(11):6652-7.
65. Summers J, Smith PM, Horwich AL. Hepadnavirus envelope proteins regulate covalently closed circular DNA amplification. Journal of virology. 1990;64(6):2819-24.
66. Summers J, Smith PM, Huang MJ, Yu MS. Morphogenetic and regulatory effects of mutations in the envelope proteins of an avian hepadnavirus. Journal of virology. 1991;65(3):1310-7.
67. Yan H, Zhong G, Xu G, He W, Jing Z, Gao Z, et al. Sodium taurocholate cotransporting polypeptide is a functional receptor for human hepatitis B and D virus. eLife. 2012;1:e00049.
68. Bruss V, Hagelstein J, Gerhardt E, Galle PR. Myristylation of the large surface protein is required for hepatitis B virus in vitro infectivity. Virology. 1996;218(2):396-9.
69. Patzer EJ, Nakamura GR, Simonsen CC, Levinson AD, Brands R. Intracellular assembly and packaging of hepatitis B surface antigen particles occur in the endoplasmic reticulum. Journal of virology. 1986;58(3):884-92.
70. Huovila AP, Eder AM, Fuller SD. Hepatitis B surface antigen assembles in a post-ER, pre-Golgi compartment. The journal of cell biology. 1992;118(6):1305-20.
71. Patient R, Hourioux C, Roingeard P. Morphogenesis of hepatitis B virus and its subviral envelope particles. Cellular microbiology. 2009;11(11):1561-70.
72. Roingeard P, Sureau C. Ultrastructural analysis of hepatitis B virus in HepG2-transfected cells with special emphasis on subviral filament morphogenesis. Hepatology. 1998;28(4):1128-33.
73. Jiang B, Himmelsbach K, Ren H, Boller K, Hildt E. Subviral hepatitis B virus filaments, like infectious viral particles, are released via multivesicular bodies. Journal of virology. 2016;90(7):3330-41.
74. Liou W, Sung YJ, Tao MH, Lo SJ. Morphogenesis of the hepatitis B virion and subviral particles in the liver of transgenic mice. Journal of biomedical science. 2008;15(3):311-6.

75. Watanabe T, Sorensen EM, Naito A, Schott M, Kim S, Ahlquist P. Involvement of host cellular multivesicular body functions in hepatitis B virus budding. Proceedings of the National Academy of Sciences of the United States of America. 2007;104(24):10205-10.
76. Kian Chua P, Lin MH, Shih C. Potent inhibition of human Hepatitis B virus replication by a host factor Vps4. Virology. 2006;354(1):1-6.
77. Slagsvold T, Pattni K, Malerod L, Stenmark H. Endosomal and non-endosomal functions of ESCRT proteins. Trends in cell biology. 2006;16(6):317-26.
78. Rost M, Mann S, Lambert C, Doring T, Thome N, Prange R. Gamma-adaptin, a novel ubiquitin-interacting adaptor, and Nedd4 ubiquitin ligase control hepatitis B virus maturation. The Journal of biological chemistry. 2006;281(39):29297-308.
79. Lambert C, Doring T, Prange R. Hepatitis B virus maturation is sensitive to functional inhibition of ESCRT-III, Vps4, and gamma 2-adaptin. Journal of virology. 2007;81(17):9050-60.
80. Grigorov B, Arcanger F, Roingeard P, Darlix JL, Muriaux D. Assembly of infectious HIV-1 in human epithelial and T-lymphoblastic cell lines. Journal of molecular biology. 2006;359(4):848-62.
81. Persing DH, Varmus HE, Ganem D. Inhibition of secretion of hepatitis B surface antigen by a related presurface polypeptide. Science. 1986;234(4782):1388-91.
82. Wang HC, Wu HC, Chen CF, Fausto N, Lei HY, Su IJ. Different types of ground glass hepatocytes in chronic hepatitis B virus infection contain specific pre-S mutants that may induce endoplasmic reticulum stress. The American journal of pathology. 2003;163(6):2441-9.
83. Kim SY, Kyaw YY, Cheong J. Functional interaction of endoplasmic reticulum stress and hepatitis B virus in the pathogenesis of liver diseases. World journal of gastroenterology. 2017;23(43):7657-65.
84. Chua PK, Wang RY, Lin MH, Masuda T, Suk FM, Shih C. Reduced secretion of virions and hepatitis B virus (HBV) surface antigen of a naturally occurring HBV variant correlates with the accumulation of the small S envelope protein in the endoplasmic reticulum and Golgi apparatus. Journal of virology. 2005;79(21):13483-96.
85. Szmuness W, Stevens CE, Harley EJ, Zang EA, Oleszko WR, William DC, et al. Hepatitis B vaccine: demonstration of efficacy in a controlled clinical trial in a high-risk population in the United States. The New England journal of medicine. 1980;303(15):833-41.
86. Simon B, Kundi M, Puchhammer E. Analysis of mutations in the S gene of hepatitis B virus strains in patients with chronic infection by online bioinformatics tools. Journal of clinical microbiology. 2013;51(1):163-8.
87. Hassemer M, Finkernagel M, Peiffer KH, Glebe D, Akhras S, Reuter A, et al. Comparative characterization of hepatitis B virus surface antigen derived from different hepatitis B virus genotypes. Virology. 2017;502:1-12.
88. Lee JM, Ahn SH. Quantification of HBsAg: basic virology for clinical practice. World journal of gastroenterology. 2011;17(3):283-9.
89. Coleman PF. Detecting hepatitis B surface antigen mutants. Emerging infectious diseases. 2006;12(2):198-203.
90. Siegler VD, Bruss V. Role of transmembrane domains of hepatitis B virus small surface proteins in subviral-particle biogenesis. Journal of virology. 2013;87(3):1491-6.
91. Kann M, Schmitz A, Rabe B. Intracellular transport of hepatitis B virus. World journal of gastroenterology. 2007;13(1):39-47.
92. Ganem D, Varmus HE. The molecular biology of the hepatitis B viruses. Annual review of biochemistry. 1987;56:651-93.
93. Gunther S, Fischer L, Pult I, Sterneck M, Will H. Naturally occurring variants of hepatitis B virus. Advances in virus research. 1999;52:25-137.
94. Kramvis A, Kew M, Francois G. Hepatitis B virus genotypes. Vaccine. 2005;23(19):2409-23.
95. Kramvis A, Arakawa K, Yu MC, Nogueira R, Stram DO, Kew MC. Relationship of serological subtype, basic core promoter and precore mutations to genotypes/subgenotypes of hepatitis B virus. Journal of medical virology. 2008;80(1):27-46.
96. Kramvis A. Genotypes and genetic variability of hepatitis B virus. Intervirology. 2014;57(3-4):141-50.
97. Kramvis A, Kew MC, Bukofzer S. Hepatitis B virus precore mutants in serum and liver of Southern African Blacks with hepatocellular carcinoma. J Hepatol. 1998;28(1):132-41.
98. Tanaka Y, Hasegawa I, Kato T, Orito E, Hirashima N, Acharya SK, et al. A case-control study for differences among hepatitis B virus infections of genotypes A (subtypes Aa and Ae) and D. Hepatology. 2004;40(3):747-55.

99. Kew MC, Kramvis A, Yu MC, Arakawa K, Hodkinson J. Increased hepatocarcinogenic potential of hepatitis B virus genotype A in Bantu-speaking sub-saharan Africans. Journal of medical virology. 2005;75(4):513-21.
100. Kramvis A. Molecular characteristics and clinical relevance of African genotypes and subgenotypes of hepatitis B virus. South African medical journal. 2018 8;108(8b):17-21.
101. Bhoola NH, Reumann K, Kew MC, Will H, Kramvis A. Construction of replication competent plasmids of hepatitis B virus subgenotypes A1, A2 and D3 with authentic endogenous promoters. Journal of virological methods. 2014;203:54-64.
102. Sugiyama M, Tanaka Y, Kato T, Orito E, Ito K, Acharya SK, et al. Influence of hepatitis B virus genotypes on the intra- and extracellular expression of viral DNA and antigens. Hepatology. 2006;44(4):915-24.
103. Bhoola NH, Kramvis A. Hepatitis B e antigen expression by hepatitis B virus subgenotype A1 relative to subgenotypes A2 and D3 in cultured hepatocellular carcinoma (Huh7) cells. Intervirology. 2016;59(1):48-59.
104. McMahon BJ. The influence of hepatitis B virus genotype and subgenotype on the natural history of chronic hepatitis B. Hepatology international. 2009;3(2):334-42.
105. Chandra PK, Biswas A, Datta S, Banerjee A, Panigrahi R, Chakrabarti S, et al. Subgenotypes of hepatitis B virus genotype D (D1, D2, D3 and D5) in India: differential pattern of mutations, liver injury and occult HBV infection. Journal of viral hepatitis. 2009;16(10):749-56.
106. Saito T, Kamimura T, Asakura H, Ishikawa M. Ultrastructural localization of Pre-S2 polypeptides in the liver tissues of patients with chronic hepatitis B virus infection. Liver. 1989;9(6):329-37.
107. Ray MB, Desmet VJ, Bradburne AF, Desmyter J, Fevery J, De Groote J. Differential distribution of hepatitis B surface antigen and hepatitis B core antigen in the liver of hepatitis B patients. Gastroenterology. 1976;71(3):462-9.
108. Gowans EJ, Burrell CJ, Jilbert AR, Marmion BP. Patterns of single- and double-stranded hepatitis B virus DNA and viral antigen accumulation in infected liver cells. The journal of general virology. 1983;64(6):1229-39.
109. Chu CM, Liaw YF. Intrahepatic distribution of hepatitis B surface and core antigens in chronic hepatitis B virus infection. Hepatocyte with cytoplasmic/membranous hepatitis B core antigen as a possible target for immune hepatocytolysis. Gastroenterology. 1987;92(1):220-5.
110. Fattovich G, Bortolotti F, Donato F. Natural history of chronic hepatitis B: special emphasis on disease progression and prognostic factors. Journal of hepatology. 2008;48(2):335-52.
111. Gish RG, Given BD, Lai CL, Locarnini SA, Lau JY, Lewis DL, et al. Chronic hepatitis B: Virology, natural history, current management and a glimpse at future opportunities. Antiviral research. 2015;121:47-58.
112. Krugman S, Overby LR, Mushahwar IK, Ling CM, Frosner GG, Deinhardt F. Viral hepatitis, type B. Studies on natural history and prevention re-examined. The New England journal of medicine. 1979;300(3):101-6.
113. Huber LA, Pfaller K, Vietor I. Organelle proteomics: implications for subcellular fractionation in proteomics. Circulation research. 2003;92(9):962-8.
114. Stasyk T, Huber LA. Zooming in: fractionation strategies in proteomics. Proteomics. 2004;4(12):3704-16.
115. Howell KE, Devaney E, Gruenberg J. Subcellular fractionation of tissue culture cells. Trends in biochemical sciences. 1989;14(2):44-7.
116. Zhang F, Tang X, Garcia T, Lok AS, Wang Y, Jia H, et al. Characterization of contrasting features between hepatitis B virus genotype A and genotype D in small envelope protein expression and surface antigen secretion. Virology. 2017;503:52-61.
117. Chisari FV, Filippi P, McLachlan A, Milich DR, Riggs M, Lee S, et al. Expression of hepatitis B virus large envelope polypeptide inhibits hepatitis B surface antigen secretion in transgenic mice. Journal of virology. 1986;60(3):880-7.
118. Julithe R, Abou-Jaoude G, Sureau C. Modification of the hepatitis B virus envelope protein glycosylation pattern interferes with secretion of viral particles, infectivity, and susceptibility to neutralizing antibodies. Journal of virology. 2014;88(16):9049-59.
119. Vigerust DJ, Shepherd VL. Virus glycosylation: role in virulence and immune interactions. Trends in microbiology. 2007;15(5):211-8.
120. Chen MT, Billaud JN, Sallberg M, Guidotti LG, Chisari FV, Jones J, et al. A function of the hepatitis B virus precore protein is to regulate the immune response to the core antigen. Proceedings of the National Academy of Sciences of the United States of America. 2004;101(41):14913-8.

121. Yu DM, Li XH, Mom V, Lu ZH, Liao XW, Han Y, et al. N-glycosylation mutations within hepatitis B virus surface major hydrophilic region contribute mostly to immune escape. Journal of hepatology. 2014;60(3):515-22.
122. Kwei K, Tang X, Lok AS, Sureau C, Garcia T, Li J, et al. Impaired virion secretion by hepatitis B virus immune escape mutants and its rescue by wild-type envelope proteins or a second-site mutation. Journal of virology. 2013;87(4):2352-7.
123. Ito K, Qin Y, Guarnieri M, Garcia T, Kwei K, Mizokami M, et al. Impairment of hepatitis B virus virion secretion by single-amino-acid substitutions in the small envelope protein and rescue by a novel glycosylation site. Journal of virology. 2010;84(24):12850-61.
124. Mustafa MZ, Schofield J, Mills PR, Priest M, Fox R, Datta S, et al. The efficacy and safety of treating hepatitis C in patients with a diagnosis of schizophrenia. Journal of viral hepatitis. 2014;21(7):e48-51.
125. Friedman JR, Voeltz GK. The ER in 3D: a multifunctional dynamic membrane network. Trends in cell biology. 2011;21(12):709-17.
126. Gorlich D, Prehn S, Hartmann E, Kalies KU, Rapoport TA. A mammalian homolog of SEC61p and SECYp is associated with ribosomes and nascent polypeptides during translocation. Cell. 1992;71(3):489-503.
127. de Brito OM, Scorrano L. An intimate liaison: spatial organization of the endoplasmic reticulum-mitochondria relationship. The EMBO journal. 2010;29(16):2715-23.
128. Schroder M, Kaufman RJ. ER stress and the unfolded protein response. Mutation research. 2005;569(1-2):29-63.
129. Ellgaard L, Molinari M, Helenius A. Setting the standards: quality control in the secretory pathway. Science. 1999;286(5446):1882-8.
130. Chisari FV, Pinkert CA, Milich DR, Filippi P, McLachlan A, Palmiter RD, et al. A transgenic mouse model of the chronic hepatitis B surface antigen carrier state. Science. 1985;230(4730):1157-60.
131. Locarnini S, Hatzakis A, Chen DS, Lok A. Strategies to control hepatitis B: Public policy, epidemiology, vaccine and drugs. J Hepatol. 2015;62(1):S76-86.

APPENDIX I: ETHICS CLEARANCE CERTIFICATE

Human Research Ethics Committee (Medical) 50 years 1966 – 2016

Research Office Secretariat: Faculty of Health Sciences, Phillip Tobias Building, 3rd Floor, Office 301,
29 Princess of Wales Terrace, Parktown, 2193 Tel +27 (0)11-717-1252 /1234/2656/2700
Private Bag 3, Wits 2050, email: zanele.ndlovu@wits.ac.za
Office email: hrec-medical.researchoffice@wits.ac.za
Website: www.wits.ac.za/research/about-our-research/ethics-and-research-integrity/

Ref: W-CJ-170308-2 08/03/2017

TO WHOM IT MAY CONCERN:

Waiver: This certifies that the following research does not require clearance from the Human Research Ethics Committee (Medical).

Investigator: Ms Thanusha Pillay (student no. 732728).

Project title: Study of the expression of HBsAg and HBeAg by different African genotypes of HBV using cellular fractionation.

Reason: This is a laboratory study using tissue culture and previously constructed plasmids. There are no human participants.

Professor Peter Cleaton-Jones

Chair: Human Research Ethics Committee (Medical)

UNIVERSITY OF THE WITWATERSRAND
PROF PE CLEATON-JONES
HREC (MEDICAL)
2017 -03- 08
JOHANNESBURG

Copy – HREC (Medical) Secretariat: Zanele Ndlovu, Rhulani Mkansi, Lebo Moeng.

Figure 31. Ethics clearance certificate

APPENDIX II: REPLICATION COMPETENT CLONE PLASMID MAPS

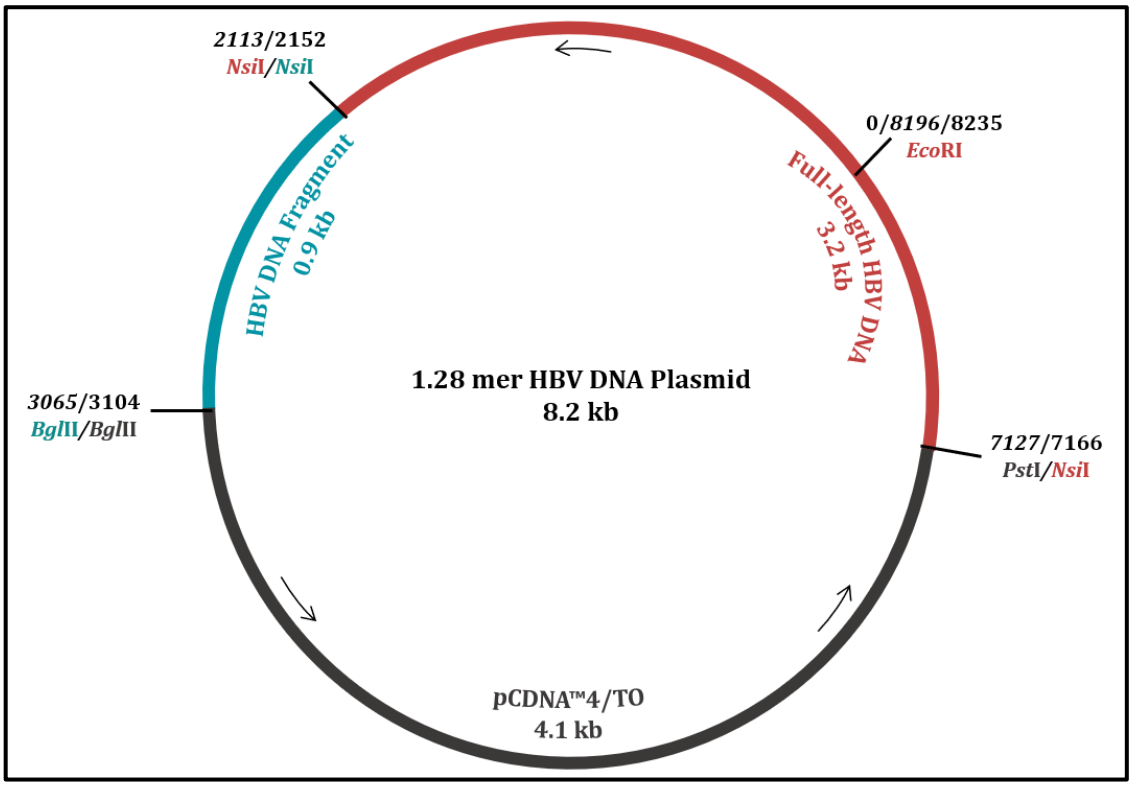


Figure 32. Schematic illustration of the 1.28 mer replication competent plasmid containing HBV wild-type subgenotype A1, A2, or D3

Restriction site locations (in base pairs) corresponding to A1- WT and A2-WT are Romanised, and D3-WT sites are indicated in *italics*.

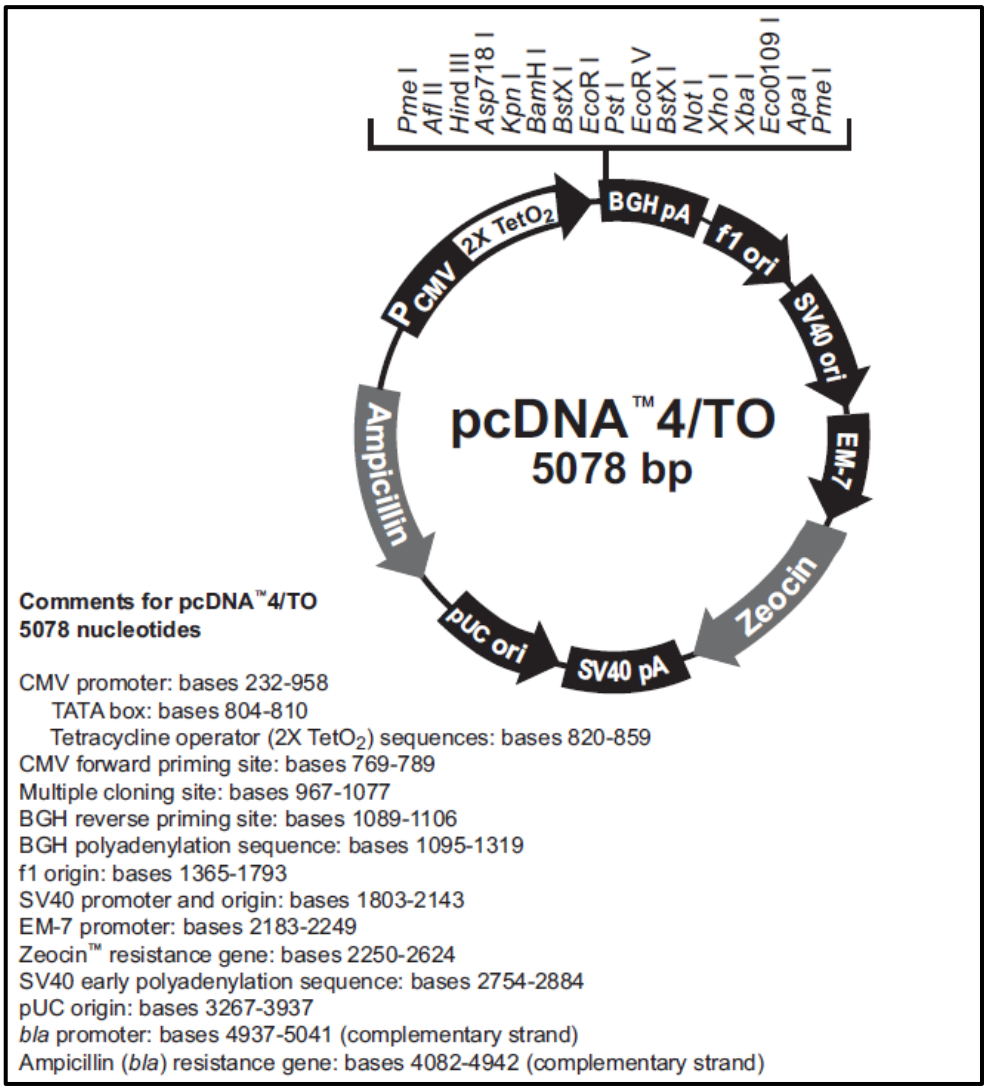


Figure 33. Schematic illustration of the pCDNA 4/TO mammalian expression vector

The pCDNA™4/TO expression vector contains an ampicillin resistance ORF, allowing only bacteria containing this vector to grow in medium containing ampicillin. The vector contains two *Bgl*II restriction enzyme recognition sites, one *Pst*I restriction enzyme recognition site which were used to generate the 1.28 mer HBV plasmidss containing an HBV authentic promoter. The vector also contains *Bam*HI, *Eco*NI and *Xba*I restriction enzyme recognition sites, which were used to confirm the presence, and correct orientation of 1.28 mer HBV DNA in the plasmid DNA (Bhoola *et al*. 2014)
(URL:https://www.thermofisher.com/order/catalog/product/V102020)

APPENDIX III: PROTOCOLS

A. Agarose Gel Electrophoresis

Agarose gel electrophoresis was performed to determine the integrity of extracted plasmid DNA, as well as to analyse DNA fragments produced during restriction digestion of the 1.28 mer HBV DNA. The 0.1 µg/µl O'GeneRuler™ 1 kb DNA Ladder (Fermentas Molecular Biology Tools) (Appendix V, Figure 35, p107)was used as reference on a 0.8% (w/v)agarose gel (Appendix IV, A1, p96) prepared in 1X TBE Buffer (Appendix IV, A7, p97) containing 3 µl/100 ml ethidium bromide (Bio Basic Inc., Ontario, Canada). The gel was allowed to run at 70V for 30 min and then 100V until the dye front reached ¾ down the gel.

B. Mycoplasma Detection

The LookOut™ Mycoplasma PCR Detection Kit allows for the high sensitivity detection of *Mycoplasma* contamination in cell cultures, with the primer set specific to a highly conserved 16S rRNA region in the *Mycoplasma* genome. Reaction tubes supplied with the kit are pre-coated with deoxyribonucleotide triphosphate (dNTPs), primers, loading dye, as well as internal control DNA.

A 100 µl aliquot of cell culture supernatant was collected from cell culture flasks containing ~90% confluent Huh7 cells and transferred to sterile 1.5 ml microcentrifuge tubes. The supernatants were heated at 95 °C for 5 min and briefly centrifuged to collect the condensation in each tube. **Table 7** illustrates the reaction set up (please refer to Appendix IV, B3, p99 for the composition of the Rehydration Buffer). The included positive control contained internal control DNA consisting of non-infectious DNA fragments from the *Mycoplasma orale* genome. The negative control consisted of a prepared reaction tube with no additional cell culture supernatant. **Table 8** describes the PCR cycling conditions using the MyCycler Thermal Cycler (Bio-Rad). PCR products were run on 0.8% (w/v) agarose gel (Appendix IV, A1, p96) at 70V for 30 min then 100V until the dye front reached ¾ down the gel.

Table 7. Reaction Set Up for the Detection of Mycoplasma in Cell Culture

Reagent	Volume (µl)		
	Test Reaction	Positive Control	Negative Control
Polymerase/Rehydration Buffer	23.0	25.0	23.0
Cell Culture Supernatant	2.0	-	-
Nuclease-Free Water	-	-	2.0
Total Volume	25.0	25.0	25.0

Table 8. Cycling Conditions for the Detection of Mycoplasma in Cell Culture

Step	Temperature (°C)	Time (min)	Cycle
Initial Denaturation	94	2:00	1
Denaturation	94	0:30	40
Annealing	55	0:30	
Elongation	72	0:40	
	4	∞	

APPENDIX IV: COMPOSITION OF REAGENTS AND SOLUTIONS

A. Plasmid Preparation

	Solution	Composition
A1.	**0.8% Agarose**	**0.8 g SeaKem® LE Agarose** (Lonza, Basel, Switzerland) **100 ml 1X TBE Buffer** (Solution: A7) **3 µl/100 ml 10 mg/ml Ethidium Bromide** Agarose powder was dissolved in 1X TBE Buffer in a microwave and the solution allowed to cool slightly prior to the addition of ethidium bromide. The agarose gel solution was then poured onto a gel tray clamped on both sides, the comb added, and the agarose gel allowed to solidify for 30 min before use.
A2.	**100 mg/ml Ampicillin**	**1.0 g Ampicillin** (Melford, Ipswich, UK) **10 ml SABAX Water** Ampicillin powder was dissolved in SABAX water for injection by vortexing and the solution filter-sterilised using a 0.2 µm Minisart® NML single-use syringe filter (Sartorius AG, Goettingen, Germany). 1 ml aliquots of the ampicillin solution were stored in foil-wrapped sterile 1.5 ml tubes and stored at -20 °C until further used.
A3.	**50 mg/ml Kanamycin**	**0.5 g Kanamycin Sulphate** (Melford) **10 ml SABAX Water** Kanamycin powder was dissolved in SABAX water for injection by vortexing and the solution filter-sterilised using a 0.2 µm Minisart® NML single-use syringe filter (Sartorius AG). 1 ml aliquots of the kanamycin solution were stored in foil-wrapped sterile 1.5 ml tubes and stored at -20 °C until further used.
A4.	**LB Medium**	**10 g Tryptone** (Melford) **5 g Yeast Extract** (Sigma-Aldrich) **10 g Sodium Chloride (NaCl)** (Saarchem) Distilled water was added to a final volume of 1 L, the solution was then autoclaved at 121 °C for 30 min and stored at 4 °C until further used.

A5.	**10 mM Tris, pH 7.5**	**0.12 g Tris** **UltraPure™ water, DNase- and RNase-free** UltraPure™ water was added to a volume of 80 ml, the solution adjusted to pH 7.5 with hydrochloric acid, 32% (v/v) and made up to a final volume of 100 ml with UltraPure™ water, DNase- and RNase-free. The solution was autoclaved at 121 °C for 30 min and stored at room temperature until further used.
A6.	**20X TBE Buffer**	**212 g Tris Base** (Roche Diagnostics GmbH by Roche Applied Science, Manneheim, Germany) **110 g Boric Acid** (Sigma-Aldrich) **18.6 g EDTA Disodium Salt** (Sigma-Aldrich) Distilled water was added to a final volume of 1 L, autoclaved at 121 °C for 30 min and stored at room temperature until further used.
A7.	**1X TBE Buffer**	**100 ml 20X TBE Buffer** (Solution: A6) **1.9 L Sterile Distilled Water** 20X TBE Buffer was dissolved in sterile distilled water and stored at room temperature until further used.
A8.	**Resuspension Buffer RES-EF**	**100 µg/ml RNase A** **Resuspension Buffer S1-EF** Prior to first time use of the kit, 100 µg/ml RNase A was dissolved in 1 ml Resuspension Buffer S1-EF by vortexing. The resulting solution was mixed thoroughly with the remaining Resuspension Buffer S1-EF. The Resuspension Buffer S1-EF containing RNase A was stored at 4 °C until further used.
A9.	**2X YT Agar Plates Supplemented with 100 mg/ml Ampicillin**	**16 g Tryptone** **10 g Yeast Extract** **5 g NaCl** **15 g Agar Bacteriological** (Saarchem) Distilled water was added to a final volume of 1 L, autoclaved at 121 °C for 30 min, and the solution allowed to cool at room temperature for 1 hour. An aliquot of 1 ml 100 mg/ml ampicillin was added, and 50 ml of this agar solution was poured into 10 cm petri dishes and allowed to dry overnight. The next day the agar

		plates were incubated at 37 °C for 30 min and stored at 4 °C until further used.
A10.	**2X YT Agar Plates Supplemented with 50 mg/ml Kanamycin**	**16 g Tryptone** **10 g Yeast Extract** **5 g NaCl** **15 g Agar Bacteriological** Distilled water was added to a final volume of 1 L, autoclaved at 121 °C for 30 min, and the solution allowed to cool at room temperature for 1 hour. An aliquot of 1 ml 50 mg/ml kanamycin was added, and 50 ml of this agar solution was poured into 10 cm petri dishes and allowed to dry overnight. The next day the agar plates were incubated at 37 °C for 30 min and stored at 4 °C until further used.
A11.	**2X YT Medium**	**16 g Tryptone** **10 g Yeast Extract** **5 g NaCl** Distilled water was added to a final volume of 1 L, autoclaved at 121 °C for 30 min and stored at 4 °C until further used.

B. Cell Culture and Transient Transfection

	Solution	Composition
B1.	**Complete Growth DMEM Medium**	**435 ml DMEM (1X) + GlutaMAX™** **50 ml Foetal Bovine Serum, Certified, Heat Inactivated & Gamma Irradiated, South American Origin** **5 ml 100X MEM Non-Essential Amino Acids** **10 ml 10000 U/ml Penicillin-Streptomycin**
B2.	**Phosphate Buffered Saline (PBS)**	**1 PBS Tablet** (Gibco™) **500 ml UltraPure™ Water, DNase- and RNase-free** (Gibco™) 1 PBS tablet was dissolved in UltraPure™ water, autoclaved at 121 °C for 30 min and stored at 4 °C until further used.

B3.	**Polymerase/ Rehydration Buffer**	**2.5 U/µl JumpStart™ *Taq* DNA Polymerase** (Sigma-Aldrich) **Rehydration Buffer** (Sigma-Aldrich) 0.5 µl 2.5 U/µl JumpStart™ *Taq* DNA Polymerase was added per 23 µl Rehydration Buffer.

C. Subcellular Fractionation, Whole Cell Lysis, and Protein Quantification

	Solution	Composition
C1.	**Cytoplasmic Extraction Buffer**	**1 µl 100X Halt Protease Inhibitor Cocktail** **100 µl CEB Stock Solution** Buffer prepared fresh when required.
C2.	**Membrane Extraction Buffer**	**1 µl 100X Halt Protease Inhibitor Cocktail** **100 µl MEB Stock Solution** Buffer prepared fresh when required.
C3.	**Nuclear Extraction Buffer**	**1 µl 100X Halt Protease Inhibitor Cocktail** **100 µl NEB Stock Solution** Buffer prepared fresh when required.
C4.	**Chromatin-Bound Extraction Buffer**	**5 µl 100 mM CaCl2** **3 µl Micrococcal Nuclease** **1 µl 100X Halt Protease Inhibitor Cocktail** **100 µl NEB Stock Solution** Buffer prepared fresh when required.
C5.	**Cytoplasmic Extraction Buffer**	**1 µl 100X Halt Protease Inhibitor Cocktail** **100 µl PEB Stock Solution** Buffer prepared fresh when required.
C6.	**25X Complete, EDTA-Free Protease Inhibitor Cocktail Stock Solution**	**1 tablet Complete, EDTA-Free Protease Inhibitor Cocktail** (Roche) **2 ml Milli-Q water** 1 tablet was dissolved in Milli-Q water and stored at 4 °C until further used.

C7.	**SDS Total Cell Lysis Buffer Stock Solution**	**50 mM Tris-HCl, pH 6.8 (5 ml of 1 M Tris-HCl, pH 6.8** (Solution:D18)**)** **2g SDS** **10 ml Glycerol** The solution was made up to 100 ml with Milli-Q water and stored at room temperature until further used.
C8.	**SDS Total Cell Lysis Buffer Working Solution**	**40 µl 25X Complete, EDTA-Free Protease Inhibitor Cocktail Stock Solution** (Solution: C6) **1 ml SDS Total Cell Lysis Buffer Stock Solution** (Solution: C7) Buffer prepared fresh when required.
C9.	**BCA Working Reagent**	BCA Reagent A was added 50 parts to 1 part BCA Reagent B, and prepared fresh when required.

D. Western Blotting

	Solution	Composition
D1.	**40% (w/v) Acrylamide-Bis-Acrylamide Solution**	**95 g Acrylamide** (Sigma-Aldrich) **5 g Bis-Acrylamide** (Bio-Rad) The solution was made up to 250 ml with sterile-distilled water and filter-sterilised with a 0.4 µm Minisart® NML single-use syringe filter. The solution was aliquoted into 50 ml polypropylene tubes wrapped in aluminium foil and stored at 4 °C until further used.
D2.	**10% (w/v) APS**	**1 g APS** (Promega Corporation) The solution was made up to 10 ml with sterile distilled water and stored in aliquots of 1 ml at -20 °C for long-term, or at 4 °C for up to 2 weeks.
D3.	**5% (w/v) Blocking Buffer**	**25g Blotting-Grade Blocker** (Bio-Rad) The solution was made up to 500 ml with TBS-T (Solution: D16) and stored at 4 °C until further used.
D4.	**4X Laemmli Buffer Stock Solution**	**250 mM Tris-HCl, pH 6.8 (12.5 ml of 1 M Tris-HCl, pH 6.8** (Solution: D18)**)** **4g SDS** (Roche) **20 ml Glycerol** (Saarchem)

		0.01 g Bromophenol Blue Sodium Salt for Electrophoresis (Sigma-Aldrich) The solution was made up to a final volume of 40 ml with Milli-Q water and stored at room temperature.
D5.	**4X Laemmli Buffer**	**2 ml β-Mercaptoethanol** (Sigma-Aldrich) **8 ml Laemmli Buffer Stock Solution** (Solution: D4) The solution was mixed in a 15ml polypropylene tube wrapped in aluminium foil and stored at 4 °C until further used. 25 µl 4X Laemmli Buffer was added per 100 µl sample.
D6.	**5M NaCl**	**146.1 g Sodium Chloride** (Saarchem) The solution was made up to a final volume of 500 ml with Milli-Q water, autoclaved at 121 °C for 30 min and stored at room temperature until further used.
D7.	**5M NaOH**	**20 g Sodium Hydroxide (NaOH) Pellets** (Saarchem) The solution was made up to a final volume of 100 ml with Milli-Q water, autoclaved at 121 °C for 30 min and stored at room temperature until further used.
D8.	**Ponceau Stain**	**5 g Ponceau S, practical grade** (Sigma-Aldrich) **10 ml Acetic Acid, Glacial** (Saarchem) The solution was made up to a final volume of 1 L with sterile-distilled water and stored at room temperature until further used.
D9.	**10% (w/v) SDS**	**1g SDS** The solution was made up to 100 ml with sterile distilled water and stored at room temperature until further used.
D10.	**SDS-PAGE Gel**	<u>12% (v/v) Separating Gel</u>: **3.4 ml Sterile Distilled Water** **2.5 ml 1.5 M Tris-HCl, pH 8.8** (Solution: D20) **4 ml 40% (w/v) Acrylamide/Bis-Acrylamide Solution** (Solution: D1) **100 µl 10% (w/v) SDS** (Solution: D9) **160 µl 10% (w/v) APS** (Solution: D2) **14 µl Tetramethyldiamine (TEMED)** (Promega Corporation)

		The separating gel was pipetted into the Mini-PROTEAN® Tetra HandCast System (Bio-Rad) until three-quarters full, immediately overlaid with 100% (v/v) isopropanol to prevent oxidation of the gel and allowed to solidify. Before preparing the stacking gel, the isopropanol was completely removed. <u>4.5 % (v/v) Stacking Gel:</u> **2.86 ml Sterile-Distilled Water** **500 µl 1 M Tris-HCl, pH 6.8** (Solution: D18) **40 µl 10% (w/v) SDS** (Solution: D9) **600 µl 40% (w/v) Acrylamide/Bis-Acrylamide Solution** (Solution: D1) **24 µl APS** (Solution: D2) **24 µl TEMED** The stacking gel was pipetted into the Mini-PROTEAN® Tetra HandCast System, the comb inserted, and allowed to solidify. The complete gel was then wrapped in a paper towel soaked with 1X SDS Running Buffer (Solution: D12) and stored at 4 °C until further used.
D11.	**10X SDS Running Buffer**	**30.3 g Tris** (Saarchem) **144.1 g Glycine** (Sigma) The solution was made up to 800 ml with sterile distilled water and autoclaved at 121 °C for 30 min. **10 g SDS** was dissolved in the solution, sterile distilled water added to a final volume of 1 L and stored at room temperature until further used.
D12.	**1X SDS Running Buffer**	**200 ml 10X SDS Running Buffer** (Solution: D11) The solution was made up to 2 L with sterile distilled water and stored at room temperature until further used.
D13.	**SuperSignal® West Dura Extended Duration Substrate Working Solution**	**300 µl SuperSignal® West Dura Stable Peroxide** **300 µl SuperSignal® West Dura Luminol/Enhancer** The solution was mixed thoroughly and prepared fresh prior to use.
D14.	**Stripping Buffer**	**25 g Blotting-Grade Blocker** **1g Sodium Azide (NaN_3)** (D.H. Laboratory Chemicals Division, The British Drug Houses Ltd., Poole, Dorset, England)

		The solution was made up to 500 ml with TBS-T (Solution: D16) and stored at 4 °C until further used.
D15.	**10X TBS**	**50 ml 1M Tris-HCl, pH 8.0** (Solution: D19) **150 ml 5 M NaCl** (Solution: D6) The solution was made up to a final volume of 1 L with Milli-Q water and stored at room temperature until further used.
D16.	**1X TBS-T**	**200 ml 10X TBS** (Solution: D15) **2 ml Tween® 20** (Saarchem) The solution was made up to a final volume of 2 L with Milli-Q water and stored at room temperature until further used.
D17.	**1 M Tris-HCl, pH 6.8 (Milli-Q)**	**12.11 g Tris** Tris was dissolved in 50 ml Milli-Q water to a final volume and adjusted to pH 6.8 with Hydrochloric Acid, 32% (v/v). The solution was made up to a final volume of 100 ml with Milli-Q water, autoclaved at 121 °C for 30 min and stored at room temperature until further used.
D18.	**1 M Tris-HCl, pH 6.8**	**30.29 g Tris** Tris was dissolved in 150 ml sterile distilled water and adjusted to pH 6.8 with Hydrochloric Acid, 32% (v/v). The solution was made up to a final volume of 250 ml with sterile distilled water, autoclaved at 121 °C for 30 min and stored at room temperature until further used.
D19.	**1 M Tris-HCl, pH 8.0**	**60.57 g Tris** Tris was dissolved in 400 ml Milli-Q water and the solution adjusted to pH 8.0 with Hydrochloric Acid, 32% (v/v). The solution was made up to a final volume of 500 ml with Milli-Q water, autoclaved at 121 °C for 30 min and stored at room temperature until further used.
D20.	**1.5 M Tris-HCl, pH 8.8**	**90.86 g Tris** Tris was dissolved in 400 ml sterile distilled water and adjusted to pH 8.8 with Hydrochloric Acid, 32% (v/v). The solution was made up to a final volume of 500 ml with sterile distilled water, autoclaved at 121 °C for 30 min and stored at room temperature until further used.

D21.	**10X Wet Transfer Buffer**	**30.3 g Tris** **144.1 g Glycine** Tris and glycine were dissolved in 800 ml sterile distilled water and adjusted to pH 8.3 with Hydrochloric Acid, 32% (v/v). The solution was made up to a final volume of 1 L with sterile distilled water, autoclaved at 121 °C for 30 min and stored at room temperature until further used.
D22.	**1X Wet Transfer Buffer**	**200 ml 10X Wet Transfer Buffer** (Solution: D21) **400 ml 100% (v/v) Ethanol** (Saarchem) The solution was made up to a final volume of 2 L with sterile distilled water and stored at room temperature until further used.

E. ELISA and PEG Precipitation

	Solution	Composition
E1.	**0.1M EDTA**	**3.72 g EDTA Disodium Salt** EDTA powder was dissolved in 100 ml sterile distilled water and stored at 4 °C until further used.
E2.	**0.1M HEPES Buffer pH 7.5**	**2.38 g HEPES Hemisodium Salt Dry Powder** (Sigma-Aldrich) HEPES powder was dissolved in 80 ml sterile dissolved water. The solution was adjusted to pH 7.5 using NaOH pellets and made up to a final volume of 100 ml with sterile distilled water.
E3.	**1M NaCl**	**4 ml 5M NaCl** (Solution: D6) **16 ml Sterile Distilled Water** 5M NaCl was added to sterile distilled water and stored at room temperature until further used.
E4.	**37% (w/v) PEG 8000**	**37 g Polyethylene Glycol (PEG) 8000** (Sigma-Aldrich) **100 ml PBS** (Solution: B2) PEG 8000 powder was dissolved in sterile PBS and stored at 4 °C until further used.
E5.	**HEPES Resuspension Buffer**	**1 ml HEPES Buffer pH 7.5** (Solution: E2) **1 ml 1M NaCl** (Solution: E3) **100 µl 0.1M EDTA** (Solution: E1)

		100 µl Nonidet™ P 40 Substitute (Sigma-Aldrich) The solution was made up to a final volume of 10 ml with sterile distilled water and prepared fresh when required.
E6.	**Substrate Solution**	**Murex HBsAg Version 3 Substrate Diluent** **Murex HBsAg Version 3 Substrate Concentrate** Immediately prior to use, one part Substrate Diluent was added to an equal volume of Substrate Concentrate.
E7.	**Wash Buffer**	**40 ml ETI-EBK PLUS Wash Buffer (25X)** The solution was made up to a final volume of 1 L with sterile distilled water and prepared fresh when required.
E8.	**Wash Fluid**	**10 ml Murex HBsAg Version 3 Wash Fluid Concentrate (20X)** Th solution was made up to a final volume of 1 L with sterile distilled water and prepared fresh when required.
E9.	**Working Enzyme Tracer Solution**	**ETI-EBK PLUS Enzyme Tracer (50X Conjugate)** **ETI-EBK PLUS Tracer Diluent** Immediately prior to use, the solution was prepared by mixing 1 part Enzyme Tracer (50X conjugate) with 49 parts Tracer Diluent.

APPENDIX V: DNA AND PROTEIN LADDERS

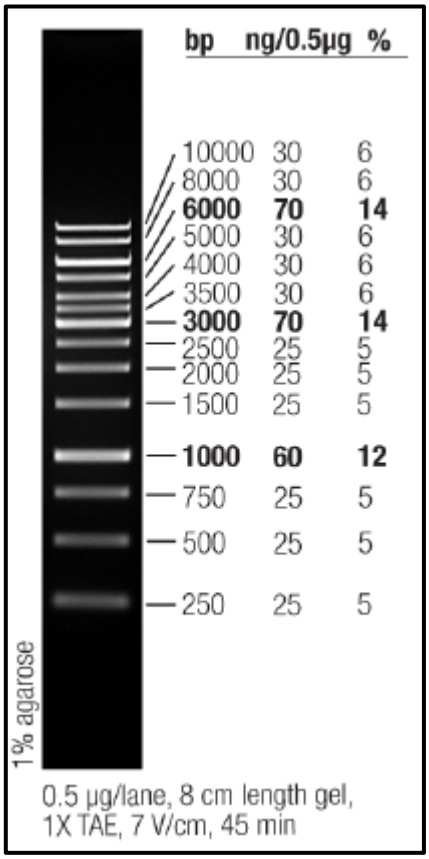


Figure 34. O'GeneRuler™ 1 kb DNA Ladder, Ready-to-Use

The Thermo Scientific™ O'GeneRuler™ 1 kb DNA Ladder, ready-to-use, is designed for sizing and approximate quantification of wide range double-stranded DNA fragments on agarose gel. The ladder is composed of fourteen chromatography-purified individual DNA (in base pairs): 10 000, 8000, 6000, 5000, 4000, 3500, 3000, 2500, 2000, 1500, 1000, 750, 500, 250. It contains three reference bands (6000, 3000 and 1000 bp) for easy orientation. The ladder is premixed with 6X Orange DNA Loading Dye for direct loading on gel.

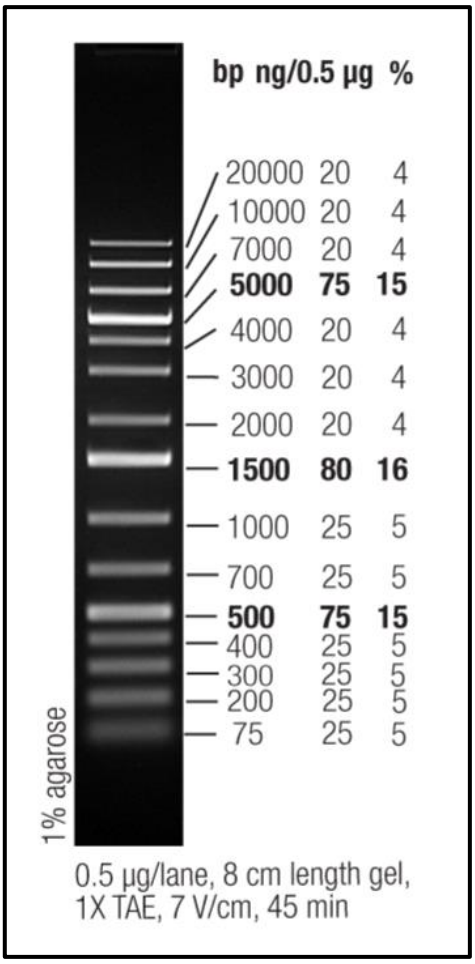


Figure 35. O'GeneRuler™ 1 kb Plus DNA Ladder, Ready-to-Use

The Thermo Scientific™ O'GeneRuler™ 1 kb Plus DNA Ladder, ready-to-use, is designed for sizing and approximate quantification of wide range double-stranded DNA fragments on agarose gel. The ladder is composed of fourteen chromatography-purified individual DNA (in base pairs): 20000, 10000, 7000, 5000, 4000, 3000, 2000, 1500, 1000, 750, 500, 400, 300, 200, and 75. It contains three reference bands (5000, 1500 and 500 bp) for easy orientation. The ladder is premixed with 6X Orange DNA Loading Dye for direct loading on gel.
(URL: http://www.thermofisher.com/order/catalog/product/SM1331)

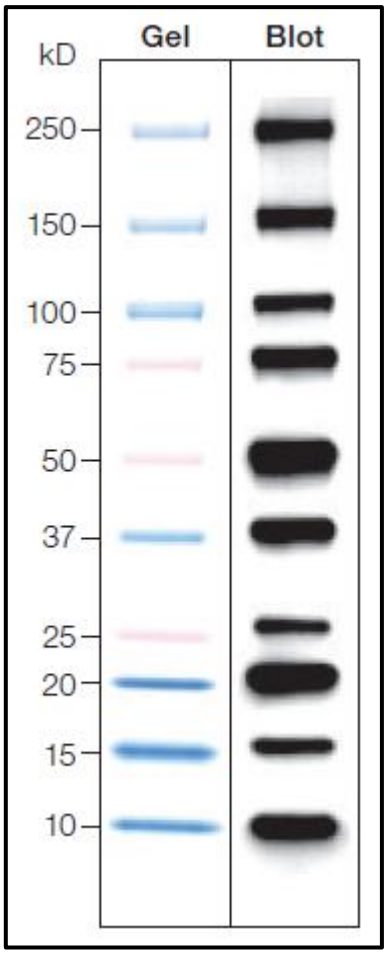


Figure 36. Precision Plus Protein™ WesternC™ Standards

Precision Plus Protein WesternC Standards offer 10 distinct, prestained protein bands broad-range protein standards that enable chemiluminescent detection when probed with StrepTactin-HRP conjugates. These protein standards contain ten highly purified recombinant proteins with molecular weights of 10, 15, 20, 25, 37, 50, 75, 100, 150 and 250 kD. Three high-intensity reference bands at 25, 50, and 75 kD bands are stained pink for easy band referencing and blot orientation.
(URL: https://www.bio-rad.com/webroot/web/pdf/lsr/literature/Bulletin_5561.pdf)

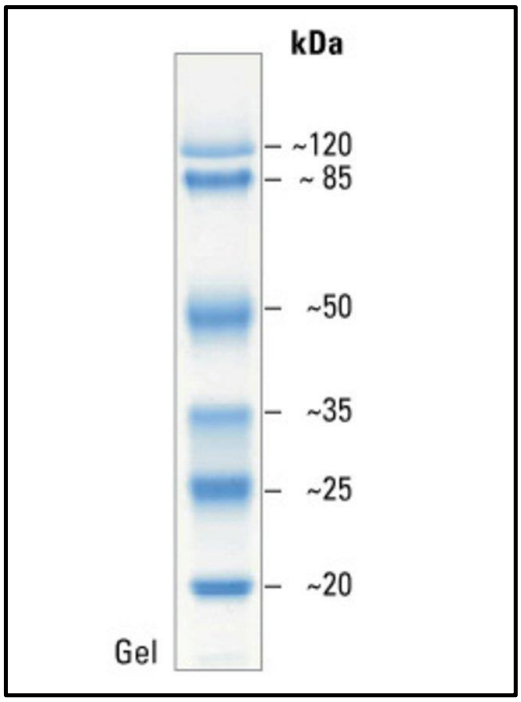


Figure 37. Pierce™ Prestained Protein MW Marker

The Pierce™ Prestained Protein MW Marker is a ready-to-use protein molecular weight marker containing six blue-stained natural proteins ranging from 20 kDa to 120 kDa.
(URL: https://www.thermofisher.com/order/catalog/product/26612)

Appendix VI: ENZYME-LINKED IMMUNOSORBENT ASSAY

96-well Plate Layout

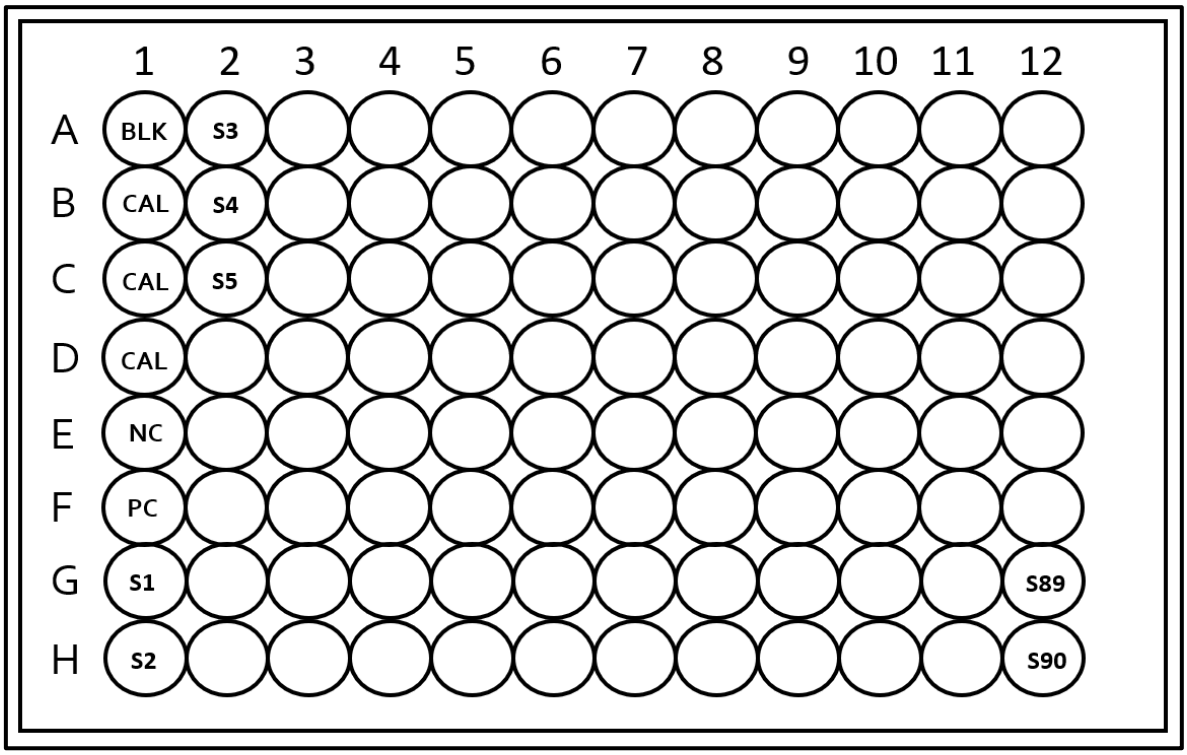


Figure 38. ETI-EBK PLUS HBeAg ELISA plate layout

Key: BLK, Blank; **CAL,** Calibrator; **NC,** Negative Control; **PC,** Positive Control; **S,** Sample.

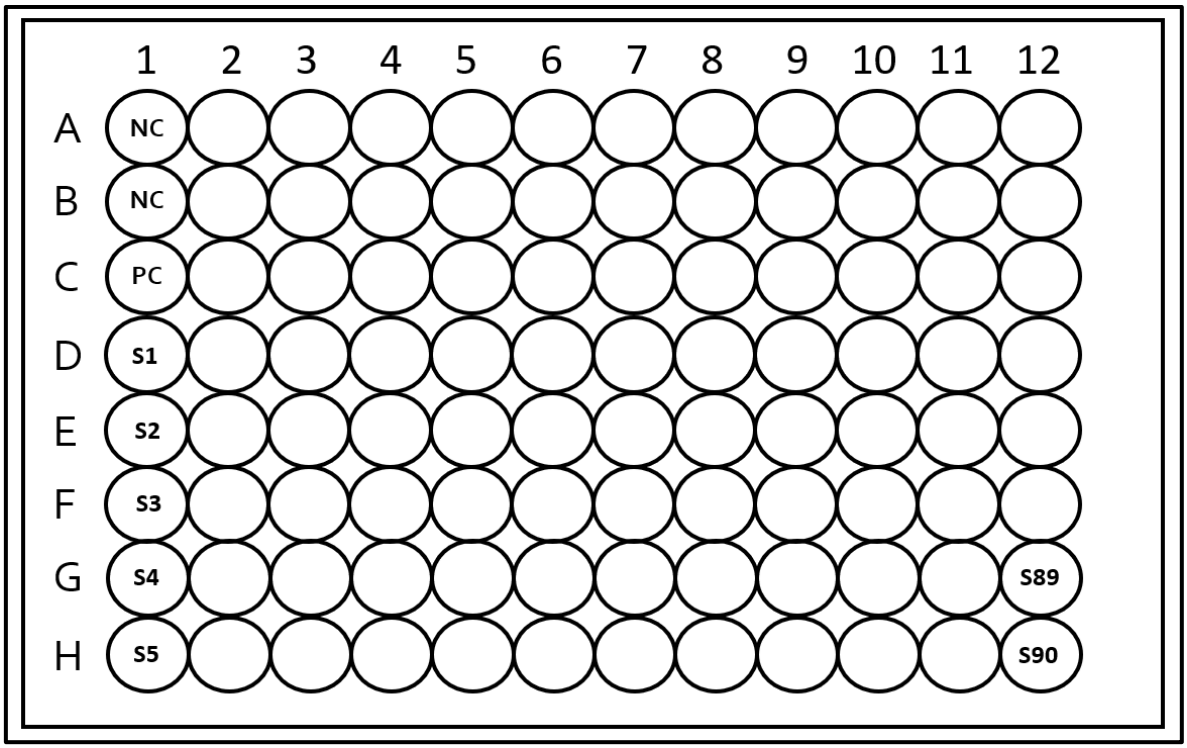


Figure 39. Murex HBsAg Version 3 HBsAg ELISA plate layout

Key: NC, Negative Control; **PC,** Positive Control; **S,** Sample.

APPENDIX VII: PLAGIARISM DECLARATION



PLAGIARISM DECLARATION TO BE SIGNED BY ALL HIGHER DEGREE STUDENTS

SENATE PLAGIARISM POLICY: APPENDIX ONE

I _____ (Student number: _____) am a student registered for the degree of _____ in the academic year _____.

I hereby declare the following:

- I am aware that plagiarism (the use of someone else's work without their permission and/or without acknowledging the original source) is wrong.
- I confirm that the work submitted for assessment for the above degree is my own unaided work except where I have explicitly indicated otherwise.
- I have followed the required conventions in referencing the thoughts and ideas of others.
- I understand that the University of the Witwatersrand may take disciplinary action against me if there is a belief that this is not my own unaided work or that I have failed to acknowledge the source of the ideas or words in my writing.

Signature: _____ Date: _____